EXAMINATION OF DESULFURIZATION BEHAVIOUR OF LADLE FURNACE SLAGS OF A LOW-SULFUR STEEL

A THESIS SUBMITTED TO
THE GRADUATE SCHOOL OF NATURAL AND APPLIED SCIENCES
OF
MIDDLE EAST TECHNICAL UNIVERSITY

BY

ENDER KESKİNKILIÇ

IN PARTIAL FULFILLMENT OF THE REQUIREMENTS
FOR
THE DEGREE OF DOCTOR OF PHILOSOPHY
IN
METALLURGICAL AND MATERIALS ENGINEERING

OCTOBER 2007

Approval of the thesis:

EXAMINATION OF DESULFURIZATION BEHAVIOUR OF LADLE FURNACE SLAGS OF A LOW-SULFUR STEEL

submitted by **ENDER KESKİNKILIÇ** in partial fulfillment of the requirements for the degree of **Doctor of Philosophy in Metallurgical and Materials Engineering Department, Middle East Technical University** by,

Prof. Dr. Canan Özgen _____
Dean, Graduate School of **Natural and Applied Sciences**

Prof. Dr. Tayfur Öztürk _____
Head of Department, **Metallurgical and Materials Engineering**

Prof. Dr. Ahmet Geveci _____
Supervisor, **Metallurgical and Materials Engineering Dept., METU**

Prof. Dr. Yavuz A. Topkaya _____
Co-Supervisor, **Metallurgical and Materials Engineering Dept., METU**

Examining Committee Members:

Prof. Dr. İshak Karakaya _____
Metallurgical and Materials Engineering Dept., METU

Prof. Dr. Ahmet Geveci _____
Metallurgical and Materials Engineering Dept., METU

Prof. Dr. Ekrem Selçuk _____
Metallurgical and Materials Engineering Dept., METU

Assist. Prof. Dr. Hasan Okuyucu _____
Metal Education Dept., Gazi University

Prof. Dr. Ümit Atalay _____
Mining Engineering Dept., METU

Date: 17.10.2007

I hereby declare that all information in this document has been obtained and presented in accordance with academic rules and ethical conduct. I also declare that, as required by these rules and conduct, I have fully cited and referenced all material and results that are not original to this work.

Name, Last Name : Ender Keskinkılıç

Signature :

ABSTRACT

EXAMINATION OF DESULFURIZATION BEHAVIOUR OF LADLE FURNACE SLAGS OF A LOW-SULFUR STEEL

Keskinkılıç, Ender

Ph.D., Department of Metallurgical and Materials Engineering

Supervisor : Prof. Dr. Ahmet Geveci

Co-Supervisor : Prof. Dr. Yavuz A. Topkaya

October 2007, 161 pages

The aim of this research was mainly to investigate desulfurization behaviour of ladle furnace slags of a low-sulfur steel. First, the change of the amount of unstable oxides (Fe_tO and MnO) in slags was studied from the converter till the end of ladle furnace treatment for different steel quality groups. It was found that the change in the amount of unstable oxides could be examined best with low-C steel qualities. Then, the change of activity of iron oxide was investigated for a member of low-C steel quality group, namely 4937K, a low-S steel. The relation between the degree of desulfurization at the ladle furnace, *% DeS (measured)*, and the change in activity of iron oxide, *% Decrease in* a_{Fe_tO}, was examined first using an empirical expression obtained from literature. Then, this relationship was studied using steel oxygen activity measurements conducted at the ladle furnace. With this method, a regression formula was proposed for 4937K slags relating activity coefficient of iron oxide, γ_{Fe_tO}, with the major slag components. The results obtained from steel oxygen activities were found to be representative for 4937K steel-slag system showing similar behaviour with the ones from the empirical expression obtained

from literature. Similar results were found using Temkin equation and the polymeric anion model. In relation to formation of less harmful inclusions to suppress adverse effects of sulfur, morphological studies of some steels produced in ERDEMİR plant were performed. D-type globular inclusions with severity values of 1-2 were observed.

Key words: Desulfurization, Activity Coefficient of Fe_tO, Activity of Fe_tO

ÖZ

DÜŞÜK KÜKÜRTLÜ ÇELİK ÜRETİMİNDE OLUŞAN POTA FIRINI CURUFLARININ KÜKÜRT GİDERME DAVRANIŞLARININ İNCELENMESİ

Keskinkılıç, Ender
Doktora, Metalurji ve Malzeme Mühendisliği Bölümü
Tez Yöneticisi : Prof. Dr. Ahmet Geveci
Ortak Tez Yöneticisi : Prof. Dr. Yavuz A. Topkaya

Ekim 2007, 161 sayfa

Bu araştırmanın amacı, genel olarak, düşük kükürtlü çelik üretiminde oluşan pota fırını curuflarının kükürt giderme davranışlarının incelenmesidir. İlk olarak, curuftaki kararsız oksitlerin (Fe_tO ve MnO) konvertörden pota fırını işlemi sonuna kadar olan değişimi farklı çelik grupları için ayrı ayrı ele alınmıştır. Kararsız oksitlerdeki değişimin en iyi şekilde düşük karbonlu çeliklerde incelenebileceği sonucuna varılmıştır. Daha sonra, demir oksitin aktivitesindeki değişim düşük karbonlu çelik kaliteleri arasında yer alan ve aynı zamanda düşük kükürtlü bir çelik kalitesi olan 4937K için ele alınmıştır. *% DeS (ölçülen)* şeklinde tanımlanan pota fırınındaki kükürt giderme ile *% Azalma* a_{Fe_tO} ile takip edilen demir oksitin aktivitesindeki değişim arasındaki ilişki, ilk olarak, literatürde yer alan empirik bir denklemin kullanılmasıyla incelenmiştir. Sonrasında bu ilişki pota fırınındaki çelik oksijen aktivitesi değerlerinin kullanılması suretiyle ele alınmıştır. Bu metodla 4937K curufları için demir oksitin aktivite katsayısının, γ_{Fe_tO}, temel curuf bileşenleriyle ilişkilendirildiği bir regrasyon denklemi elde edilmiştir. Çelik oksijen aktivitesi değerleri kullanılarak elde edilen sonuçların 4937K çelik-curuf sistemi

için temsil edici olduğu sonucuna varılmış, literatürdeki denklem kullanılarak elde edilen sonuçlarla benzer bir eğilim sergilediği görülmüştür. Temkin denkleminin ve polimerik anyon modelinin kullanılmasıyla da benzer sonuçlar elde edilmiştir. Kükürdün olumsuz etkilerini önlemek için daha az zararlı inklüzyonların oluşturulması gerekliliği noktasında ERDEMİR'de üretilen bazı çeliklerin inklüzyon morfolojileri incelenmiştir. İncelemelerde şiddet değeri 1-2 olan D-tipi küresel inklüzyonlar gözlenmiştir.

Anahtar kelimeler: Kükürt Giderme, Fe_tO Aktivite Katsayısı, Fe_tO Aktivitesi

ACKNOWLEDGEMENTS

The author wishes to express his great appreciation to his supervisor Prof. Dr. Ahmet Geveci and co-supervisor Prof. Dr. Yavuz A. Topkaya for their guidance, advice and encouragements throughout the thesis. The author also thanks to his committee members, who offered valuable help and support.

The author would also like to thank Recep Sarı for XRF analysis of slag samples and Ramazan Tütük for SEM-EDS analysis of steel specimens.

All staff of Quality Metallurgy and RD Department of ERDEMİR is greatly acknowledged.

Thanks also go to my elder brother, İlker, for his valuable advices.

Finally, it must be mentioned that in all stages of this work, the patience and support of my family are the key factors of completion of the PhD thesis.

TABLE OF CONTENTS

LIST OF TABLES

TABLES

LIST OF FIGURES

FIGURES

CHAPTER 1

INTRODUCTION

Demand for clean steel is continuously increasing as the World steel production is increasing year by year. Nowadays, clean steel production necessitates certain treatments to be performed and some precautions to be taken starting from the very beginning of ironmaking stage till the end of continuous casting.

As far as the steelmaking from hot metal is concerned, even choices of iron ore have vital importance since some impurity elements (e.g. Cu, Ni, As etc.) coming from the iron ore can not be separated from the steel metallurgically. These tramp elements do not only lead to some problems during hot rolling (i.e. Hot shortness) but also cause deterioration in mechanical properties of the final product. Likewise, being one of the hazardous elements to human health, arsenic (As) content of the steel should be strictly controlled especially for the tin plated steel qualities since the end use of the tin plated product is generally a food can.

Again considering steelmaking from the hot metal, efforts should be performed to refine hot metal and steel at the pretreatment (e.g. desulfurization, dephosphorization, desiliconization), converter, secondary metallurgy and casting stages. Refining of steel includes mainly removal of impurities either to slag or gas phase, and shape control of inclusions. Different metallurgical operations should be conducted to obtain a casted product that has only limited number of impurities and desired inclusion morphology so that it can ensure the mechanical and physical properties demanded by the customer.

One of the elements that is generally regarded as a tramp element in steelmaking is sulfur. Except for the resulfurized grades, sulfur is an impurity that decreases impact strength, transverse ductility and weldability, and is therefore highly undesirable in applications where these properties are important, such as pipeline, ship plate. Sulfur can also cause hot shortness problem in steels having low manganese content [1].

In order to overcome the problems associated with the presence of sulfur, there are mainly two remedies: 1. Removal of sulfur from the steel, 2. Formation of stable sulfide compounds that are solid at hot rolling temperatures and have suitable shapes. The first item is commonly named as "Desulfurization", which is performed both at the hot metal pretreatment and steelmaking stages. In the scope of the second item, manganese is generally used to form stable sulfide compound, manganese sulfide (MnS), which is solid at hot rolling temperatures. At the secondary metallurgy, the shape control of both the oxide and the sulfide type inclusions are generally conducted using calcium and this operation is known as "Calcium Treatment" [2].

One of the requirements of the desulfurization at the secondary metallurgy is the necessity of low oxygen potential in the steel-slag system [3]. Oxygen potential of the system can be described either with oxygen activity of the steel melt or iron oxide activity in the slag. Presence of unstable oxides in the steelmaking slags hinders the desulfurization treatment. Therefore, efforts should be made to decrease the percentage of them in ladle slags. The most important unstable oxides are known as FeO and MnO.

The aim of this research was to investigate the behaviour of steelmaking slags of ERDEMİR with regard to steel cleanliness and especially desulfurization. Briefly, in the scope of this thesis work, first the variations of unstable oxides in ERDEMİR converter and ladle slags were studied for different steel qualities. Then, the degree of desulfurization of a low-sulfur steel quality (4937K, DIN EN 10149-2 1995

GRADE S355MC) was studied in relation to the change in the oxygen potential at the ladle furnace, in detail. In connection with the formation of less harmful inclusions in the system worked, morphological investigation of inclusions were performed on the steels concerned using image analyzer and SEM-EDS.

CHAPTER 2

LITERATURE REVIEW

2.1 Effect of Sulfur on Steel

Sulfur is one of the tramp elements in steelmaking. Tramp element is defined as an element that serves no useful purpose in the furnace charge. Tramp element may report to the molten bath, and/or to the slag, and/or to the furnace atmosphere. Tramp elements that report to the bath, if present in sufficient quantity, almost always have adverse effect on steel properties, ease and cost of steel production, and/or have undesirable environmental characteristics. e.g. S, P, Pb, Sn, Sb, Zn, Cd, Hg. Sulfur decreases impact strength, transverse ductility, and weldability, and is therefore highly undesirable in applications where these properties are important, such as pipeline, ship plate. Sulfur is detrimental to surface quality, and may lead to hot shortness in low Mn steels. In EAF and BOF, sulfur is only removable using a basic slag practice at high temperatures. Generally accepted sulfur content of the steels is illustrated in Table 2.1.

Table 2.1 Generally accepted sulfur content of the steels [4]

QUALITY CATEGORY vs. TYPICAL S CONTENT *	STRUCTURAL STEELS	ENGINEERING STEELS	COMMERCIAL QUALITY	DRAWING QUALITIES
S	Usually 0.04% max.	Usually 0.02% max.	Usually 0.03% max.	Usually 0.015% max.

* These are the max. contents allowable. Depending on the specific applications, the sulfur content of the steels are restricted to lower values. These steels are sometimes called “low sulfur” (e.g. sulfur content being 50 ppm max.) and “ultra low sulfur” (e.g. sulfur content being around ~ 10-20 ppm max. or even less).

As an addition to the molten steel, sulfur's only useful role is to improve machinability in product applications where tensile strength and other properties are not critical. When added to improve machinability, sulfur appears in the solidified steel as FeS and other sulfide inclusions that act as "chip breakers" during machining. Unless added for machinability, S is considered to be an impurity [4].

2.2 Sulfur in Iron and Steelmaking

Solubility of sulfur in liquid iron is infinitely large whereas it is quite small in solid iron. Therefore, sulfur containing inclusions form during solidification. Careful examination of Fe-S equilibrium phase diagram reveals that beyond a specific sulfur content there exists a liquid phase when going above 1261K (Figure 2.1 and Figure 2.2).

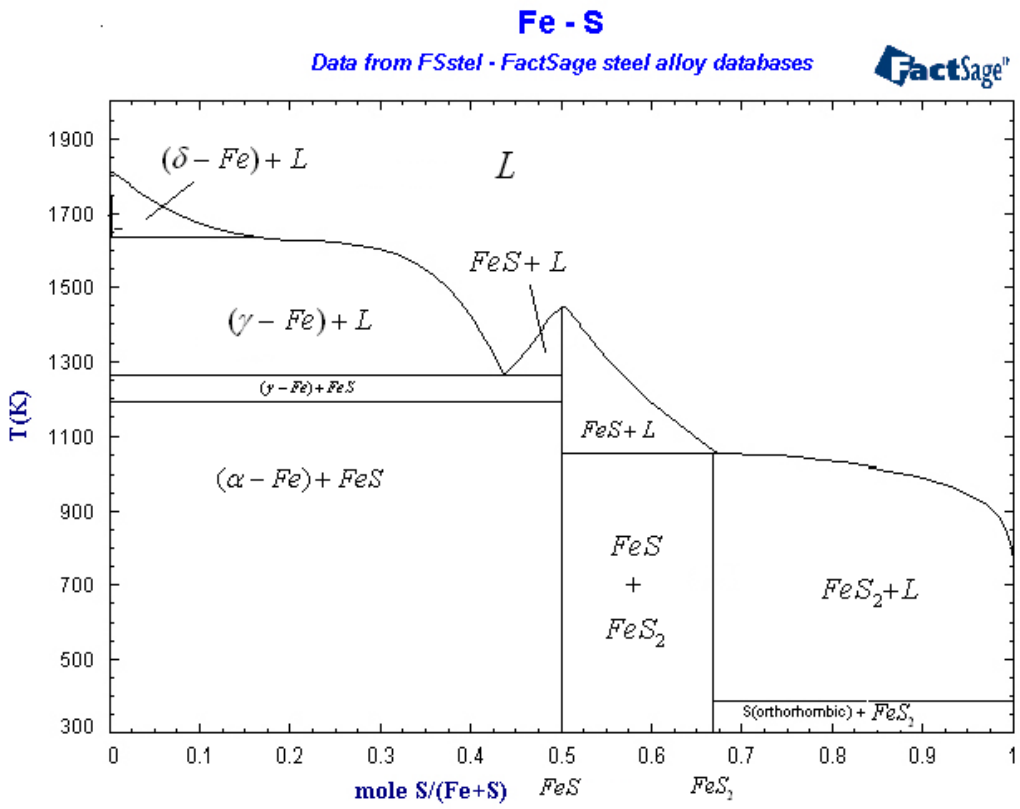

Figure 2.1 The Fe-S phase diagram [5]

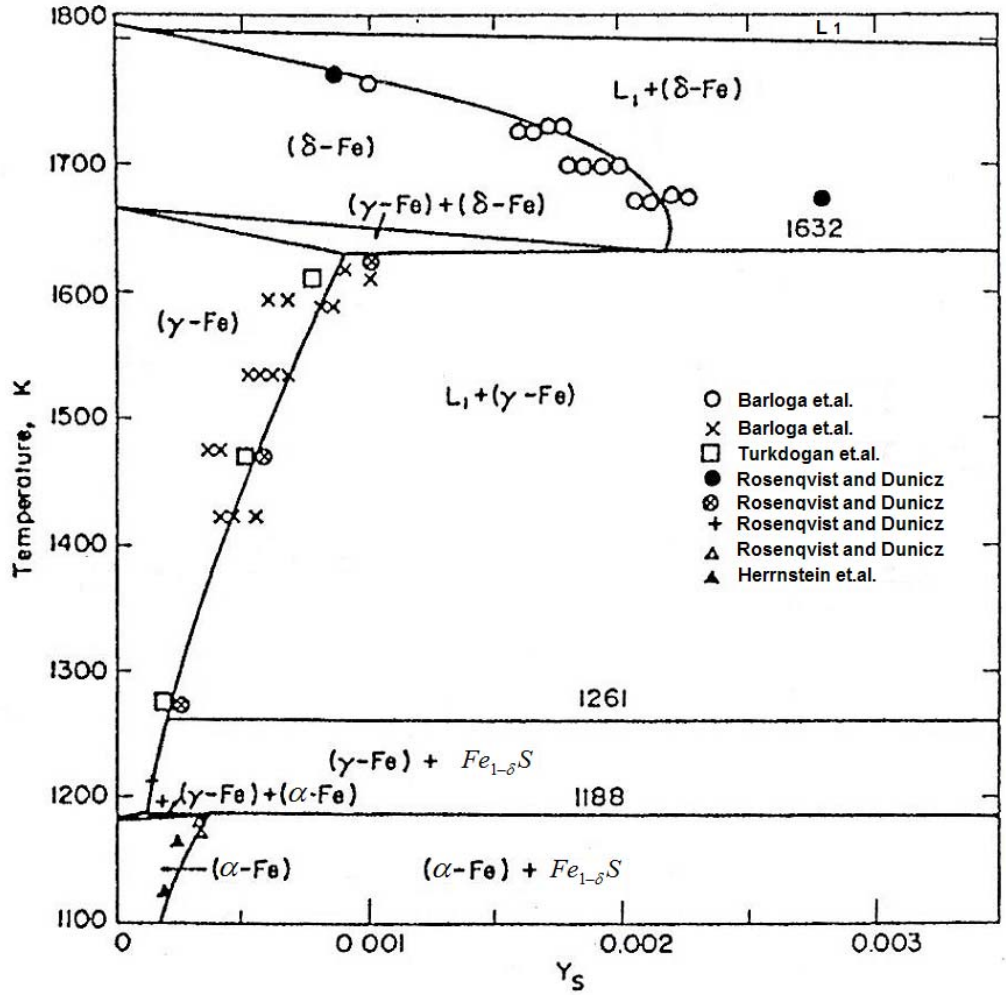

Figure 2.2 The iron-rich portion of the Fe-S phase diagram; comparison between the calculated diagram involving $\delta - Fe$, $\alpha - Fe$ and $\gamma - Fe$ and the experimental data [6].

At hot rolling (plastic deformation) temperatures presence of such liquid phase causes hot shortness, which is one of the main problems encountered during hot rolling process. To overcome this problem, there are two remedies: The first one is to lower sulfur by some means during different stages of ironmaking and steelmaking. The second one is to add element M, which has high sulfur affinity, to the liquid iron or steel to form MS compound having high melting temperature such that no liquid phase could be present at hot rolling temperatures. Ease of

formation of stable sulfur containing compounds can be seen by comparing the lines of each elements of the Ellingham diagram which is defined for pure elements and pure sulfides (see Appendix A for Ellingham Diagram)[7] .

In steelmaking, in order to form S-containing compound having high melting temperature, generally Mn is used. If one examines the sulfur potential lines of the Ellingham diagram [7], MnS is more stable than FeS at steelmaking temperatures. MnS is solid at hot rolling temperatures therefore hot shortness problem will not come into picture.

Solubility of oxygen in solid iron is quite small so inclusions formed will contain oxides and oxides-sulfides. Due to presence of oxygen, formation of sulfur containing inclusions should be studied with Fe-S-O ternary system. In this simple case, it is assumed that no other element is present in the system. Therefore, existence of other elements necessitates the study of more complex phase systems.

Various types of inclusions form during solidification. Studies [8] revealed that the most important parameter defining the morphology of inclusions is O / S ratio: FeO-rich inclusions form at the beginning of solidification with globular shape whereas inclusions containing less FeO (i.e. FeS-rich inclusions) form at later stages of solidification with rod or plate shape [9].

For a particular alloy, the higher the ratio of O / S, the richer the most of the inclusions formed during solidification as far as FeO content of them is considered. Therefore, the most of the inclusions present in the system are globular shape and are randomly distributed throughout the dendrites. On the other hand, the most of the inclusions are found to be precipitated along the grain boundaries in the alloys having lower O / S ratio [8].

There exists a liquid phase upon heating a Fe-S-O alloy above 915 ^{o}C which is ternary eutectic point and plastic deformation applied at these temperatures can

cause hot shortness (Ternary phase diagram of Fe-S-O system is shown in Appendix B) [10]. Actually there is a certain solubility of sulfur in solid iron. Therefore below specified sulfur content, formation of a liquid phase at hot rolling temperatures can be prevented. In the oxygen free Fe-S system sulfur content below 100 ppm is necessary not to have liquid phase at rolling temperatures. This amount should be less than 70 ppm while considering wustite-saturated iron in austenite form [8].

In Fe-Mn-S-O system, there exists an oxi-sulfide phase having low melting temparature [11]. In such systems, in order not to have liquid phase, there should be a certain amount of manganese in the metal. At 900 ^{o}C, 0.001% Mn should be present in the metal while 1% Mn is necessary at 1200 ^{o}C. For the oxygen free systems (i.e. Fe-Mn-S) to prevent formation of liquid phase, the necessary amount of manganese is relatively small, being 0.01% at 1200 ^{o}C. Therefore, when a strong deoxidizer is used, small amount of manganese is enough to prevent liquid phase formation [11].

Another method to prevent liquid phase formation is the use of elements like Ce, La and Ca which have high sulfur affinity so that stable sulfides can form [12]. It was understood that hot shortness could be eliminated by forming solid MnS compounds.

Depending on the steel composition, MnS inclusions formed during solidification of steel can be present with three different shapes according to Sim and Dahle's classification [13].

I. type: Inclusions having different sizes, separated from one another, randomly distributed through steel matrix, globular shape
II. type: Inclusions like thin rods, along the grain boundaries
III. type: Randomly distributed like the first type, separated from one another, inclusions having cornered surfaces.

According to studies [14] conducted for the morphologies and formation mechanisms of MnS inclusions, it was revealed [14] that morphologies of these inclusions were dependent on O / S ratio. If O / S ratio is large enough the inclusions are the first type while second and third types are observed when this ratio is small. First and second types are formed with the same mechanism: First type forms at the beginning of solidification whereas second type forms at later stages of solidification. The formation mechanism of the third type is not quite known, on the other hand it forms at the beginning of solidification with solid phase [9,15].

MnS inclusions formed during solidification affect physical, chemical and mechanical properties of steel adversely [16]. For a specified sulfur content, the second type inclusions are the ones that affect mechanical properties adversely most. For the same conditions, the ones that affect these properties least are the first type. It was found that mechanical properties of steel were badly affected with increasing S content [16].

2.3 Sulfur Reactions in Iron and Steelmaking

At steelmaking temperatures, the stable form of sulfur is the gas. Sulfur is soluble in liquid iron and slag. Therefore, the reactions happening at the gas-slag and metal- slag interfaces are important for the removal of sulfur [17].

Sulfur in the gaseous form gets into the solution according to the reaction given below:

$$\frac{1}{2}S_2(g) = \underline{S}(\%) \qquad (1)$$

In the literature, to study the behavior of sulfur when it is present with very small concentrations an experimental set up was prepared to set the following equilibrium [18]:

$$\underline{S}(\%) + H_2(g) = H_2S(g) \quad (2)$$

Sulfur activity in liquid iron at 1600 ^{o}C is calculated by using Henry's activity coefficient concept as below:

$$a_i = f_i \cdot \%i \quad (3)$$

where

$$\log f_i = \sum e_i^j \cdot \%j \quad (4)$$

In the case of higher element concentrations, it is more suitable to use the following relation:

$$\log f_i = \sum \log f_i^j \quad (5)$$

In relation (4), it is assumed that $\log f_S^j$ varies linearly with $\%j$. As shown in Figure 2.3, this assumption holds when $\%j$ values are small. On the other hand, at higher $\%j$ values, $\log f_S^j$ does not change linearly with $\%j$.Therefore, at higher concentrations graphical method or second order interaction coefficients, r_i^j, should be used. When second order interaction coefficients are used, activity coefficient of sulfur is calculated with the relation given below:

$$\log f_S = \sum e_S^j \cdot (\%j) + \sum r_S^j \cdot (\%j)^2 \quad (6)$$

As an example, activity coefficient of S in the liquid iron containing S, Si, C and Mn can be written as follows:

$$\log f_S = e_S^S \cdot (\%S) + e_S^{Si} \cdot (\%Si) + e_S^C \cdot (\%C) + e_S^{Mn} \cdot (\%Mn) + r_S^S \cdot (\%S)^2 + r_S^{Si} \cdot (\%Si)^2 + r_S^C \cdot (\%C)^2 + r_S^{Mn} \cdot (\%Mn)^2 \quad (7)$$

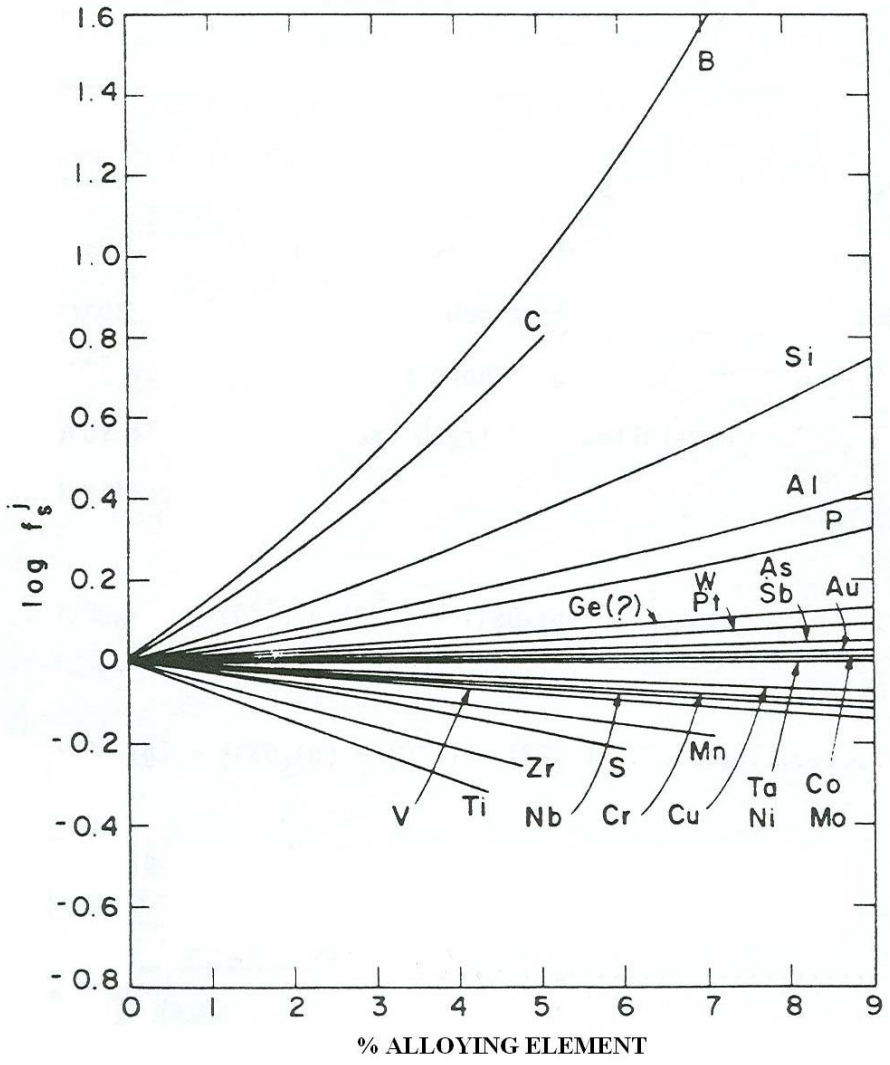

Figure 2.3 Variation of activity coefficient of sulfur with the alloying elements in liquid iron [19]

For liquid iron systems at 1600 ^{o}C, both the first order and the second order interaction coefficients can be found in literature [20]. When considering activity coefficient of sulfur, in turn removal of sulfur, C and Si have special importance. As it can be seen from Figure 2.3, the activity coefficient of sulfur increases as C

and/or Si content of the liquid iron increases. The activity coefficient of sulfur in liquid metal at blast furnace hearth region where concentrations of these elements are relatively high are larger than the one in liquid steel where C and Si concentrations are relatively small. Therefore, just from the comparison of activity coefficients in these two different systems, it can be said that separation tendency of sulfur from the metal is higher in blast furnace.

2.4 Sulfide Capacity (C_S)

The solubility of sulfur in slags is limited to certain extent (1% - 10%) [21]. It is expressed with the following relation:

$$\frac{1}{2}S_2(g)+(O^{2-})=(S^{2-})+\frac{1}{2}O_2(g) \tag{8}$$

The equilibrium constant is given by

$$K=\frac{(a_{S^{2-}})\cdot P_{O_2}{}^{1/2}}{(a_{O^{2-}})\cdot P_{S_2}{}^{1/2}} \tag{9}$$

where $a_{S^{2-}}$ is equal to $\gamma_{S^{2-}}\cdot(\%S)$.

Richardson and Fincham [22] defined C_S as

$$C_S=(\%S)\cdot\frac{P_{O_2}{}^{1/2}}{P_{S_2}{}^{1/2}} \tag{10}$$

C_S is called as sulfide capacity that shows a slag's ability to absorb sulfur. It increases as slag basicity increases. At first glance, a slag with high sulfide capacity indicates the ability of that slag to absorb sulfur is high. On the other hand, this should not lead to draw misleading conclusions since sulfur amount present in the

slag depends on partial pressure of oxygen in the system. In other words, a slag with high sulfide capacity can contain a little amount of sulfur in oxidizing conditions.

Ability of a slag to absorb sulfur from the phase in contact with it depends upon the basicity of the slag and oxygen potential of the system: The more basic the slag and the less oxidizing conditions available, the more sulfur is present in that slag [23].

Sulfide capacities for various slags have been calculated from experimental data and examples are shown in Figure 2.4 and Figure 2.5 [24].

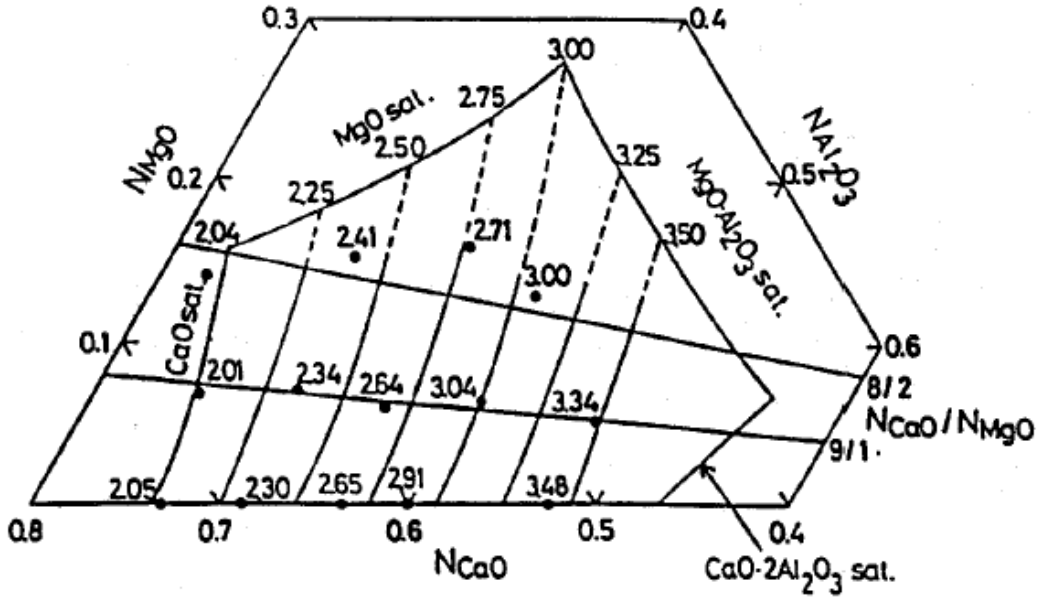

Figure 2.4 Iso-sulfide capacity curves for CaO-Al_2O_3-MgO slags at 1600 ^oC. Numerical values show - log C_S [24].

Sulfide capacities are usually expressed in log units, for example: log C_S = -3.2. The less negative the logarithmic unit (larger the actual number), the better the sulfur removing capacity of the slag, i.e., a slag with log C_S = -1 has a better sulfur removing capacity than a slag with a log C_S = -3 [24].

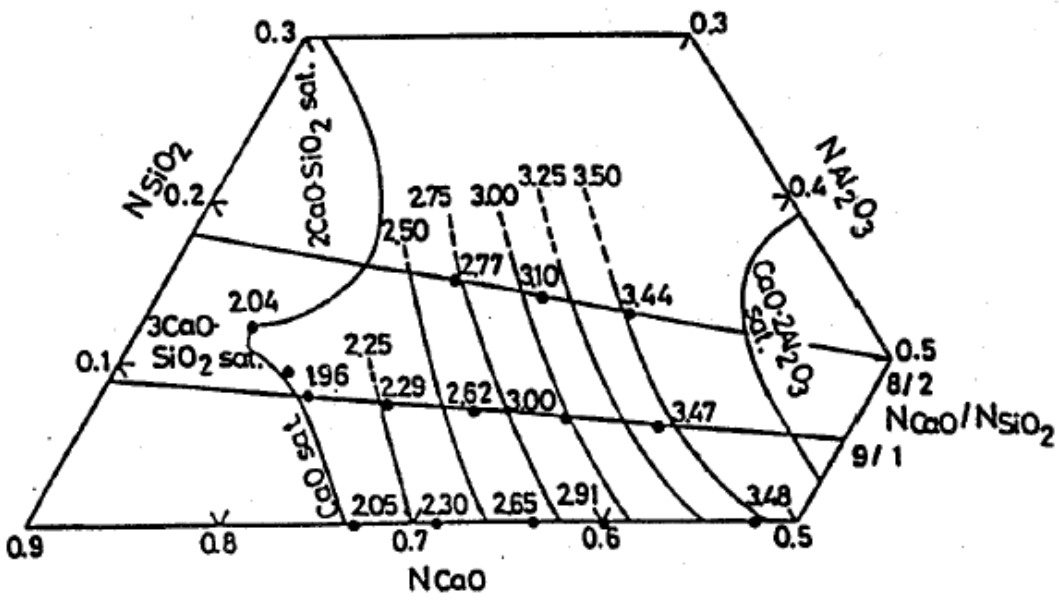

Figure 2.5 Iso-sulfide capacity curves for $CaO\text{-}Al_2O_3\text{-}SiO_2$ slags at 1600 ^oC. Numerical values show - log C_S [24].

2.5 Slag Models

Almost in the middle of twentieth century, some chemical solution models for slags were generated. According to researches conducted for silicate melts, Toop and Samis expressed the equilibrium conditions for the reaction [25].

$$2O^- \Leftrightarrow O^0 + O^{2-} \qquad (11)$$

Silicate slags consist of 3-dimensional (3-D) interconnected networks of SiO_4^{4-} tetrahedra in which silicons are joined by bonding oxygen atoms (O^0). The gradual addition of cations (e.g. Na^+, Ca^{2+}) results in the progressive breaking of these oxygen bonds with the formation of non-bridging oxygens (NBO), denoted O^- and eventually the formation of free oxygen, O^{2-}, ions [26].

Equilibrium constant of reaction (11) is given below:

$$K = \frac{(O^0)\cdot(O^{2-})}{(O^-)^2} \tag{12}$$

where the components in parentheses represent the equilibrium number of each. It was proposed that this equilibrium constant K be dependent only on the temperature and be characteristics of the cations present in the melts.

From charge balance calculations,

$$2(O^0) + (O^-) = 4N_{SiO_2} = \text{total number of silicon bonds} \tag{13}$$

Rearranging yields;

$$(O^0) = \frac{4N_{SiO_2} - (O^-)}{2} \tag{14}$$

Toop and Samis suggested the free energy of mixing MO (metal oxide) and SiO_2 is given by:

$$\Delta G^M = -\frac{(O^-)}{2}\Delta G^o \tag{15}$$

where $(O^-)/2$ is the actual number of moles of oxygen ions reacted, and ΔG^o is the standard free energy of for reaction (11) [25].

Melt species activities are computed on the basis of Temkin fused salt notation, given as:

$$a_{MO} = \left[M^{v+}\right]\left[O^{2-}\right] = \frac{(M^{v+})}{\sum cations} \times \frac{(O^{2-})}{\sum anions} \tag{16}$$

According to relation (16), the thermodynamic activity of the molten oxide is the activity product of ionic fractions over cationic and anionic matrices. Terms in brackets denote activities and terms in parentheses number of moles [27].

According to the polymeric anion model proposed by Masson et.al. [28], it is considered that liquid silicates may be treated as condensation polymers derived from the "monomer" SiO_4^{4-}.The distribution of anions in such a system may be considered in terms of the equilibrium between the ion SiO_4^{4-} and any species of chain length n to yield the next higher member and a free oxygen ion:

$$SiO_4^{4-} + Si_nO_{3n+1}^{2(n+1)-} \Leftrightarrow Si_{n+1}O_{3n+4}^{2(n+2)-} + O^{2-} \quad (17)$$

The equilibrium constants derived by Masson and co-workers [28] are given as follows:

$$k_{1n} = k_{11} \cdot \frac{(3n+1)\cdot(3n+2)}{2\cdot(2n+3)\cdot(n+1)} \quad (18)$$

The equilibrium constants are designated as k_{1n}, where 1 shows the number of Si atoms in the first complex of the above reaction, and n is the number of Si atoms in the second complex.

As seen from the relations, knowledge of only one k value (e.g. k_{11} for the simplest.) enables one to calculate equilibrium constant for any other reaction. According to the polymeric anion model [28], the activity of the basic oxide can be calculated using Temkin equation given in relation (16).

Later on, the models for simple slag systems were tried to be extended for complex metallurgical slags. In the previous decades, there were some studies [29-31]

conducted to enlighten the thermochemical behavior of multicomponent slag systems. In relation to steelmaking process, these were important especially to evaluate the sulfide capacities and to estimate oxide activities of different types of slags. Some of the slag models obtained with these studies will be summarized in the following sections.

2.5.1 Optical Basicity Model

In an effort to perform acid-base characterization of solids, especially glassy materials, Duffy and Ingram [29] introduced optical basicity concept in seventies. Optical basicity, denoted as Λ, expresses the basicity of a glass (or other oxidic medium) in terms of the electron density carried by the oxygens; i.e. their ability to donate negative charge. Originally, optical basicity was obtained from spectroscopic shifts (in the ultra-violet region) of ions such as Tl^{+} and Pb^{2+} dissolved as probes for sensing the electron donor power of the oxygens. The accumulation of optical basicity data revealed, in time, that it was possible to calculate Λ for an oxidic system from its composition. For example, optical basicity of $CaO\text{-}P_2O_5$ glass system (1:1 mole ratio) can be calculated as follows:

The Ca^{2+} ion neutralizes one-sixth of the oxygen atoms (in the formal oxidation state of -2) and the P^{5+} ion neutralizes five-sixths. It was also argued that the polarizing power of phosphorus was greater than that of calcium, and that a parameter could be introduced to express this difference (termed the 'basicity moderating parameter', γ, defined in the following paragraphs). Therefore, for the mentioned glass, it made sense to express the experimental value of optical basicity [32] as:

$$\Lambda = \left(\frac{1}{6\gamma_{Ca}} + \frac{5}{6\gamma_{P}} \right) \tag{19}$$

The expression given by Duffy for the optical basicity is as follows:

$$\Lambda = \frac{X_A^{a+}}{\gamma_A} + \frac{X_B^{b+}}{\gamma_B} + ..., \quad (20)$$

where X_A^{a+}, X_B^{b+},… are the equivalent fractions of A^{a+}, B^{b+} … and γ_A, γ_B … are the corresponding basicity moderating parameters [33]. Since for single oxides $1/\gamma = \Lambda$, relation (20) can also be expressed as below:

$$\Lambda = X_A\Lambda_A + X_B\Lambda_B + ... \quad (21)$$

By use of relation (21) it is possible to calculate the bulk or average value of Λ for a slag of any composition involving these oxides. X is the equivalent cation fraction, based on the fraction of negative charge "neutralized" by the charge on the cation concerned. The most convenient representation of cation fraction is:

X = [mole fraction of component x number of oxygen atoms in oxide molecule] / [Σ mole fraction of component x number of oxygen atoms in oxide molecule] (22)

Thus in a CaO-Al_2O_3-SiO_2 melt, for example:

$$X_{CaO} = \frac{N_{CaO}}{N_{CaO} + 3N_{Al_2O_3} + 2N_{SiO_2}} \quad (23)$$

$$X_{Al_2O_3} = \frac{3N_{Al_2O_3}}{N_{CaO} + 3N_{Al_2O_3} + 2N_{SiO_2}} \quad (24)$$

$$X_{SiO_2} = \frac{2N_{SiO_2}}{N_{CaO} + 3N_{Al_2O_3} + 2N_{SiO_2}} \quad (25)$$

where N in each case is the mole fraction of the component involved [34].

Basicity moderating parameter, γ, represents the tendency of an oxide-forming cation to reduce the donor properties (i.e. the basicity) of oxide ions within the field. The larger the value of γ, the more the electron charge clouds of the oxygen atoms would be contracted, thereby reducing their basicity.

$$\gamma_M = \frac{Z_M \cdot r_M}{|Z_O| \cdot \Lambda_{MO}} \tag{26}$$

where Z_M is the oxidation number of cation M in MO, r_M is the stoichiometric ratio between the number of cations M and the number of oxide ions, and $|Z_O|$ represents the oxidation number of the oxide ion in MO [27].

Probe ion spectroscopy was found to provide optical basicity values for few oxides because UV transparency is impaired. It does not permit obtaining theoretical Λ for transition metal oxides. After making a large number of measurements, mainly using Pb^{2+} as the probe ion, it was discovered that optical basicity of an oxide is related to the Pauling electronegativity, χ. Optical basicity is inversely proportional to Pauling electronegativity. Optical basicity and electronic polarizability ($\alpha_{O_2^-}$) of the oxide species were also well connected. It was found that ($\alpha_{O_2^-}$) increases with the increasing basicity of the medium [33].

Average electronegativity parameter, χ_{av}, was defined as below:

$$\chi_{av} = \frac{\sum_{i=1}^{N} \chi_i \cdot n_i}{\sum_{i=1}^{N} n_i} \tag{27}$$

where χ_i is the Pauling electronegativity and n_i the number of atoms of the *i*th element. N is the number of elements present in the compound. Using Duffy's

analysis and their modifications, Reddy et.al. [33] derived empirical relations for the optical basicity (Λ) and electronic polarizability ($\alpha_{O_2^-}$):

$$\Lambda = \frac{0.75}{\chi_{av} - 1.35} \tag{28}$$

$$\gamma = \frac{\chi_{av} - 1.35}{0.75} \tag{29}$$

and

$$\alpha_{O_2^-} = \frac{\chi_{av} - 1.35}{\chi_{av} - 1.80} \tag{30}$$

Sosinsky and Sommerville [34] studied the composition dependence of sulfide capacity by using optical basicity concept and derived an empirical expression between the optical basicity, the temperature and the sulfide capacity of an oxide slag at temperatures between 1400 and 1700 ^{o}C as follows:

$$\log C_S = \left(\frac{22690 - 54640 \cdot \Lambda}{T} \right) + 43.6 \cdot \Lambda - 25.2 \tag{31}$$

where T is the temperature and Λ is the optical basicity for the multicomponent slag. Young et.al. [35] modified this expression incorporating further slag-metal data with regression analysis as given in relation (32) and (33). These equations were found to be superior to the previous formula, but squared optical basicity terms were needed to be used.

$\Lambda < 0.8$:

$$\log C_S = -13.913 + 42.84 \cdot \Lambda - 23.82 \cdot \Lambda^2 - \left(\frac{11710}{T} \right) - 0.02223 \cdot (\%SiO_2) - 0.02275 \cdot (\%Al_2O_3) \tag{32}$$

$\Lambda \geq 0.8$:

$$C_S = -0.6261 + 0.4808 \cdot \Lambda + 0.7197 \cdot \Lambda^2 + (1697/T) - (2587 \cdot \Lambda / T) + 0.0005144 \cdot (\%FeO) \qquad (33)$$

2.5.2 IRSID Slag Model

The optimization of high temperature reactions taking place in steelmaking systems necessitates a precise evaluation of thermodynamic relationships. For oxide systems, thermodynamic information concerns slag phase diagrams and component activities in multicomponent systems. Use of this information is possible with thermodynamic models. The 'cell model', also called as IRSID slag model developed by Gaye and co-workers [30,36] is one of these models.

The statistical thermodynamics 'cell model' is based on an idea originally proposed by Kapoor and Frohberg [37] for describing binary and ternary liquid oxide systems. Gaye et.al. extended it further to represent systems containing a large number of components. The model calculates both slag component activities and a phase diagram [38].

For a liquid mixture of an arbitrary number of oxides, presence of two overlapping sublattices is considered. One sublattice is filled with oxygen anions, and the other one with the various cations. The structure is then described in terms of cells consisting of one oxygen anion surrounded by two cations and as noted (i-A-j) [30]. S^{2-} and $(2F)^{2-}$ anions were then incorporated in the model. The cationic sub-lattice is filled with the different cations in decreasing order of their charge.

For oxide systems, usually two types of parameters are sufficiently used to evaluate the energy of the system :

1. The energies for the formation of asymmetric cells from the corresponding symmetrical ones. For a mixture of oxides only, these energies are noted W_{ij}^{O} and correspond to the reaction:

½(i-O-i) + ½(j-O-j)→(i-O-j) (34)

2. The interaction energies between cells, corresponding to one parameter per couple of cations. For a mixture of oxides only, these parameters are noted E_{ij}^{O} and represent the interaction between a symmetrical cell (i-O-i) and an asymmetric one (i-O-j) [36].

The general rule is that the same number of anions must be provided from both cations in the constituent with two different cations. The mole fraction of the "component oxides", i.e. the cells with only one type of cation, are for n cations:

$$x_i = \frac{y_i + \sum_{j \neq i}^{n} v_j y_{ij}}{Q} \tag{35}$$

$$Q = \sum_{i=1}^{n} (y_i + \sum_{j \neq i}^{n} v_j y_{ij}) \tag{36}$$

where v_j is oxygen stoichiometry of the oxygen in the component oxide of the cation M, M_{u_i}, O_{v_i} [39]. As an example, for CaO-SiO_2 system, three parameters are needed to ensure an accurate description over the entire composition range [40]. The constituents are (CaO, SiO_2, $(CaO)_2$ SiO_2) and the quantities are as follows [39]:

$$x_{CaO} = \frac{y_{CaO} + 2y_{Ca_2SiO_4}}{Q} \tag{37}$$

$$x_{SiO_2} = \frac{y_{SiO_2} + y_{Ca_2SiO_4}}{Q} \tag{38}$$

$$Q = y_{CaO} + y_{SiO_2} + 3y_{Ca_2SiO_4} \tag{39}$$

Once the free energy and component activities are computed for the metastable liquid, confrontation with the stabilities of compounds (or in some instances solid solutions of compounds) allow the calculation of the phase diagram.

It was found that the IRSID model describes very satisfactorily the most important slag systems [40]. As an example, Figure 2.6 shows a comparison of the computed and experimental phase diagrams and silica activity in the $CaO\text{-}SiO_2\text{-}Al_2O_3$ system at 1550 ^oC. The agreement for composition regions representative of blast furnace slags, ladle metallurgy slags, and most actual inclusion precipitation regions are quite satisfactory. The only serious discrepancy concerns the silica-rich side of the binary $SiO_2\text{-}Al_2O_3$ system. In this respect, Gaye and co-workers indicated the necessity of a slight change of the model in order to reflect the amphoteric nature of alumina [38].

Together with the further extensions, the slag model can be used for calculations in the system $SiO_2\text{-}TiO_2\text{-}Ti_2O_3\text{-}Cr_2O_3\text{-}Al_2O_3\text{-}Fe_2O_3\text{-}CrO\text{-}FeO\text{-}MgO\text{-}MnO\text{-}CaO\text{-}CaF_2\text{-}S$ [36].

The multiphase equilibrium calculation code, Chemical Equilibrium Calculation for the Steel Industry (CEQCSI) was developed at IRSID for very specific applications related to steelmaking: Calculation of slag crystallization path, calculation of slag-metal equilibrium in order to determine the transfer from the slag to the metal of trace elements, calculation of inclusions precipitation to determine, from the overall steel analysis, the amount, composition and origin of endogeneous inclusions and precipitates [36]. As an example, using the CEQCSI code, Gaye et.al investigated the kinetics of precipitation of non-metallic inclusions during solidification of steel. In their work, the authors made a model based on both classical nucleation and mixed controlled growth, to analyze the precipitation of TiN as the steel solidification proceeds, as well as final size of precipitates for low sulfur concentration. The authors experimentally showed that growth of TiN

precipitates is controlled by diffusion and interfacial reaction [41]. Thereafter, they extended their model to the precipitation of multicomponent liquid oxides [42].

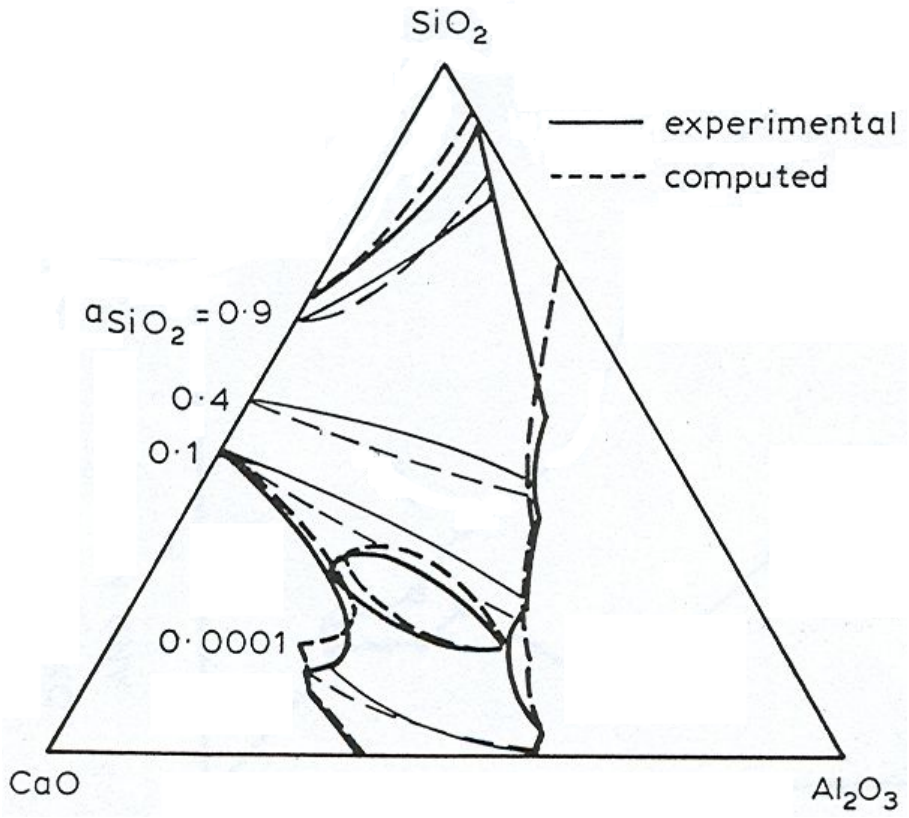

Figure 2.6 Computed and experimental phase diagram and silica activity in CaO-SiO_2-Al_2O_3 system at 1550 ^oC (reproduced from Gaye, H., Riboud, P.V., and Welfringer, J.) [38]

2.5.3 KTH Slag Model

In an effort to obtain a reliable description of sulfide capacities in the multicomponent system, Al_2O_3-CaO-Cr_2O_3-FeO-Fe_2O_3-MgO-MnO-SiO_2, a model was developed at the Royal Institute of Technology, KTH (Kungliga Tekniska Högskolan), Sweden [31]. The main goal of the model development was to be able to predict the sulfide capacities of slags containing more than three components using solely the information from the corresponding lower order systems.

The expression of sulfide capacity is represented with the following relationships using Richardson and Fincham's definition [22]:

$$K_1 = \exp(-\frac{\Delta G^O}{R \cdot T}) \tag{40}$$

and

$$\frac{a_{O^{2-}}}{f_{S^{2-}}} = \exp\left(-\frac{\xi}{R \cdot T}\right) \tag{41}$$

where

$$\xi = \sum (X_i \cdot \xi_i) + \xi_{mix} \tag{42}$$

where ΔG^O is the Gibbs free energy of reaction (8) and R is the gas constant. In relation (42), *i* represents component *i* and X_i is the molar fraction of component *i* in the multicomponent system. The term ξ_i is expressed as a linear function of temperature for each component in the slag in the absence of interaction between different species. ξ_{mix} stands for the mutual interactions (binary and ternary) between different species in the slag. ξ_{mix} is dependent on slag composition and temperature [23]. In other words, ξ_{mix} term is described in terms of polynomials in both temperature and composition. In order to make reliable predictions, the relevant binary and ternary interaction parameters need to be optimized using well determined sulfide capacity data in the corresponding binary and ternary systems. In order to meet such requirements, a series of experimental studies were carried out. The optimized model parameters related to unary, binary and ternary interactions were listed in the work of Nzotta et.al. [31]. Composition dependence is indicated with cation fraction, y_i, representing the cation fraction of cation i, defined as the number of the cations of i over the total number of the cations:

$$y_i = \frac{N_i}{\sum_{j=1}^{n} N_j} \tag{43}$$

As an example, using a modified Temkin approach, ternary interaction parameter of Al_2O_3-CaO-SiO_2 is calculated using the following relation:

$$\xi_{\text{int}eraction}^{Al_2O_3-CaO-SiO_2} = y_{Al^{3+}} \cdot y_{Ca^{2+}} \cdot y_{Si^{4+}} \cdot [-2.03579264 \cdot 10^6 + 6.86044695 \cdot 10^2 \cdot T] \tag{44}$$

Using relation (42), the expression of ξ for the Al_2O_3-CaO-MgO-MnO-SiO_2 slag is presented in the following page [31].

Nzotta et.al. [31] studied some multicomponent systems to obtain their sulphide capacities using gas-slag equilibration technique. The reliability of the model obtained by the same authors in a previous work was also examined. The mentioned model predicted the sulphide capacities of multicomponent systems using the information of lower order systems. Comparison of the model predictions with the experimental results revealed that the sulfide capacity model developed in their laboratory could be successfully used in predicting the sulphide capacities of some multicomponent slags. Considering interactions between the different species, an expression was also proposed for the prediction of sulphide capacities of the slags in the Al_2O_3-CaO-MgO-MnO-SiO_2 system. Nzotta et.al. [43] also worked on sulfide capacities of iron-oxide containing slags. Sulfide capacities of some types of iron-oxide containing slags were experimentally determined again using gas-slag equilibration technique. The experimental data were used to predict sulfide capacities of the FeO-Al_2O_3-CaO-MgO-MnO-SiO_2 six component system. The results of their previously mentioned model was found to agree well with the experimental data. The model was also employed to predict to sulfide capacities of some typical BOF, EAF and LF slags.

$$\xi = X_{Al_2O_3}\xi_{Al_2O_3} + X_{CaO}\xi_{CaO} + X_{MgO}\xi_{MgO} + X_{MnO}\xi_{MnO} + X_{SiO_2}\xi_{SiO_2} + \xi_{\text{int}eraction}^{Al_2O_3-CaO} + \xi_{\text{int}eraction}^{Al_2O_3-SiO_2} + \xi_{\text{int}eraction}^{Al_2O_3-MnO} + \xi_{\text{int}eraction}^{CaO-SiO_2} + \xi_{\text{int}eraction}^{MgO-SiO_2} + \xi_{\text{int}eraction}^{MnO-SiO_2}$$
$$+ \xi_{\text{int}eraction}^{Al_2O_3-CaO-MgO} + \xi_{\text{int}eraction}^{Al_2O_3-CaO-SiO_2} + \xi_{\text{int}eraction}^{Al_2O_3-MgO-SiO_2} + \xi_{\text{int}eraction}^{Al_2O_3-MgO-MnO} + \xi_{\text{int}eraction}^{Al_2O_3-MnO-SiO_2} + \xi_{\text{int}eraction}^{CaO-MgO-SiO_2} + \xi_{\text{int}eraction}^{CaO-MnO-SiO_2} + \xi_{\text{int}eraction}^{MgO-MnO-SiO_2}$$

(45)

Hao et.al. [44] presented some results of the experiments conducted in Capital Steel. In their work, slag samples were taken at the ladle furnace and sulfide distribution ratios (L_S) were examined according to KTH model and optical basicity model. During plant trials, slag sampling was made in four heats. Four slag samples were taken for each heat at certain stages of ladle refining. It was found that calculated L_S values were much bigger than the measured ones before ladle furnace treatment. This was attributed to the fact that slag and steel were not in equilibrium before ladle metallurgy stage. During secondary metallurgy period L_S was found to increase showing tendency to reach slag-metal equilibrium. The results obtained with KTH model were reported to agree well with the measured ones, whereas optical basicity model predicted much higher L_S values since it did not consider the mutual interactions between the different components in the slag.

Wang et.al. [45] studied sulfide capacities of typical COREX slags of which there was no sufficient knowledge in the literature. Using gas-slag equilibrium technique and sulfide capacity definition obtained by Richardson and Fincham [22], it was shown that at a fixed Fe_tO and Al_2O_3 contents and a fixed $(CaO+MgO)/SiO_2$ ratio, C_S value was found to decrease while MgO content increased. It was also reported that at a constant (CaO/SiO_2) ratio and MgO and Al_2O_3 contents, C_S value increased together with the increase in Fe_tO amount. Increasing slag basicity, denoted as CaO/SiO_2, at a constant MgO, Fe_tO and Al_2O_3 contents led to a significant increase in sulfide capacity.

Ban-ya et.al. [46] studied sulfide capacity and the solubility of CaS in the $CaO-Al_2O_3$ and $CaO-Al_2O_3-CaF_2$ slag systems. From the molecular theory, the desulfurization reaction was written as:

$$1/2\,S_2(g)+(CaO)=1/2\,O_2(g)+(CaS) \qquad (46)$$

The molar sulfide capacity was formulated as below:

$$C'_S = N_{CaS} \cdot (P_{O_2} / P_{S_2})^{1/2} \quad (47)$$

It was found that the molar sulfide capacity, C'_S, increased as CaO and CaF_2 contents and temperature increased. It was also reported that the solubility of CaS in the above mentioned slags increased with the increase in CaO and CaF_2 components. The temperature dependence of CaS solubility on the other hand could not be enligtened clearly [46].

2.6 Sulfur Slag-Metal Distribution Ratio (L_S)

Desulfurization reaction in the ionic form can be written as [47]

$$\underline{S}(\%) + (O^{2-}) = (S^{2-}) + \underline{O}(\%) \quad (48)$$

The equilibrium constant is given by

$$K_{46} = \frac{(a_{S^{2-}}) \cdot a_{\underline{O}}}{(a_{O^{2-}}) \cdot a_{\underline{S}}} \quad \text{where} \quad a_{S^{2-}} = \gamma_{S^{2-}} \cdot (\%S) \quad \text{and} \quad a_{\underline{S}} = f_S \cdot \%\underline{S} \quad (49)$$

$$L_S = \frac{(\%S)}{\%\underline{S}} = K \cdot \frac{a_{O^{2-}}}{\gamma_{S^{2-}}} \cdot f_S \cdot \frac{1}{a_{\underline{O}}} \quad (50)$$

The left-hand side of the relation (50) was defined as the sulfur slag-metal distribution ratio, or sulfur partition ratio in some literature. From the above equation it can be concluded that there are 4 factors affecting on sulfur slag-metal distribution ratio [17]:

- Metal composition
- Slag composition

- Oxygen potential of the system
- Temperature

Metal Composition

Sulfur slag-metal distribution ratio increases as the activity coefficient of sulfur in metal increases. Elements like B, C and Si were found to increase the activity coefficient of sulfur in the metal. Simple calculations show that activity coefficient of sulfur in blast furnace metal is 4 times greater than activity coefficient of sulfur in converter metal [19,17].

Slag Composition

Sulfur slag-metal distribution ratio increases as slag basicity (in turn, sulfide capacity) rises. The relation between sulfur partition ratio and sulfide capacity can be obtained by combining the reactions (8) and (48) as follows [23]:

$$\underline{S}(\%)+\frac{1}{2}O_2(g)=\underline{O}(\%)+\frac{1}{2}S_2(g) \tag{51}$$

The equilibrium constant of relation (51) is given in literature as:

$$\log K_{51}=-\frac{935}{T}+1.375 \tag{52}$$

Using sulfide capacity definition given in (10), K_{51}, can be written as:

$$K_{51}=\frac{a_{\underline{O}}}{a_{\underline{S}}}\cdot\sqrt{\frac{P_{S_2}}{P_{O_2}}}=\frac{(\%S)}{\%\underline{S}}\cdot\frac{a_{\underline{O}}}{f_S\cdot C_S} \tag{53}$$

By combining (10), (52) and (53), the following expression for the equilibrium sulfur slag-metal distribution ratio, L_S, is obtained [23]:

$$\log L_S = \log \frac{(\%S)}{\%\underline{S}} = -\frac{935}{T} + 1.375 + \log C_S + \log f_S - \log a_{\underline{O}} \qquad (54)$$

Oxygen Potential of System

Oxygen potential of the system can be expressed either by oxygen activity of the metal or by FeO activity of the slag [47]. Removal of sulfur from the metal enhances when $a_{\underline{O}}$ is small (i.e. reducing conditions). When $a_{\underline{O}}$ values of converter and blast furnace are calculated, it is found that oxygen potential of converter is 100 times greater than the one in blast furnace [17].

Temperature

According to the studies conducted, no significant effect of temperature on sulfur slag-metal distribution ratio was found in the systems as long as metal and slag compositions remained constant [17].

Sulfur partition ratio for different Al contents for $CaO\text{-}Al_2O_3$ type slags is shown in Figure 2.7. Sulfur distribution ratio for $CaO\text{-}Al_2O_3\text{-}SiO_2$ slags at 1600 ^oC is illustrated in Figure 2.8 for steel containing 0.03%Al.

In the literature it was reported that increase in slag basicity was found to increase the sulfur slag-metal distribution ratio [23]. However, all basic oxides do not show the same effect considering their power of sulfur removal. Ward [7] calculated desulfurization ability of the following oxides when that of CaO is assumed as unity:

Oxides	Desulfurization ability
FeO	0.325
MnO	0.25
MgO	0.0075
Na_2O	1070

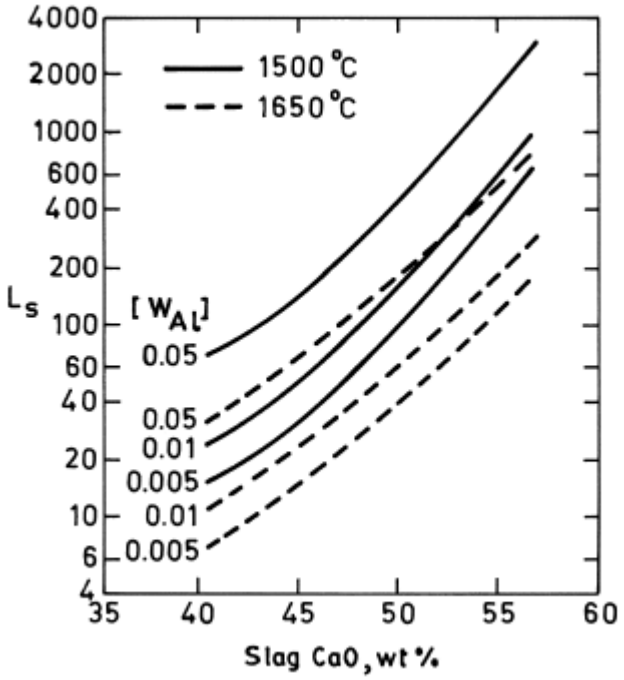

Figure 2.7 Equilibrium sulfur partition ratio between liquid iron with dissolved Al and CaO-Al_2O_3 slags [48]

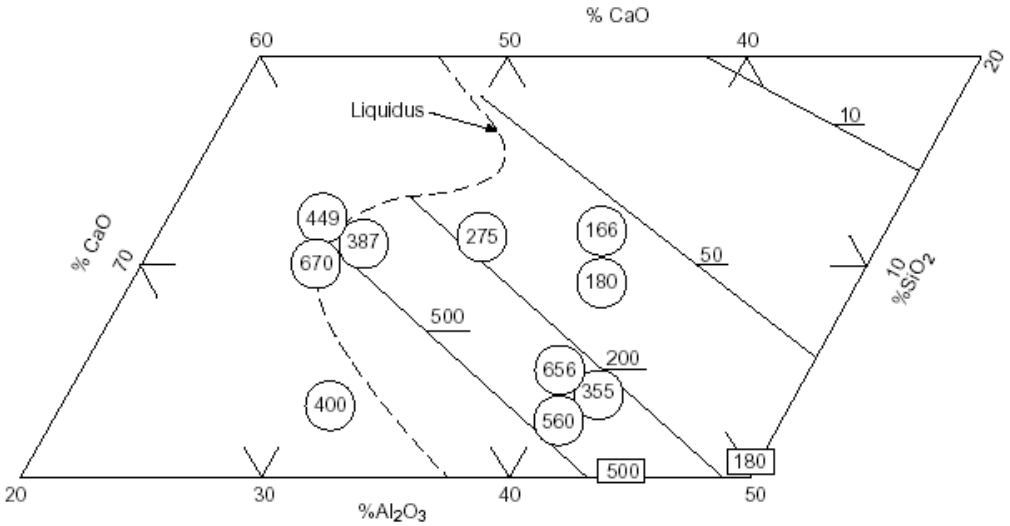

Figure 2.8 Sulfur distribution for CaO-Al_2O_3-SiO_2 slags at 1600 ^oC and steel containing 0.03% Al [49]

Desulfurization ability of Na_2O is much higher than the others. However, alkali oxides should not be present in the metals of blast furnace and converter since they are detrimental to the ironmaking and steelmaking operations for many respects [17]. Hot metal desulfurization behaviour of some Na_2O containing slag systems will be given in the following section.

One of the most important aspects that is frequently overlooked when evaluating and discussing slags, is that most slags consist of two fractions, i.e., a liquid fraction and a solid fraction. Slag fluidity in basic slags is controlled by the liquid and solid fractions of the slag. The higher the solid fraction of the slag - the lower the fluidity of the slag (higher viscosity). A basic slag that is completely liquid has maximum fluidity. In many calculations of sulfur removal, the total composition of the slag is sometimes mistakenly considered. It is the lime dissolved in the liquid fraction of the slag that is removing sulfur from the steel and not lime as determined by the chemical analysis of the "total" slag. The undissolved lime in the slag does not remove any sulfur [24].

A general recommendation is the total reducible oxides in ladle slags should be less than 2% (Reducible oxides: FeO and MnO). The effect of amount of reducible oxides in ladle slags on the desulfurizing efficiency is shown in Figure 2.9 [24].

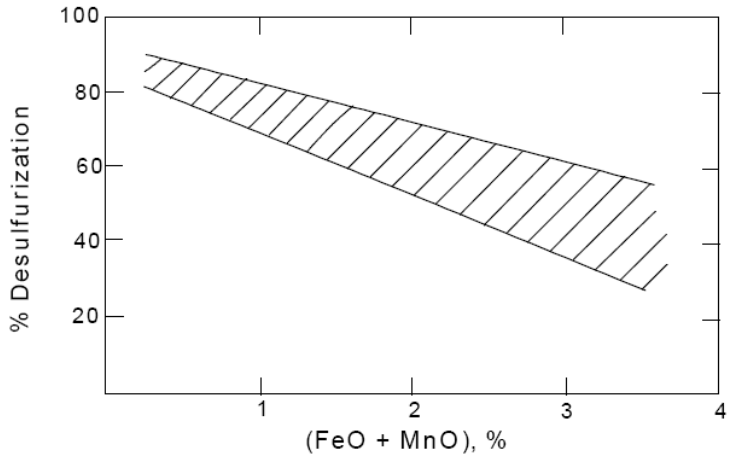

Figure 2.9 Effect of (FeO + MnO) in slag on desulfurization [24]

2.7 Hot Metal Desulfurization

In blast furnace, sulfur content of the metal can be reduced by increasing

- Slag volume
- Slag basicity
- Hearth temperature

Performing these operations on the other hand cause an increase in coke rate and a decrease in production rate [50]. Therefore, some alternative methods were generated in the past. These methods involve sulfur removal by sending materials having high sulfur affinity to the hot metal bath before steelmaking stage. These methods are suitable since the activity coefficient of sulfur in hot metal bath is sufficiently high and oxygen potential of the system is relatively low compared to steelmaking environment.

The materials used for desulfurization are calcium carbide, Mg and its alloys, Mg soaked materials, lime, sodium compounds and synthetic slag mixtures. The most important desulfurization materials are lime, calcium carbide, Mg (and its different forms) and Na_2CO_3 [17].

2.7.1 Lime (CaO)

Desulfurization reaction of CaO can be written as follows:

$$CaO(s) + S(\%) + C(s) = CaS(s) + CO(g) \tag{55}$$

The standard Gibbs free energy change of this reaction [51] is

$$\Delta G^{O}{}_{55} = 27500 - 27.16 \cdot T \ \ cal \tag{56}$$

Equilibrium constant of reaction (55) is

$$K_{55} = \frac{a_{CaS} \cdot P_{CO}}{a_{CaO} \cdot a_S \cdot a_C} \quad \text{where} \quad a_{\underline{S}} = f_S \cdot \%\underline{S} \quad \text{and} \quad a_{CaS} = a_{CaO} = a_C = 1 \quad (57)$$

$$\%\underline{S} = \frac{P_{CO}}{K_{55} \cdot f_S} \quad (58)$$

Taking P_{CO} as 1 atm and f_S as 5, %S values are calculated for 1500 ^oC, 1400 ^oC and 1300 ^oC and given as:

%S = 5.7 ppm 1500 ^oC,
%S = 9 ppm 1400 ^oC,
%S = 15.3 ppm 1300 ^oC.

For P_{CO}=0.1 atm,

%S = 0.57 ppm 1500 ^oC,
%S = 0.9 ppm 1400 ^oC,
%S = 1.53 ppm 1300 ^oC.

From these data, it can be inferred that desulfurization by CaO is enhanced by increasing temperature and/or decreasing CO partial pressure. Upon reaction of CaO with S, a layer of CaS formed around CaO particles causing a decrease in reaction rate. Therefore, the efficiency of desulfurization can be increased by use of CaO with particle size as small as possible (increase in reaction surface area) [52].

Use of $CaCO_3$ instead of CaO is another alternative. $CaCO_3$ decomposes into CaO (with very fine particle size) and CO_2(g), which combines with C and forms CO(g) (Taking advantage of gas mixing) [53].

Seshadri et.al. [54] postulated a kinetic model for hot metal desulfurization by injection of lime-based powders. In their work, it was stated that hot metal

desulfurization was governed by the contribution of three processes: Top-slag contribution through emulsification at the slag-metal interface, bubble-metal interface where entrapment of desulfurizer particles become important and behaviour of dispersed particles in the melt. Effects of some parameters acting on the transient and permanent reactions were examined. It was concluded that contribution of permanent reactor increased as the total gas flow rate, temperature, top-slag volume and slag-metal interface area increased. Considering the permanent reaction contribution, it was reported that the carry-over slag should be eliminated as far as possible since it decreases the activity of the desulfurizer and increases the oxygen activity. It was also emphasised that the transient reactor contribution could be improved by optimizing depth of injection, powder flow rate, particle size and solid/gas ratio.

Chushao et.al. [55] studied desulfurization kinetics of hot metal containing vanadium. The effect of transitory and permanent-contact reaction on desulfurization rate was investigated using CaO-CaF_2 powder injection. Through rate constant calculation for permanent contact reaction, it was found that the rate constant increased remarkably with increasing CaF_2 in CaO flux in the range of 0-10%. It was reported as further increase in CaF_2 was not effective to increase rate constant. It was also shown that both the permanent-contact reaction and the transitory-contact reaction affected sulfur removal rate significantly.

2.7.2 Calcium Carbide (CaC_2)

Sulfur removal by CaC_2 can be expressed by

$$CaC_2(s) + \underline{S}(\%) = CaS(s) + 2C(s) \quad (59)$$

The standard Gibbs free energy change of this reaction [21] is

$$\Delta G^{O}_{59} = -86560 + 26.47 \cdot T \ \ cal \quad (60)$$

Equilibrium constant of reaction (59) is

$$K_{59} = \frac{a_{CaS} \cdot a_C{}^2}{a_{CaC_2} \cdot a_S} \qquad \text{where } a_{\underline{S}} = f_S \cdot \%\underline{S} \quad \text{and} \quad a_{CaS} = a_{CaC_2} = a_C = 1 \quad (61)$$

$$\%\underline{S} = \frac{1}{K_{59} \cdot f_S} \quad (62)$$

Taking $f_S = 5$, %S values were calculated for 1500 ^oC, 1400 ^oC and 1300 ^oC. %S values are very small for the temperatures indicated. Therefore, it is theoretically possible to drop to very small sulfur concentrations. %S content of the steel decreases as the desulfurization temperature decreases (opposite to CaO). Efficiency of desulfurization was found to increase as the initial sulfur concentration increased [56].

Zou et.al. [57] examined the kinetics of co-injection of calcium carbide and magnesium. Considering the desulfurization rate they concentrated on the three basic parameters: First, the penetration ratio (PR) of injected powder into the melt. Second, the residence time distribution (RTD) of the injected powder in the bath. Third, the homogeneous mixing time (HMT) of the bath. Small variations were observed in the concentrations of magnesium and sulfur in the metal after powder injection indicating that the equilibrium was attained almost completely during powder injection. Having larger particle sizes than MgS precipitates, CaC_2 was reported to serve as nucleation core of inclusions and therefore enhancing the desulfurization efficiency of magnesium. The rate of desulfurization corresponding to both materials was found to be different: At the beginning of injection, the desulfurization rate of CaC_2 was larger than that of Mg. After the first couple of minutes just the opposite holded and the desulfurization rate of Mg dominated. It was therefore adviced to optimize the powder injection by using only CaC_2 at the beginning, then the mixture of CaC_2 and Mg.

Coudure and Irons [58] studied the effect of calcium carbide particle size distribution on the kinetics of hot metal desulfurization. The authors examined the particle size-reaction rate relationship to obtain optimum particle size to guide both steelmakers and reagent producers. It was found that the desulfurization reaction was a first-order, diffusion controlled type. Laboratory scale experiments showed that at the very beginning of desulfurization process, an incubation period of 20 to 40 sec. was observed while no change in sulfur content took place. This incubation period was attributed to the fact that there was no top-slag in those experiments so the desulfurization products were found to revert the melt at the beginning. Being non-wetted by liquid iron, only 20-40% of the calcium carbide particles were found to be in contact with the melt, the remaining particles were on the carrier gas bubbles interfaces. The rate constant of desulfurization process was reported to increase as the particle diameter decreased. On the other hand, it was encountered that the reaction rate did not improve as expected while particle size decreased. As the particle diameter became smaller, the particle-liquid contact was reported to be hindered more. Moreover, related to the flowability of powders, tendency towards agglomeration was observed with the finer particles.

2.7.3 Magnesium (Mg)

Magnesium reacts with S according to the reaction below:

$$Mg(g) + \underline{S}(\%) = MgS(s) \tag{63}$$

The standard Gibbs free energy change of this reaction [21] is

$$\Delta G^{O}{}_{63} = -102830 + 43.48 \cdot T \ \ cal \tag{64}$$

Equilibrium constant of reaction (63) is

$$K_{63} = \frac{a_{MgS}}{P_{Mg} \cdot a_S} \qquad \text{where } a_{\underline{S}} = f_S \cdot \%\underline{S} \quad \text{and} \quad a_{MgS} = 1, P_{Mg} = 1 \text{ atm.} \tag{65}$$

$$\%\underline{S} = \frac{1}{K_{63} \cdot f_S} \tag{66}$$

Taking $f_S = 5$, %S values were calculated for 1500 ^{o}C, 1400 ^{o}C and 1300 ^{o}C. Theoretical %S values are very small for the temperatures indicated. %S content of the steel decreases as the desulfurization temperature decreases.

Magnesium boils at 1107 ^{o}C; the way of addition of magnesium to the liquid metal gains much importance [59]. There have been several methods generated so far [60]:

- Addition of magnesium in its alloy form
- Soaking (Magnesium soaked coke, magnesium soaked steel chips)
- Controlled blowing together with a carrier gas (With this method, efficiency of magnesium changes between 60% and 80%) [59]
- Blowing vaporized magnesium to the liquid iron
- Addition of magnesium to the ladle having closed top.

Magnesium soaked coke is placed into a graphite bell which is situated in the liquid hot metal to increase the reaction rate and to provide effective use of desulfurization material [61]. In that system, removal of sulfur by magnesium enhances at low temperatures. The efficiency of hot metal desulfurization with magnesium soaked coke was reported to increase when gas mixing was provided after completion of rapid vaporization of magnesium [62].

Jin et.al. [63] proposed a kinetic model for powder injection desulfurization. In their work, desulfurization kinetics of CaO-based flux and Mg-based flux were compared. It was found that the desulfurization rate obtained by using Mg-based flux was much larger than the one obtained by using CaO-based flux. In this respect, CaO-CaF_2 flux was also compared with calcium aluminate flux. The

desulfurization rates of the former and the latter were reported to be almost the same. On the other hand, $CaO\text{-}CaF_2$ fluxes are hazardous to environment therefore efforts were made to replace them with calcium aluminate type fluxes which is obtained from the waste of the aluminum industry. The kinetic model proposed by the authors [63] was composed of two reactions: First, the transitory-contact reaction with the ascending powder. Second, the permanent-contact reaction with top slag. The proposed overall rate of the process was the sum of the two reactions. The role of transitory-contact reaction was found to be more pronounced than the permanent contact reaction. The effect of the size of desulfurizer was also studied. It was found that the rate of desulfurization increased while powder size decreased to certain extent.

2.7.4 Sodium Carbonate (Na_2CO_3)

The difference of sodium carbonate from the other desulfurization materials is its ability to lower silicon and phosphorus content of liquid iron. There are two mechanisms offered for desulfurization of liquid metal by sodium carbonate [17]:

1. Sulfur removal reaction was proposed as

$$2Na(g) + \underline{S}(\%) = Na_2S(l) \tag{67}$$

The standard Gibbs free energy change of this reaction [7] is

$$\Delta G^{O}{}_{67} = -118000 + 63.8 \cdot T \ \ cal \tag{68}$$

Equilibrium constant of reaction (67) is

$$K_{67} = \frac{a_{Na_2S}}{P_{Na}{}^{2} \cdot a_S} \qquad \text{where} \ \ a_{\underline{S}} = f_S \cdot \%\underline{S} \ \ \text{and} \qquad a_{Na_2S} = 1, P_{Na} = 1\,\text{atm.} \tag{69}$$

$$\%\underline{S} = \frac{1}{K_{67} \cdot f_S} \tag{70}$$

Taking $f_S = 5$, %S values were calculated for 1500 ^oC, 1400 ^oC and 1300 ^oC. It was found that theoretical values are not so small. In reality, it was reported that it was hardly possible to lower sulfur content of liquid iron below 0.01% [64].

2. While small-size liquid Na_2O-SiO_2 slag particles rise up in iron melt, the sulfur removal takes places according to the reaction given below:

$$\underline{S}(\%) + (O^{2-}) = (S^{2-}) + \underline{O}(\%) \tag{48}$$

It was found that the higher the amount of Na_2O in Na_2O-SiO_2 slags formed, the higher the sulfide capacity of these slags. It was expected result since sulfide capacity increases with increasing slag basicity and Na_2O is a basic oxide [64]. Slag basicity can be increased by addition of CaO and/or MgO [52].

Second mechanism described over here is more pronounced in literature due to small particle size (i.e. larger surface area) slags with high sulfide capacity. It was reported that final content of sulfur in liquid iron decreases as slag volume and/or sulfide capacity increases [64].

Suito et al. [65] investigated simultaneous dephosphorization and desulfurization of carbon saturated iron by sodium carbonate-sodium sulfate flux. Similarly, Moriya and Fujii [66] analysed dephosphorization and desulfurization of molten pig iron by Na_2CO_3. In both studies, it was reported that the degree of desulfurization was found to increase with decreasing temperature.

Iwai et.al. [67] studied desulfurization and simultaneous desulfurization and dephosphorization of molten iron by Na_2O-SiO_2 and Na_2O-CaO-SiO_2 fluxes. Through the examination of Na_2O-SiO_2 type fluxes, the extent of desulfurization

was found to increase as the ratio of (%Na_2O/%SiO_2) increased. Presence of NaF in the flux led to an increase in degree of desulfurization while CaO additions caused the opposite. The authors also investigated the behaviour of Na_2O-CaO-SiO_2 type fluxes and showed that the decrease in the ratio of (%Na_2O/%CaO) with the addition of CaO gave rise to a considerable decrease in degree of desulfurization. The effect of silicon and carbon content of the hot metal was also studied. Increase in silicon content was reported to increase the extent of desulfurization slightly. On the other hand, increase in carbon concentration was found to decrease it. This behaviour was attributed to reduction of some Na_2O with carbon according to the following reaction:

$$(Na_2O) + \underline{C} = 2Na_{(g)} + CO_{(g)} \qquad (71)$$

Hernandez et.al. [68] analysed dephosphorization and desulfurization behaviour of hot metal with CaO-SiO_2-CaF_2-FeO-Na_2O slags. It was shown that these type of slags had low enough melting points and could easily absorb sulfur. The maximum desulfurization obtained was reported as 90-95% with a slag consisting of 6% FeO, 6% Na_2O, 20% CaF_2 and $CaO/SiO_2 = 4$.

Choi et.al. [69] investigated desulfurization kinetics of molten pig iron in slag systems of CaO-SiO_2-Al_2O_3-Na_2O. During desulfurization of hot metal with Na_2O containing systems, one of the main problem was indicated as the decrease in Na_2O of the slag with time due to evaporation. For such systems, it was found that desulfurization rate increased as Na_2O content of the slag, temperature and the slag basicity increased while Al_2O_3 content decreased. It was also reported that desulfurization was controlled either by the interfacial chemical reaction or slag phase mass transfer.

Van Niekerk and Dippenaar [70] investigated the slag-metal distribution ratio of sulfur between the carbon satutared iron and Na_2O-SiO_2, Na_2O-SiO_2-CaO and Na_2O-SiO_2-CaO-CaF_2 slag systems at 1350 ^oC. It was found that sulfide capacity of

both silicate and lime based slags increased significantly with the addition of Na_2O. Considering sulfur partition ratio, L_S, it was reported that 3.3% addition of CaO to the slag would yield the same increase in L_S as a 1% addition of Na_2O. Therefore, Na_2O-equivalent of CaO was determined to be 0.30. Slag-metal distribution ratio of sulfur were found to increase as (%CaO/%Na_2O) ratio decreased. It was also shown that sulfur partition ratio decreased as the amount of CaF_2 in these slags increased. Moreover, examination of flourspar containing soda-lime-silicate based slags revealed that CaF_2 did not enhance the extent of desulfurization of liquid iron. CaF_2 additions were found to decrease the sulfide capacity of the slags mentioned above. It was therefore suggested that only enough CaF_2 should be provided to the slag to ensure that they remain liquid.

Due to corrosive nature of Na_2O slags formed during desulfurization by Na_2CO_3, refractory wear in the process is tremendous. Gaseous reaction products lead to environmental problems. As the amount of Na_2O decreases by time, the possibility of sulfur going back to metal phase increases. Therefore, it is crucial to take desulfurization slag away from metal as quickly as possible [52].

2.8 Ladle Desulfurization

Production of ultra-low sulfur steel qualities includes addition of a material, which forms a stable sulfide so that sulfur can be removed from the metal. The elements that have high sulfur affinity are prone to react with oxygen. Therefore, these elements first combine with oxygen according to the reaction below:

$$MO(s) + \underline{S}(\%) = MS(s) + \underline{O}(\%) \qquad (72)$$

For the systems where rare-earth materials (e.g. Ce, La oxides) are used rare earth oxysulfides form instead of MS type sulfides.

Taking activities of MS and MO as unity, equilibrium constant of the above reaction can be approximated as:

$$K_{70} = \frac{\%\underline{O}}{\%\underline{S}} \tag{73}$$

During desulfurization with the above-mentioned elements and/or oxides of them, the final sulfur content of the metal depends on the steel oxygen content. Therefore, to increase the degree of desulfurization, deoxidation with strong deoxidizer is a must.

Ce and La oxides and sulfides are very stable compounds. However, the sulfur removal reactions with rare-earth elements reach equilibrium slowly. In literature, Turkdogan [71] stated solubility product values related to rare earths. In the limits of permitted concentrations of rare earths in steels, it is not possible to decrease sulfur content of the steel below 0.02%. Use of rare earth elements together with CaO increases the degree of sulfur removal. In these type of desulfurization processes, rare earth elements combine with oxygen (deoxidation) and CaO takes sulfur.

For the case when steel is deoxidized with a strong deoxidizer, Ca or CaO becomes an effective desulfurizer. The most common element used for deoxidation is Al [17]:

$$2\underline{Al}(\%) + 3\underline{O}(\%) = Al_2O_3(s) \tag{74}$$

In literature, it was stated that production of ultra-low S steels (S < 10 to 20 ppm) necessitates powder injection process which will be outlined in the following section [72]. Otherwise, desulfurization with top slag was found to be satisfactorily conducted. Principal additions during top-slag process can be listed as follows:

- CaO
- Al
- CaF_2, SiO_2, Al_2O_3

The necessity of CaO is for the formation of limy slag which is to basic for efficient desulfurization. Al is added at the ladle furnace is to deoxidize the liquid steel and to collect the deoxidation product, Al_2O_3, to the slag. Al reacts also with SiO_2 to some extent. Additions like CaF_2, SiO_2, Al_2O_3 are performed to obtain desired synthetic slag composition for sulfur removal [72]. Another important role of the synthetic slag formed is to provide following slag-metal reaction so that sulfur in the metal can be lowered [47]:

$$\underline{S}(\%) + (O^{2-}) = (S^{2-}) + \underline{O}(\%) \tag{48}$$

In ladle desulfurization conducted with CaO-Al_2O_3 slags, sulfur content of the metal is governed by the following reaction [47]:

$$(CaO) + \underline{S}(\%) + \frac{2}{3}\underline{Al}(\%) = (CaS) + \frac{1}{3}(Al_2O_3) \tag{75}$$

As CaO/Al_2O_3 ratio of the slag increases, the sulfur slag-metal distribution ratio increases. The best desulfurization can be achieved with the slags saturated with CaO. Aluminum content of the metal to be desulfurized is also important according to above reaction: The degree of desulfurization increases as the aluminum content of the metal increases. In the systems deoxidized with Al and desulfurized with CaO-Al_2O_3 slags, very high values of (%S)/[%S] can be obtained [52].

Andersson et.al. [73] developed a thermodynamic and kinetic model of reoxidation and desulfurization in the ladle furnace. In their work, two dimensional fluid-flow model was merged with the thermodynamic equations of reoxidation and

desulfurization. Ladle vacuum treatment of a gas-stirred ladle was simulated. In the slag-metal mixing zone, besides the desulfurization reaction, four slag-metal reactions were considered. In that respect, activities of SiO_2 and Al_2O_3 and activity coefficients of Fe_tO and MnO were calculated using the relations obtained by Ohta and Suito [74]. The proposed model was found to be useful for the prediction of loss of aluminum and desulfurization in the steel and the reduction of FeO and MnO in the slag [73].

The generated model by Andersson et.al. was also used to predict some thermodynamic properties of slags. It was found that with the static and dynamic modelling using computational fluid dynamics (CFD), theoretical desulfurization conditions and vacuum degassing operation could be described in sulfur refining process at Ovako Steel AB. It was reported that the dynamically predicted final S contents in molten steel were in good agreement with plant data. It was also concluded that the ratio of ($\%Al_2O_3/\%CaO$) had a substantial effect on sulfur partition ratio [75]. The authors previously calculated sulfur slag-metal distribution ratio by using sulfide capacities obtained by KTH model and activity of Al_2O_3 determined from the empirical relation given by Ohta and Suito [74]. Together with these findings, they studied the effect of carbon and aluminum content of the steel, temperature, alumina and lime content of the slag on sulfur partition ratio. Increase in carbon and aluminum content of the steel led to an increase in sulfur slag-metal distribution ratio, as did the temperature of the steel melt. As ($\% Al_2O_3/\%CaO$) ratio increased, sulfur slag-metal distribution ratio was found to decrease. This was mainly because of a decreased sulfide capacity and an increased oxygen activity [76]. The results of the experiments also revealed that an increase in the iron oxide content in the top slag significantly lowered the desulfurization rate, as cited in the literature [75].

Patsiogiannis et.al. [77] conducted laboratory scale refining studies on low carbon Al-killed steels using synthetic fluxes. Low carbon steel melts were deoxidized using Al in zirconia crucibles. Reoxidation and desulfurization behavior of these

steel melts were examined, in detail. It was indicated that the rate of the deoxidation reaction was very rapid and it was more or less similar to that of aluminum melting and dissolution in the steel. The slowest step in the whole deoxidation process was the removal of alumina inclusions from the steel melt to the slag. Therefore, total amount of oxygen present in the steel bath was controlled by this slowest step, the rate of separation of the inclusions.The authors found that it was better to examine the rate of reoxidation from the soluble Al content of the steel rather than instantaneous steel oxygen activities since the latter do not consider the amount of alumina inclusions formed in the bath.

It was also shown that the use of fluxes was indespensible to decrease the reoxidation of the steel melt. Removal of oxide inclusions were found to necessitate liquid final slags which better trapped inclusions formed due to deoxidation and reoxidation. The best results were obtained with the final slags having CaO/Al_2O_3 ratio of around 1. In relation to inclusion removal, CaF_2 addition was found to have no significant effect.

Considering desulfurization behavior of the above mentioned steel melts, it was stated that the rate of sulfur removal was controlled by the liquid phase mass transfer occurring at the slag-metal interface. Desulfurization reaction was shown as a first order type as far as the kinetics of the process was concerned. Rate constant of the permanent contact reaction was linearly proportional with the liquid phase mass transfer coefficient (m_s) so the change of the rate of sulfur removal was determined simply by comparing m_s values. It was reported that the mass transfer coefficient was relatively independent of the initial sulfur content of the metal.

Addition of FeTe to the steel melt was reported to cause a decrease in m_s values. This behavior was explained with the nature of Te which is a surface active element and it therefore reduced the slag-metal interfacial area and so the rate of desulfurization.

Addition of small amounts of CaF_2 to the flux was found to have no effect on the rate of desulfurization, whereas higher additions (i.e. 21 wt% in the slag) were

reported to have a detrimental effect on desulfurization behavior [77]. This result was parallel to the observations [78] that fluorine ions in the slag hinder the degree of desulfurization of liquid iron.

BaO addition to the flux was shown to be useful to increase the mass transfer coefficient when it was used in significant quantities [76].

Patsiogiannis et.al. [79] studied incorporation of elements like S and Cl in synthetic slags which had similar chemical compositions with the ladle slags. Incorporation of such elements to the slag is important not only to improve steel cleanliness but also to use these slags in some industries. Using differential thermal analysis (DTA) and electron microprobe analysis (EMP), the authors examined CaO-Al_2O_3-SiO_2 type slags and showed that the optimized ladle steelmaking slags could incorporate chlorine and sulfur in their structure in the form of phases based on the crystal structure of the mayenite ($12CaO.7Al_2O_3$).

Turkdogan [80] studied the slag composition variations in relation to extent of dephosphorization and desulfurization in oxygen steelmaking. Based on the plant data of basic oxygen process (BOS) and bottom-blown steelmaking process (OBM), it was found that the extent of dephosporization and desulfurization were mostly affected by the iron oxide content of the slag. It was also reported that unpredictible variations in slag composition from one heat to the next changed the degree of both. It was indicated that for a given slag basicity, steel dephosphorization and desulfurization were governed primarily by iron oxide content of the slag but not by dissolved oxygen in the steel over a wide range of carbon contents of steel. The equilibrium relations described by $\frac{(\%S)}{[\%S]}\cdot[\%O]$ and $\frac{(\%S)}{[\%S]}\cdot[\%FeO]$ were found to increase as the slag basicity increased and SiO_2 and P_2O_5 contents of the slag decreased. The changes in the slag composition, especially the variations of SiO_2 and FeO were shown to be responsible for the change in the extent of desulfurization and dephosphorization.

In literature, activity coefficient of Fe_tO, γ_{Fe_tO}, was determined experimentally for different slag systems. Ohta and Suito [74] studied the activities of SiO_2 and Al_2O_3 and activity coefficients of Fe_tO and MnO in CaO-SiO_2-Al_2O_3-MgO slags. They obtained empirical expressions for a_{SiO_2}, $a_{Al_2O_3}$, γ_{MnO} and γ_{Fe_tO}. They noted that the empirical formula should only be applied within the following slag composition ranges: 10-60 wt% CaO, 10-50 wt% SiO_2, 0-50 wt% Al_2O_3 and 0-30 wt% MgO. It was reported that the composition range of SiO_2 could be extrapolated below 10 wt% [23]. The empirical expressions were generated for 1600 ^oC. However, it was found that the activity coefficients did not change much with temperature and so it was assumed that they were constant in the studied temperature range [74].

Ohta and Suito [74] expressed γ_{Fe_tO} values as a function of slag composition using a multiple regression analysis as follows:

$$\log \gamma_{Fe_tO} = \frac{[0.676(\%MgO) + 0.267(\%Al_2O_3) - 19.07]}{(\%SiO_2)} + 0.0214(\%CaO) - 0.047 \qquad (76)$$

This regression analysis was based on the author's works on CaO-SiO_2-Al_2O_3-MgO slags and their previous studies on CaO-SiO_2-Al_2O_3 and CaO-SiO_2-Al_2O_3-MgO slags. They previously measured the activity coefficients of Fe_tO and MnO in a CaO-SiO_2-Al_2O_3- Fe_tO(< 5 wt%)-MnO(< 10 wt%) system at 1873 K using an Al_2O_3 or CaO crucible [74].

2.9 Desulfurization with Powder Injection

Desulfurization with powder injection involves continuous injection of solid powdered reagents inside molten steel along with a stream of gas (generally argon). A schematic view of powder injection system is illustrated in Figure 2.10. As shown in Figure 2.10, there are 3 different zones in powder injection system considering the kinetics of the process [72].

1. Transitory contact zone:

The powder materials are in contact with the melt and desulfurization reaction happens between the ascending powder and the melt.

2. Permanent contact zone:

The desulfurization reactions takes place between the metal and the slag. Emulsification in the slag-metal interface increases the surface area available for the reaction and therefore increases the reaction rate.

3. Breakthrough zone:

The gas sent to the system with the powder, depending upon the extent of the flow rate may form some openings in the slag layer and therefore steel melt contacts with the air and reoxidation of the melt and nitrogen pick up takes place. Excessive slag-metal emulsification due to high flow rates is therefore undesirable. In modern injection metallurgy, gas flow rates are adjusted to lower levels and formation of breakthrough zone is prevented.

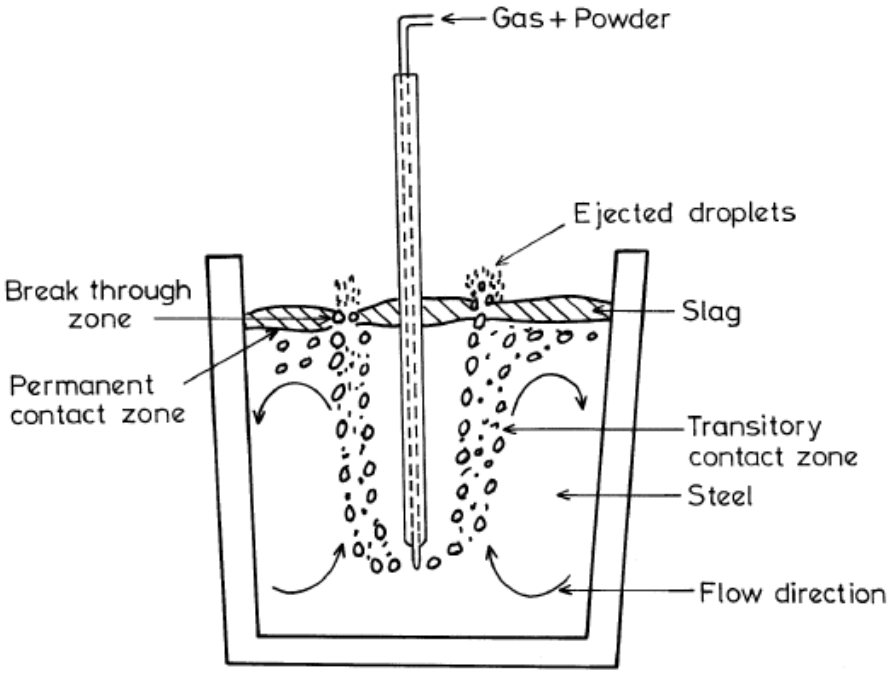

Figure 2.10 Zones in the ladle injection process [72]

The researches on the physical interaction between the melt and the particle showed that injection causes much more rapid mixing as compared to that for only gas purging. Since the transitoric reaction is dispersed in the melt it partially eliminates bulk inhomogenities in sulfur concentration. Another reason is that the gas-particle jet has much higher momentum as compared to a simple gas jet. Multihole lances were found to be more effective in desulfurization. Minimum depth of the immersion was suggested to be 1.5 meters. As indicated previously, the gas flow rate should be adjusted so that no breakthrough zone can be observed. Argon gas flow rates of 0.001-0.003 Nm^3/min was reported to be successful. 0.1 to 0.3 kilograms of calcium silicide powder must be maintained per ton of steel. For effective desulfurization rates to be achieved, the diameter of the powder should be smaller than 1 mm. Nowadays, industrially produced powders are generally less than 0.1 mm size [72].

Continuous powder injection method was found to be successful for deep-desulfurization. Continuous injection of reagents in wire form inside molten metal was more traditional method and was reported to give satisfactory results in relation to inclusion shape control, which will be discussed in the next sections. On the other hand, with wire feeding primarily only inclusion modification can be achieved [72].

Tsujino et.al. [81] studied the desulfurization behavior of ladle furnace refining with powder injection at reduced pressures. Ladle treatment with injection of CaO-10% CaF_2 mixture was applied both at the reduced pressures like 1 torr and at the atmospheric pressure. Sulfur removal data, number of inclusions, oxygen content of steel and stirring energy density were the parameters examined in both cases. At the same rate of powder consumption, reduced pressure was reported to provide lower S contents. The number of inclusions and oxygen content of steel were found to be higher during treatment at reduced pressures while higher stirring energy density were obtained due to vacuum process. Electron microprobe analysis (EPMA) results indicated that compositions of non-metallic inclusions resembled

that of the top-slag showing top-slag entrapment. After the desulfurization treatment, the number of inclusions and oxygen content of the steel were found to have values that were equivalent to those achieved by powder injection under atmospheric pressure. This was attributed to the coalescence of non-metallic inclusions under reduced pressures, which could be very effective in the flotation of the inclusions. It was concluded that ladle desulfurization by powder injection under reduced pressure provided a high stirring force, activated the entrapment of top slag and accelerated the desulfurization reaction.

2.10 Inclusion Shape Control by Calcium Treatment

As mentioned previously, sulfide inclusions should be small sized and globular in shape distributed randomly in steel. As stated earlier, this type of inclusion is obtained at the beginning of solidification. MnS inclusions formed after a strong deoxidation have not such properties. They elongate to the rolling direction causing anisotropy [14]. Shape control of sulfide inclusions includes formation of stable sulfide compounds, which precipitated with a small size and globular shape so that no deformation of inclusions can happen during rolling.

In the literature, sulfide inclusions formed by Ce and Mn were compared according to their time of formation (In 1% Mn, 0.05% Ce, 0.01% S steel). It was reported that Ce-sulfide started to precipitate during cooling of steel (fully liquid) whereas Mn-sulfide formed after 94% of solidification [71]. Wang et.al. [82] summarized the recent studies related to the use of rare earth metals in steel industry. One role of rare earth metals was reported as the inclusion shape control in that precipitation of globular rare earth oxy-sulfides instead of elongated MnS inclusions and other types of brittle oxides were important considering the enhancement of product performance in final use of steels.

The most widely used element for sulfide shape control is calcium. Calcium fed into the Al-deoxidized steel with either in powder form with a carrier gas or in wire form combines with small size Al_2O_3 particles and produces $CaO\text{-}Al_2O_3$ particles.

These particles become liquid if sufficient amount of calcium is provided. It is known that Al_2O_3 inclusions can cause nozzle blockage. Therefore, formation of liquid CaO-Al_2O_3 eliminates nozzle blockage problem [83].

The fluidity of the steel with its inclusions will be influenced by the Ca/Al ratio. Effect of calcium on the flow of aluminum deoxidized steels through nozzles is illustrated in Figure 2.11. In order to obtain low melting calcium aluminates, Ca/Al ratio must be larger than around 0.12 [84]. The effect of calcium was also studied with log (%Ca/Al x10^4) parameter. It was indicated that the value of log (%Ca/Al x10^4) must exceed about 3, in order to avoid high melting Al_2O_3 and CaO.6Al_2O_3 deposits in the tundish nozzle. At the higher ratios, CaO.2Al_2O_3, CaO.Al_2O_3, and 12CaO.7Al_2O_3 are formed, depending on the Ca content [12].

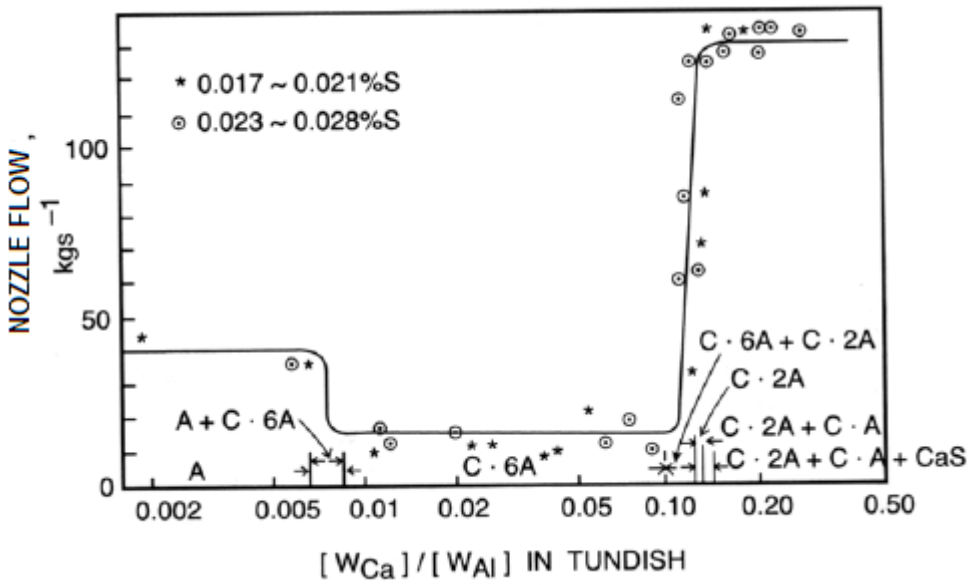

Figure 2.11 Influence of dissolved calcium on the flow of an aluminum-killed steel melt through the tundish nozzle [84]

It was found that formation of the high-melting Al_2O_3 rich Ca aluminates must be avoided, by increasing the CaO content of the inclusions. In order to avoid blockage or hard stringer formation, the CaO.2Al_2O_3, CaO.Al_2O_3, and 12CaO.7Al_2O_3 compositions should be formed [12].

Due to their high sulfide capacity and low oxygen potential of the system, CaO-Al_2O_3 inclusions take some part of sulfur in the metal. During solidification, sulfur present in these inclusions precipitates as CaS. Therefore, there exist globular shape inclusions of CaO-Al_2O_3 surrounded by CaS rim [85]. Schematic illustration of modification of inclusion morphology as a result of calcium treatment is shown in Figure 2.12.

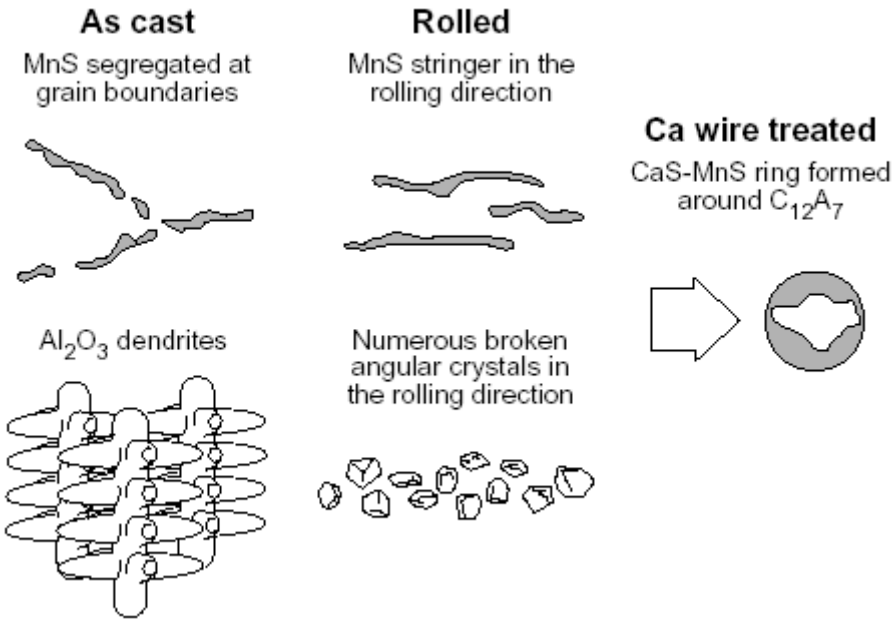

Figure 2.12 Schematic illustration of modification of inclusion morphology as a result of calcium treatment [85]

Change of composition due to calcium treatment is illustrated in Figure 2.13 for CaO-Al_2O_3-SiO_2 system together with the binary CaO-Al_2O_3 and CaO-SiO_2 systems. In Al-Si deoxidized steels, the inclusion compositions are in the areas I and II respectively, depending on the Al and Si levels. When Ca is added, the inclusion composition areas move in the directions of the arrows, resulting in the formation of new inclusion compositions [12].

Blais et.al. [86] outlined the need for inclusion characterization. In this respect, image analysis, scanning electron microscopy and energy dispersive spectrometry were indicated as the methods to obtain more details about the chemistry of inclusions. The authors reviewed the basic principles of inclusion characterization methodology. It was reported that optimum shape control of MnS type inclusions was achieved with the Ca/S ratio of around 0.7. It was also found that the mean diameter of circular inclusions slightly decreased as the Ca/S ratio increased.

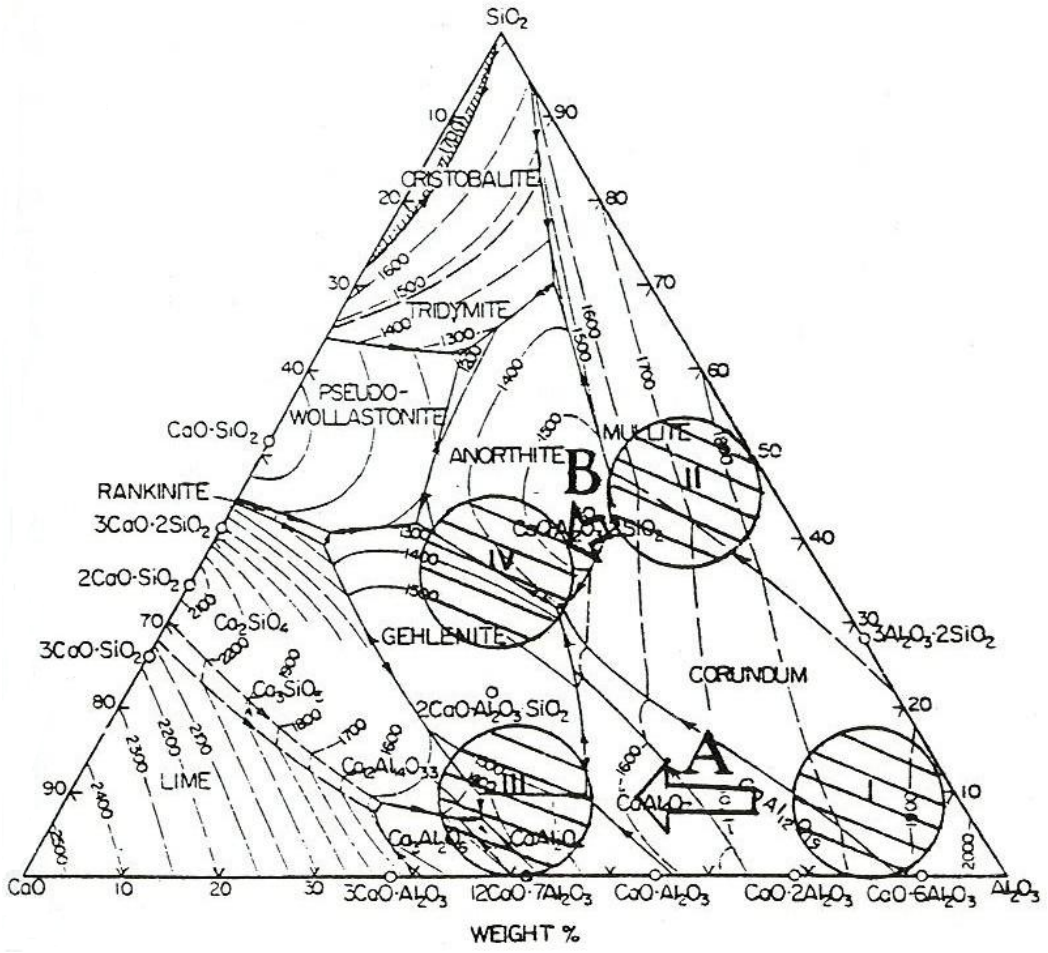

Figure 2.13 Influence of calcium treatment on the composition of inclusions in the system of $CaO\text{-}Al_2O_3\text{-}SiO_2$ [12]

Ito et.al. [87] studied the kinetics of shape control of alumina inclusions with calcium treatment in line pipe steel (S: 0.001%) for sour service ($H_2S_{(g)}$ containing

fluid or liquid). It was shown that the shape control proceeded as the time passed from the wire injection. The degree of shape control was found to be enhanced with the increase in the stirring energy and with the decrease in time between deoxidation and calcium-silicon addition. With the application of unreacted core model, the rate determining step was reported as the calcium diffusion in the calcium aluminate product layer (Figure 2.14).

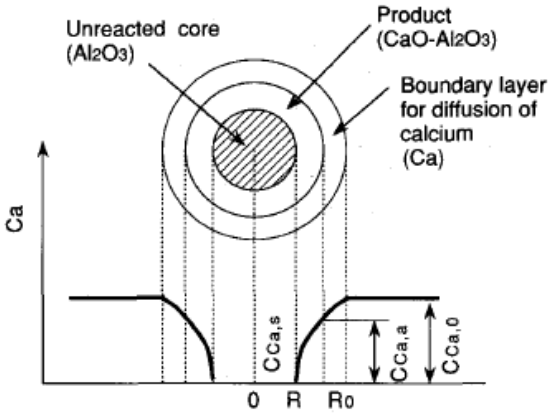

Figure 2.14 Schematic view of shape control of Al_2O_3 with Ca by unreacted core model [87]

Through calcium treatment, transformation of alumina particles to liquid calcium aluminates proceeds with the proposed sequence as $Al_2O_3 \rightarrow CA_6 \rightarrow CA_2 \rightarrow CA \rightarrow CA_x$ where C and A denote calcium oxide and aluminum oxide, respectively. This transformation sequence can be seen in $CaO\text{-}Al_2O_3$ phase diagram given in Figure 2.15. In this respect, Z.J. Han et.al. [88] studied the rate of this type of trasformation with the reactions between Al_2O_3 and CaO in a resistance furnace. It was stated that there were two stages in inclusion modification: 1. Formation of liquid calcium aluminate with interaction and reaction of dissolved Ca and O ions with solid alumina particle. 2. Progress of modification through interaction between liquid calcium aluminate and solid alumina. It was found that chemical reaction at the alumina / calcium aluminate interface was the rate controlling step. On the other hand, in the SEM-EDS analysis, no intermediate phases mentioned above were reported. This was attributed to the fact that all intermediate phases are

solid ones and diffusion in the solid state is very slow. Z.J. Han et.al. also proposed a kinetic model for modification of alumina inclusion by using the measured rate constant and the unreacted-core model. However, it was concluded that the interaction between the solid alumina particles and dissolved calcium were not fully understood [88].

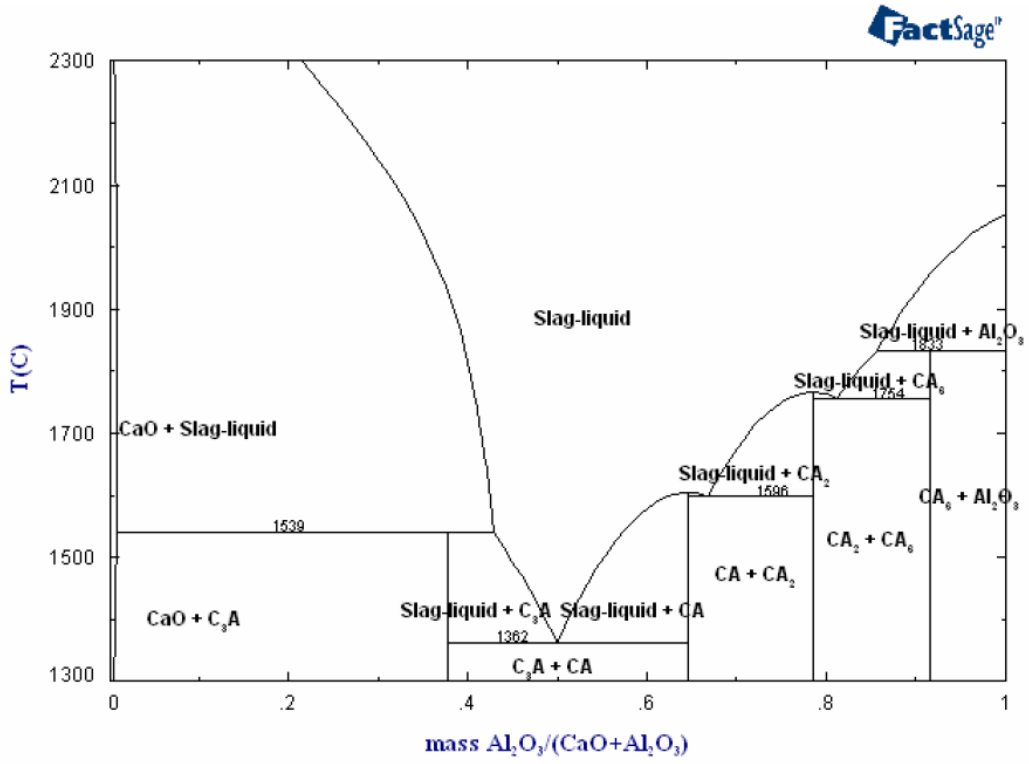

Figure 2.15 CaO-Al_2O_3 phase diagram [89]

Ye et.al. [90] reviewed the use of thermodynamic data in describing calcium modification of aluminum oxide inclusions. Using different sources for thermodynamic data, they calculated the activities of CaO and Al_2O_3 which are to be known to examine the extent of Ca-treatment. Mechanism of Al_2O_3 modification was studied with the unreacted core model. It was indicated that during treatment, inclusion became CaO-rich as moving from the core to the outer shell and a layer of solid CaS ring was formed on CA_x due to the low oxygen activity in equilibrium with CA_x.

2.11 Kinetics of Ladle Desulfurization

2.11.1 Sulfur Removal Equilibrium

The main sulfur removal mechanism is the transfer of sulfur from the metal to the slag phase. The following parameters are important for good sulfur removal from the metal to the slag:

- Liquid and fluid slag with a high dissolved lime content; high sulfide capacity (C_S).
- Higher temperature, which improves both thermodynamics and kinetics.
- Low oxygen content of the steel and low oxidation state of the slag.
- Higher slag volume removes more S, for the same S distribution ratio.
- Mixing (stirring) of the steel; kinetics of mass transfer to slag metal interface.
- The extent of slag and metal inter-mixing at the interface (stirring intensity and slag fluidity) [24].

The overall desulfurization reaction consists of the following kinetic steps:

1. Transfer of sulfur dissolved in liquid iron to slag–metal interface
2. Transfer of O^{2-} from the bulk of the slag to the slag–metal interface
3. Chemical reaction at the interface, governed by:

$$\underline{S}(\%) + (O^{2-}) = (S^{2-}) + \underline{O}(\%) \qquad (48)$$

4. Transfer of S^{2-} from the interface into bulk slag
5. Transfer of [O] from the interface into the bulk metal phase
6. Mixing in slag phase
7. Mixing in metal phase

Industrial desulfurization kinetics is intimately linked with slag formation kinetics as well as other disturbing side reactions. The slag consists of the following components:

- Slag carried over from the BOF vessel
- Deoxidation products
- Worn ladle lining
- Remaining slag from the previous heat
- Added slag-forming components such as lime, limestone, dolomite, and fluorspar [72].

2.11.2 Mathematical Interpretation of Rate of Desulfurization

While thermodynamics describe the driving force and extent or limits of sulfur transfer from metal to slag, the actual change achieved in the allotted treatment time depends on a number of kinetic factors. It has been established that mass transfer of sulfur in the metal to the slag-metal interface, limits the overall kinetics of sulfur transfer to the slag. This means that the rate at which sulfur is transferred from the bulk metal to the slag-metal interface and transfer across the boundary layer close to the interface, are the slowest and thus rate limiting step, which is mainly affected by stirring in the metal. The mixing of the metal is thus the main limiting parameter, as controlled by the inert gas stirring through porous plugs or electro magnetic stirring.

Instantaneous rate of change in sulfur content as a function of the sulfur content at time t (%S) and the equilibrium sulfur content ($\%S^{eq}$) is given by the equation (77) below:

$$\frac{d\%S}{dt} = -k(\%S - \%S^{eq}) \qquad (77)$$

Integration of equation (77) yields;

$$\ln\frac{(\%S-\%S^{eq})}{(\%S^{o}-\%S^{eq})}=-kt \tag{78}$$

where $\%S^{o}$ is the initial S content. Since the rate is controlled by mass transfer in the metal, the most important parameter determining the value of k, kinetic constant, would be the stirring intensity in the metal. The magnitude of the kinetic constant can be determined from actual plant conditions by sampling and analysis of metal sulfur content over time intervals. Typical variation of the sulfur content with time is illustrated in Figure 2.16 for different k values [24].

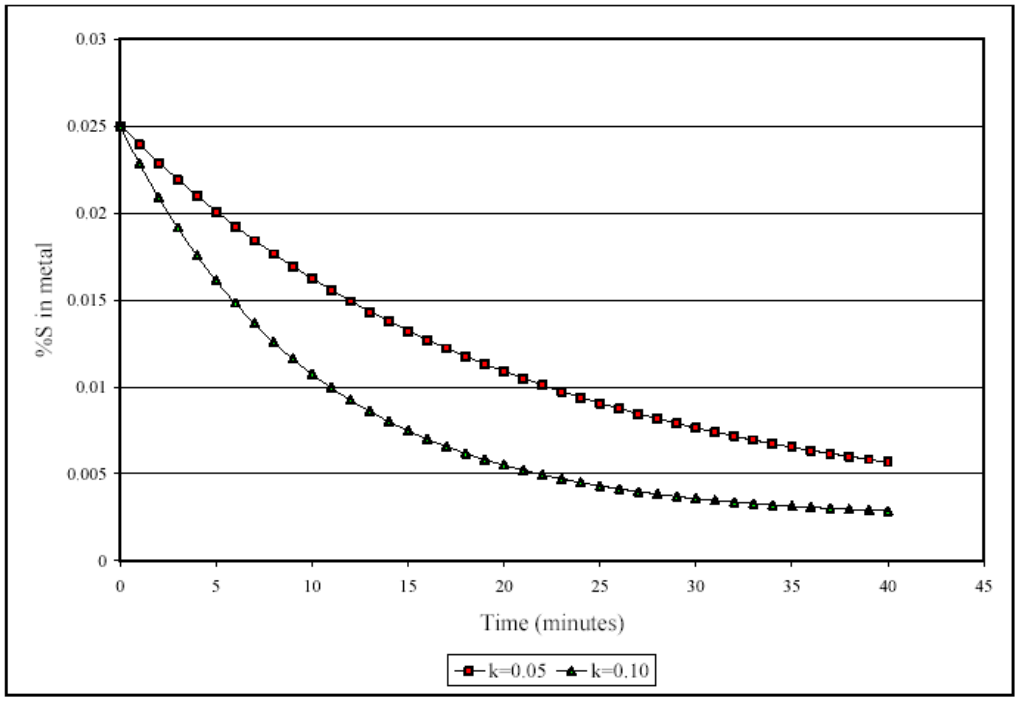

Figure 2.16 Example of %S versus time for different k values [24]

CHAPTER 3

EXPERIMENTAL

In this chapter, in relation to the experiments conducted at the secondary metallurgy, a brief information about the ladle furnace of ERDEMİR steelmaking plant was presented. The experimental procedure followed as to the slag sampling and slag analysis technique were briefly discussed. Chemical composition and process route of the low-sulfur steel quality, 4937K, were then outlined.

3.1 Ladle Furnace (LF & LT)

Adjacent to the No. 3&4 Continuous Casting Machines of ERDEMİR, there are two ladle stations for the secondary metallurgical operations: The Ladle Treatment (LT) and the Ladle Furnace (LF). The former has identically same properties with the latter except for the absence of heating facility. Heating in the Ladle Furnace is provided with 3 submerged electrodes having 45 cm diameter each. Argon gas can be introduced to the system both from the top lance and from the porous plug at the bottom of the ladle. The other important constituents of the furnace are the alloy bins and the Al and CaSi wire feeding machines. The ladle coming from the converter is first subjected to argon gas blown from the porous plug. At the end of 3 minutes of argon gas blowing, temperature measurement is performed and analysis sample is taken. Depending on the chemical analysis requirements of the steel grade to be produced, necessary alloying materials are introduced into the steel bath. At the same time, considering the temperature requirement of the continuous casting machine, heating and/or cooling of ladle is conducted. Then, temperature of the steel bath is again measured and analysis sample is obtained. According to these results, heating/cooling and alloying steps can still be applied. After final 3 minutes of argon gas blowing followed by sampling, the ladle is ready for the caster [91].

At the ladle furnace, working with slag enables one to play with the slag composition to deal special processes related to steel cleanliness such as slag deoxidation and desulfurization. Since heating operation is performed with electricity rather than aluminum addition, reheating cases, most of the time, are not worrying compared with the chemical heating considering steel cleanliness.

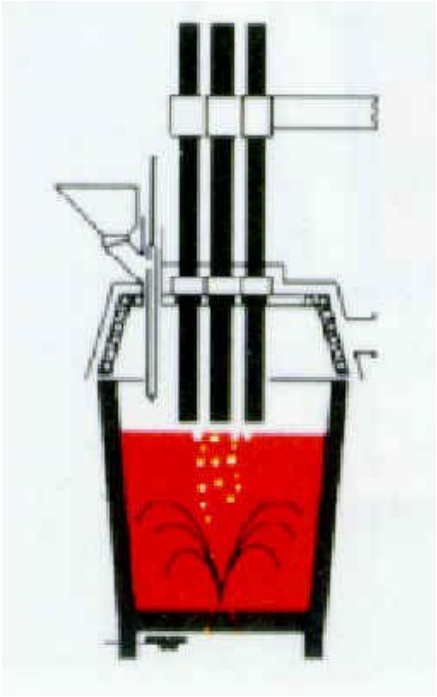

Figure 3.1 A typical Ladle Furnace (LF) [91]

3.2 Slag Sampling and Slag Chemical Analysis Procedure

According to the experimental programme, slag sampling at the ladle furnace was performed in the following way: First, the ladle coming from the converter was heated and stirred for 3 minutes period. The first slag sample was generally taken during this period, CaO and dross (obtained from Al melting with a composition of 20-70% metallic Al, 35% min. Al_2O_3 and 10% max. SiO_2) were added to the ladle afterwards. Proper heating and alloying stages were conducted for each heat according to usual practices. At the end of ladle treatment, second slag sample was

taken just before sending the ladle to the continuous caster (For the qualities in which CaSi injection is performed at the end of ladle treatment, slag sampling was performed before the CaSi injection). For some of the heats, slag sampling was also conducted at the converter, to see the chemical composition of the converter slag as well as to visualize the effect of carry over slag on the secondary metallurgy process.

Slag sampling during tapping from the converter was made by inserting a relatively long steel rod into the slag that floats on the steel. The corresponding sampling at the ladle furnace was conducted from the top of the ladle through the inspection hole where temperature and steel oxygen activity measurements as well as the steel sampling were conducted. A similar type of steel rod was employed for slag sampling purposes.

Slag samples arrived to the X-Ray laboratory were first recorded and stored. The slag samples were ground with disc grinder to a particle size of - 100 microns. Then, the powder of slag particles was placed in hollow cylindrical shape steel, with a base covered by cellulose (See Figure 3.2). The material used as a back up for slag powder is cheap, easy to be pressed and has no chemical interaction with the oxide samples analyzed. By using mechanical press (Herzog), the powder of slag together with the cellulose was pressed and tablet-shape specimens (3.5 cm diameter) were obtained. Very thin layer of slag over the cellulose material were obtained as shown in Figure 3.3. Specimen prepared with this method was ready for chemical analysis.

Chemical analysis of slag specimens was conducted with X-Ray Fluorescence (XRF) technique (ARL Model). The XRF-machine gave results of 12 components for each sample: Fe (total), SiO_2, MnO, Al_2O_3, CaO, MgO, P_2O_5, S, Na_2O, K_2O, TiO_2 and Cr_2O_3. Sum of all components was generally different from 100% (before and after Fe_tO conversion) so normalization procedure was applied for slag samples. During activity calculations only 6 components of slag were incorporated:

Fe_tO, SiO_2, MnO, Al_2O_3, CaO, MgO. Therefore, other components were not taken into account.

Figure 3.2 Powder of slag particles placed in hollow cylindrical shape steel, with a base covered by cellulose

Figure 3.3 Pressed sample; Thin layer of slag sample (gray) over cellulose material (white)

Other than Fe_tO and MnO, one of the least stable oxides in slag systems is P_2O_5. Therefore, it should be considered as a component of a slag system which contains considerable amount of P_2O_5. On the other hand, amount of P_2O_5 in ladle slags is relatively small and the main source of P_2O_5 is the slag carryover from the converter. Since phosphorus removal from hot metal mostly takes place in converter during steelmaking, there exists a substantial quantity of P_2O_5 in

converter slags. However, together with the additions during tapping from the converter and ladle furnace stages, the amount of P_2O_5 is reduced to much lower levels. This was confirmed by the chemical analysis of the slag samples taken both at the beginning and at the end of ladle treatment. As an average, the first slag sample of the ladle contained P_2O_5 as 0.x %. On the contrary, in the end sample, amount of P_2O_5 was found as 0.0x %. Phosphorus reversion to the steel phase occurs only when a large quantity of slag carryover happens. In ERDEMİR, slag carryover from the converter is limited to acceptable levels by using slag free tapping systems such as E.M.L.I. Slag Indication System [92] and thermal cameras (see also Appendices C and D: Slag Free Tapping System, Theoretical Calculation for Carry-over Slag). In conclusion, due to reasons given above, P_2O_5 present in ladle furnace slags was not taken into consideration throughout this thesis work.

No wet chemical analysis was performed for iron oxide. Iron oxide present in the ladle slag was evaluated using Fe(total) result of X-ray fluorescence analysis. Fe (total) contains metallic iron, and, iron as FeO and Fe_2O_3. As explained in the literature, most of the iron oxide present in the steelmaking slags are in the form of FeO [93,94]. Therefore, in the current study iron oxide component was assumed to appear only as FeO for the ease of calculations. To eliminate metallic iron from the slag, specimens were passed through a magnet before X-ray analysis. By this way, metallic iron in the slag was almost completely eliminated so the remaining part was simply FeO. At the end of spectrometer analysis the value of Fe (total) was converted to its oxide form by simple stoichiometric multiplication of Fe (total) with molecular weight of FeO/Atomic weight of Fe factor. The iron oxide calculated with this method was denoted as Fe_tO.

3.3 4937K Steel Quality

4937K (DIN EN 10149-2 1995 GRADE S355MC) is a chassis steel quality produced by ERDEMİR containing maximum 50 ppm. of sulfur. Chemical composition of 4937K steel is shown in Table 3.1 [95]. While tapping from the 120-ton LD-converter, typical alloying additions are FeMn (both low and high

carbon) and FeNb as deoxidation is accomplished with the addition of aluminum. At the ladle furnace, specified amount of CaO and Al-dross are added at the beginning of the operation to obtain $CaO-Al_2O_3$ type liquid slag. Specification of Al-dross currently used at the secondary metallurgy is 20-70% metallic Al, 35% min. Al_2O_3 and 10% max. SiO_2, particle amount with size below 0.5 mm being maximum 5.0% of weight of the slag [96].

Table 3.1 Specification values of 4937K steel quality [95]

Chemical Comp.(%)	C	Mn	P	S	Si	Al	Cu	N(ppm)
4937K	0.04-0.08	0.65-0.85	0.020 max.	0.005 max.	0.030 max.	0.020-0.060	0.12 max.	120 max.
O (ppm)	Cr	Mo	V	Ni	Nb	As	Pb	Sn
100 max.	0.080 max.	0.020 max.	0.010 max.	0.100 max.	0.020-0.040	0.025 max.	0.010 max.	0.015 max.

Steel qualities are classified according to chemical composition, mechanical properties and final use of the product, and so on. Generally accepted classification method uses carbon which is the most important component in steels considering casting of steels and mechanical properties such as yield strength, tensile strength, ductility, hardness and toughness of the final product. Therefore, in ERDEMİR steelmaking plant, steel qualities are generally classified according to their carbon content as given in Table 3.2 [97]. The steel qualities given in the content of this thesis work are called according to classification illustrated here.

In the current work, temperature values used in activity calculations correspond to the first and the last temperature measurement of ladle treatment. Therefore, time of temperature measurement was assumed more or less the same as that of slag sampling.

Table 3.2 Quality groups of steels according to C content [97]

Steel Quality Group	% C
Ultra Low Carbon Steel (ULC)	Less than and equal to 0.005
Low Carbon Steel (LC)	0.005-0.08
Peritectic 1 Steel (P1)	0.08-0.12
Peritectic 2 Steel (P2)	0.12-0.17
Medium Carbon Steel (MC)	0.17-0.25
High Carbon Steel (HC)	Higher than 0.25

Activity, activity coefficient and mole fraction calculations were conducted using Mathcad. Regression analysis and statistical interpretation of data were performed with Statistica software.

Sulfur content of steel samples was determined by using optical emission spectrophotometer whose quantitative working range for S is 3 ppm to 4000 ppm. Standard samples and calibration samples are regularly used for checking accuracy of the results. Sulfur content was also checked with CS-344 device, which is a microprocessor-based instrument for measuring the carbon and sulfur content of metals, ores, ceramics, etc. The accuracy of sulfur measurement is ± 0.0002% or ± 5% of sulfur present (for S<0.1%) [98,99].

In ERDEMİR, 'Heat Nr.' is a six digit number, where the first digit denotes the year (e.g. 5 means 2005), the second digit indicates converter number (1, 2 or 3) and the remaining 4 digit shows the heat number of the converter.

In most of the tables of this thesis work; there exists a column as 'Sample Nr.' in which 1, 2 numbers or converter word is written. 1 corresponds to the first slag sample at the ladle furnace (i.e. SMP) while 2 corresponds to second slag sample at the ladle furnace (i.e. before sending ladle to the continuous casting machine). Converter phrase indicates that the sample was taken during tapping from the converter. In some of the tables, there is a column named as 'Sampling Time'. In

this column, 5 different word groups are given as an abbreviation, and the exact meaning of them is explained below:

- *Converter Tapping:* Slag sample was taken from the converter during tapping.
- *SMP (3 min):* Slag sample was taken from the ladle furnace in first 3 min period (heating+mixing)
- *SMP finish:* Slag sample was taken from the ladle furnace at the end of secondary metallurgy process (i.e. just before sending the ladle to the continuous caster)
- *SMP (Before CaSi addition):* It is almost same phrase as *smp finish*. At the ladle furnace, for the qualities containing Ca and Si, the alloy addition is made by CaSi wire injection at the end of secondary metallurgy. Slag sampling is generally carried out before CaSi wire injection to get a slag analysis showing the exact effect of ladle operations on the slag composition.
- *SMP (After CaSi addition):* Slag sampling was carried out after CaSi injection at the ladle (although not preferred).

During secondary refining, slag sampling was conducted considering the following criteria so the heats that were not produced according to standard practices were not examined:

- Heats tapped from the converter in rimmed condition were excluded, i.e. Slag sampling was carried out only for the heats deoxidized at the converter stage.
- Heats in which reblowing event had occurred were not sampled at the ladle furnace.
- Regraded (steel quality change) heats were not taken into account.

- Slag sampling was not performed at the ladle treatment station (LT: no heating facility avaliable).

Morphological investigation of inclusions were performed according to ASTM E45-97 (Reapproved 2002) standard [100] and will be discussed in Chapter 4, in detail.

Experimental procedure followed during the thesis work is illustrated with the flowsheet shown in Figure 3.4.

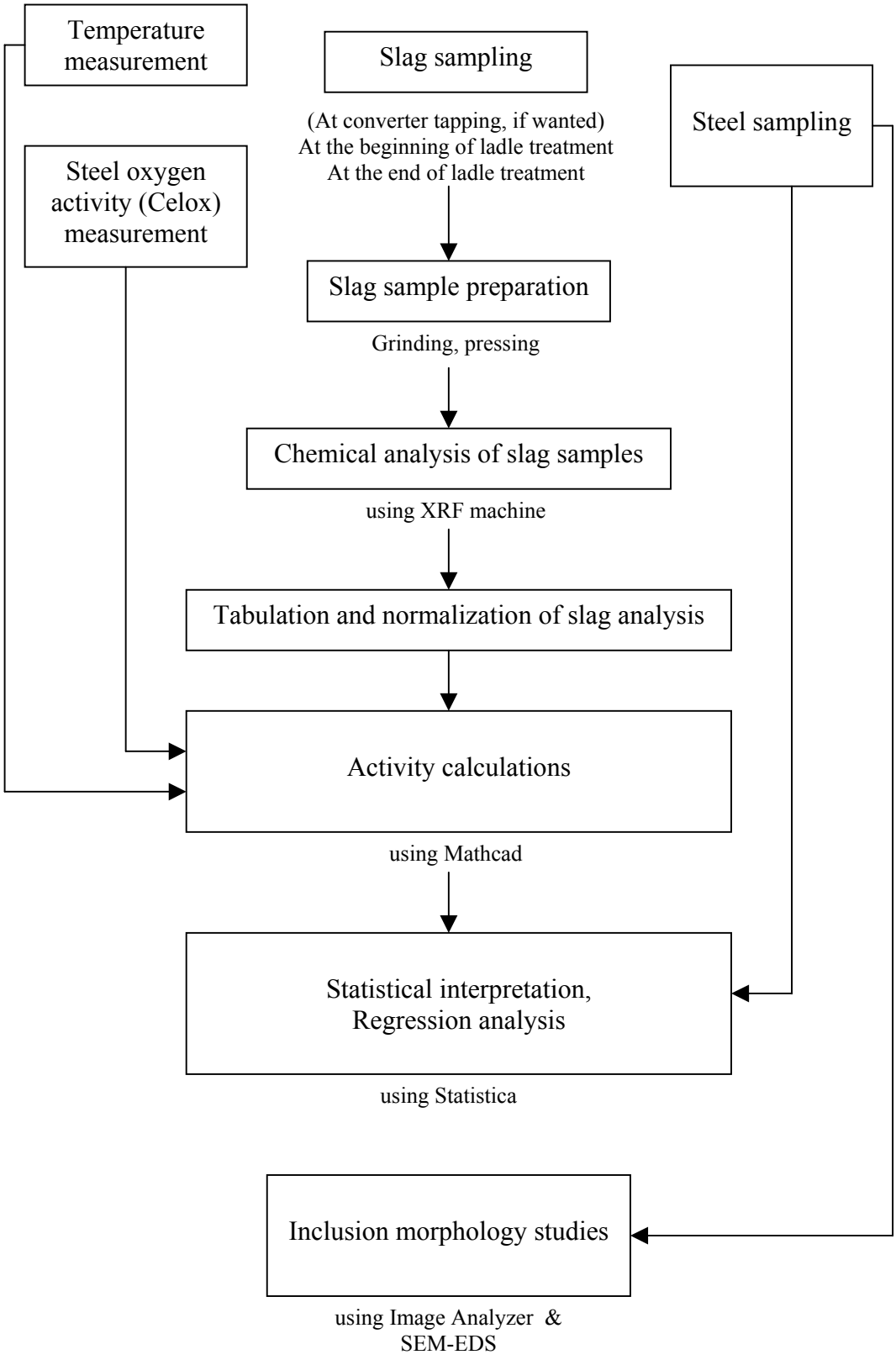

Figure 3.4 General flowsheet of the experimental procedure

CHAPTER 4

RESULTS AND DISCUSSION

4.1 Results of Examination of Unstable Oxides (Fe_tO and MnO) in Converter and Ladle Furnace Slags

The slag samples taken at the converter (BOF) and at the secondary metallurgy (LF) and amount of unstable oxides (FeO and MnO) in the slags were examined for different steel qualities. Iron oxide present in the slags was calculated according to the method given in Chapter 3 and denoted as Fe_tO [93,94] and presented in the following pages.

Steel qualities subjected to slag analysis are listed with numerical order in Table 4.1 below. The explanation in the brackets for each quality shows type of quality that is described according to classification of steels for carbon content, which is given in Table 3.2 [97]. Detailed chemical analysis of each grade is illustrated in Table 4.2 [95]. Slag samples taken at the converter and at the ladle furnace were sent to X-Ray laboratory for XRF analysis. The results of chemical analysis of slag samples were discussed from the point of view of change of Fe_tO and MnO contents for each quality group separately in the following sections (Low carbon, medium carbon, peritectic 1 and peritectic 2).

Table 4.1 Steel qualities subjected to slag analysis

3937K (Peritectic 1 Steel)	6341K (Peritectic 2 Steel)
3942K (Peritectic 2 Steel)	6424K (Low Carbon Steel)
4242K (Medium Carbon Steel)	7110K (Low Carbon Steel)
4940K (Peritectic 1 Steel)	7112K (Low Carbon Steel)
6223K (Low Carbon Steel)	7612K (Low Carbon Steel)

Table 4.2 Chemical composition requirements of steel qualities subjected to slag analysis [95]

STEEL QUALITY	CHEMICAL COMPOSITION (wt%)*									
	C	Mn	P	S	Si	Al	Cu	N (ppm)	O (ppm)	Ca (ppm)
3937K	0.07-0.11	0.35-0.55	0.020	0.010	0.100	0.025-0.060	0.12	100	100	20-60
3942K	0.12-0.16	0.60-0.80	0.020	0.010	0.100	0.025-0.060	0.12	100	100	20-60
4242K	0.15-0.19	0.85-1.05	0.020	0.020	0.030	0.025-0.100	0.12	120	100	
4940K	0.06-0.10	1.05-1.25	0.020	0.010	0.100	0.020-0.060	0.12	120	100	20-60
6223K	0.02-0.06	0.15-0.30	0.020	0.020	0.035	0.020-0.080	0.09	120	100	
6341K	0.14-0.18	1.00-1.20	0.020	0.015	0.10-0.30	0.020-0.100	0.12	120	100	
6424K	0.02-0.05	0.10-0.25	0.015	0.015	0.030	0.020-0.080	0.06	100	100	
7110K	0.02-0.06	0.15-0.30	0.020	0.020	0.030	0.020-0.080	0.10	90	100	
7112K	0.02-0.04	0.10-0.20	0.015	0.015	0.030	0.025-0.070	0.08	60	100	
7612K	0.02-0.04	0.10-0.20	0.015	0.015	0.030	0.020-0.060	0.06	70	100	

Table 4.2 Chemical composition requirements of steel qualities subjected to slag analysis (cont'd) [95]

STEEL QUALITY	CHEMICAL COMPOSITION (wt%)*								
	Ti	Cr	Mo	V	Ni	Nb	As	Pb	Sn
3937K	0.010	0.060	0.015	0.010	0.100	0.008	0.025	0.010	0.010
3942K	0.010	0.060	0.015	0.010	0.100	0.008	0.025	0.010	0.015
4242K	0.010	0.080	0.015	0.010	0.100	0.008	0.025	0.050	0.015
4940K	0.015-0.035	0.080	0.020	0.030-0.050	0.100	0.020-0.040	0.025	0.010	0.015
6223K	0.010	0.050	0.010	0.005	0.060	0.005	0.020	0.010	0.010
6341K	0.010	0.080	0.020	0.010	0.100	0.008	0.025	0.050	0.015
6424K	0.010	0.030	0.005	0.005	0.040	0.005	0.020	0.010	0.005
7110K	0.010	0.080	0.010	0.005	0.060	0.005	0.015	0.010	0.005
7112K	0.010	0.030	0.005	0.005	0.050	0.005	0.015	0.010	0.005
7612K	0.010	0.050	0.005	0.005	0.050	0.005	0.015	0.010	0.005

* Single values indicate the maximum allowable content of the element in the steel

4.1.1 Results of Slag Analysis of Low Carbon Steel Group

At least two samples were taken from the heats of which results of analysis will be presented and discussed. Sample from slags was obtained as explained in Figure 3.4 (i.e. One sample at the converter tapping, one sample at the beginning of ladle treatment and one at the end of ladle treatment). Qualities subjected to slag

analysis were 6223K, 6424K, 7110K, 7112K and 7612K. During tapping from the converter, generally no bulk alloying such as FeMn, FeSi is performed for these qualities. Al and some coke are added for deoxidation purposes, while CaO is added to obtain a suitable ladle slag which is composed of added lime and common deoxidation product, Al_2O_3. These heats are especially suitable to examine the slag behaviour starting from the converter till the end of ladle operation due to the fact that almost no alloy addition is made during tapping from the converter. This enables the analysis of the slag sample to be made with less interference since these additions surely affect the aimed ladle slag compositions and may cause difficulties for observing the change of slag composition from *converter* to *SMP finish*. Although it is accurately determined by end blow oxygen value of liquid steel for a specific heat, aluminum of 200-220 kg is added to liquid steel of 120 tons for deoxidation purposes. 40 kg of coke are also sent to the system for predeoxidation. Approximately 600 kg of CaO is added during tapping for synthetic slag formation.

Heats of low carbon steels being processed in ladle furnace are first heated and stirred for 3 minutes. This practice is valid for almost all steel qualities processed in ERDEMİR. During this period, first slag sample was taken from the top of the steel bath before any additions to the ladle. For these types of grades, an average of 100 kg of Al-dross and 120-150 kg of CaO are added to ladle as a common practice. Ladle process takes around 40 minutes depending on the chemical adjustment and temperature requirement of a specific grade. If needed, Al (wire) and FeMn are the basic materials added to steel to provide analysis required by the specifications. Second slag sample was taken at the end of ladle operations (i.e. Before sending the ladle to the continuous caster). Slag analysis of low carbon steel group is given in Table 4.3.

Change of (%Fe_tO + %MnO) content in the slag is important to understand oxygen content of the steel and the oxidation state of the slag. Desulfurization at the secondary metallurgy is currently performed with the addition of slag making additives (CaO and Al-dross) to obtain sufficiently fluid liquid slag containing less

amount of Fe_tO and MnO, which are not stable oxides in steelmaking slags (i.e. sources of oxygen). Presence of such oxides beyond a certain limit causes a decrease in degree of desulfurization.

Table 4.3 Normalized slag analysis of low carbon steel group

			Normalized values (%)					
Heat Nr.	Steel Quality	Sample Nr.	Fe_tO	SiO_2	MnO	Al_2O_3	CaO	MgO
532296	7612K	1	4.13	4.16	2.11	30.21	54.03	4.89
		2	3.93	3.52	1.56	32.80	53.07	4.75
512827	6424K	1	5.29	3.68	1.29	26.80	58.73	3.79
		2	3.90	3.72	1.36	25.79	61.19	3.66
512828	6223K	1	8.19	5.56	1.88	24.17	54.93	4.57
		2	7.51	3.65	2.37	26.91	54.02	4.95
512829	6424K	1	7.95	5.12	2.27	22.09	58.28	3.22
		2	7.69	3.24	1.55	22.49	60.14	4.38
532708	6424K	1	12.76	2.76	3.04	30.33	48.11	2.54
		2	2.76	3.09	1.36	33.17	55.77	3.59
512831	6223K	1	8.33	3.54	3.00	27.49	54.12	2.91
		2	9.43	2.62	1.93	22.84	59.87	2.96
513417	7112K	Converter	17.47	12.59	6.41	3.30	55.16	2.00
		1	4.40	5.13	2.72	33.80	49.41	3.90
523178	7112K	Converter	17.76	12.53	6.52	1.16	56.56	2.69
		1	4.96	4.94	0.85	30.79	54.38	3.60
		2	1.68	4.67	1.09	32.74	55.68	3.81
523198	7110K	1	10.30	4.50	2.88	17.13	62.21	2.04
		2	5.17	4.30	2.46	22.09	62.87	2.40
533281	7110K	1	6.48	4.39	2.58	24.44	57.63	3.67
		2	4.13	4.00	1.53	27.69	58.19	4.00

Change of $\%Fe_tO$ in the slag for low carbon steel qualities are given in Figure 4.1. The change of $\%Fe_tO$ for 10 different heats was examined for this purpose. For 2 heats, sampling at the converter was also made. In the figure, the data of each specific heat is separated from the others by vertical lines. The experimental data

for 10 heats are given in one figure to visualize %Fe_tO change during the stages of the steelmaking and to compare the results.

The heats in which converter sampling was made is important first to see %Fe_tO content of the slag obtained at the end of oxygen blowing (i.e. valuable metal loss to the slag phase) and to understand its adverse affect on ladle slag formed due to slag carry-over during tapping from the converter to the ladle. Therefore, special attention is needed for these heats. Heat numbered by 513417 belongs to 7112K quality, which is well known, frequently produced low carbon steel quality. The converter slag sample analysis gains much importance for this point of view since more or less it represents converter slag of many heats in ERDEMİR. Typical converter slag contains 18% Fe_tO, 12% SiO_2, 8% MnO, 45% CaO, 3% MgO and 1% Al_2O_3 as the main components. These values, of course, are not exact and depend on hot metal analysis, steel quality aimed to be produced, O_2-blowing practices and the type of furnace refractory material, and so on. For the specific heat mentioned above, Fe_tO content is reported as 17.47%, while the slag contains 12.59%SiO_2, 6.41% MnO, 3.30% Al_2O_3, 55.16% CaO and 2.00% MgO.

For the specific heat mentioned, 220 kg of Al and 600 kg of CaO were added during tapping. Then, the ladle was sent to the ladle furnace for secondary metallurgy. In the period of 3 minutes during heating and mixing, slag sample was taken for analysis. The results of the chemical analysis indicate that slag contains 4.40% Fe_tO, 5.13% SiO_2, 2.72% MnO, 33.80% Al_2O_3, 49.41% CaO and 3.90% MgO. It can be directly concluded that 4.40% Fe_tO in the ladle slag comes from the converter during tapping (carry-over slag). Almost all of the Al_2O_3 present in the ladle slag comes from steel deoxidation reaction; so it can be a starting point to calculate amount of slag in the ladle, and in turn amount of slag carry-over. This calculation is given in Appendix D. Fe_tO content of the slag changes from 17.47% to 4.40% from converter to SMP. %Fe_tO + %MnO value of ladle slag is found as 7.12%, which is a fairly good starting value considering oxidation state of the slag and for steel desulfurization at the ladle furnace.

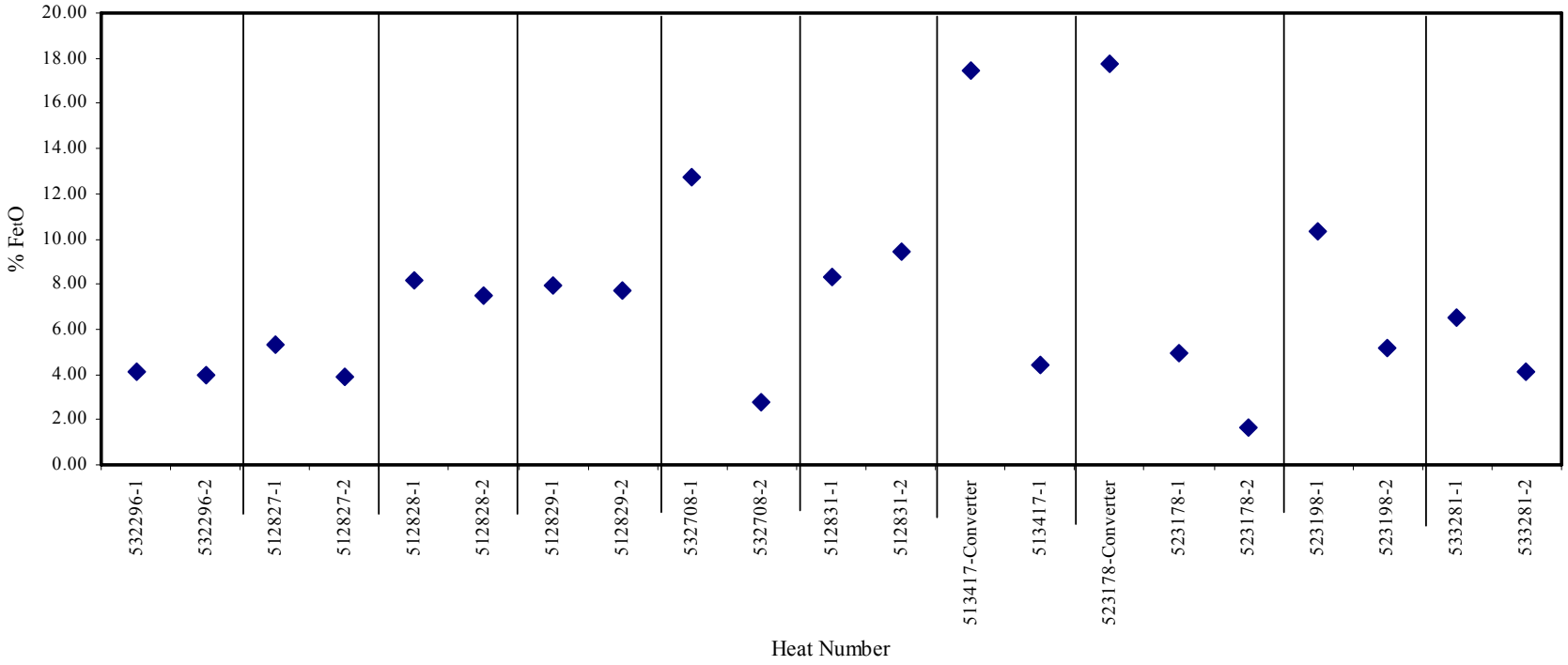

Figure 4.1 Change of $\%Fe_tO$ in converter and ladle slag for low carbon steel qualities

Change of Fe_tO content from converter to *SMP finish* can also be seen from the heat numbered as 523178 (7112K). Fe_tO content of the converter slag is reported as 17.76%, while *SMP (3 min)* value is found as 4.96%, and *SMP finish* is obtained as 1.68%. Considering *SMP finish* data $\%Fe_tO$ + %MnO is found as 2.77%, which shows that the slag is suitable for steel desulfurization. Careful examination of *SMP (3 min)* and *SMP finish* values of most of the heats indicate that with proper slag making additives and with sufficient process time, $\%Fe_tO$ values decrease during ladle operations to almost desired levels. These results for low carbon steels (low Si content also) are important since low carbon and/or low Si qualities are difficult qualities for steel desulfurization [19].

4.1.2 Results of Slag Analysis of Medium Carbon Steel Group

Slag analysis was performed at the ladle furnace and at the converter. During tapping from the converter, Al, some coke and lime are added just as in the case of low carbon steel group. Other than these additions, around 1 ton of high carbon ferromanganese is sent to the system to provide relatively high manganese content of the steel. The basic principles and practices are similar to the ones in low carbon steel group.

At the ladle furnace, sampling times are the same as that of low carbon steels. For these types of grades, an average of 80 kg of Al-dross and 160 kg of CaO are added. If necessary, Al (wire), coke and ferromanganese are added as alloy additions to the system. Slag analysis of medium carbon steel group is given in Table 4.4.

Change of $\%Fe_tO$ in the slag for medium carbon steel qualities are shown in Figure 4.2. The change of $\%Fe_tO$ for 2 heats is studied. In one of the two heats, slag sampling at the converter stage was also performed. In the graph, experimental data for the two heats are divided by a vertical line.

Table 4.4 Normalized slag analysis of medium carbon steel group

			Normalized values (%)					
Heat Nr.	Steel Quality	Sample Nr.	Fe_tO	SiO_2	MnO	Al_2O_3	CaO	MgO
513424	4242K	Converter	14.91	15.19	8.02	1.59	55.48	1.56
		1	1.72	7.18	6.88	25.03	53.76	4.70
		2	1.22	7.42	3.58	26.90	55.91	4.49
533273	4242K	1	6.63	5.14	3.07	21.74	59.90	3.07
		2	1.23	4.95	2.77	23.62	63.97	3.14

In the heat numbered by 513424, converter slag sample was taken. For this heat, Fe_tO content is reported as 14.91%. The other constituents and their amounts are 15.19% SiO_2, 8.02% MnO, 1.59% Al_2O_3, 55.48%CaO and 1.56% MgO. During tapping from the converter, 120 kg of Al, 160 kg coke, 400 kg CaO and 1100 kg FeMn were added. *SMP (3 min)* analysis indicates that slag contains 1.72% Fe_tO, 7.18% SiO_2, 6.88% MnO, 25.03% Al_2O_3, 53.76% CaO and 4.70% MgO. Second sampling at the ladle furnace was conducted just before sending the ladle to the continuous caster *(SMP finish)*. This slag consists of 1.22% Fe_tO, 7.42% SiO_2, 3.58% MnO, 26.90% Al_2O_3, 55.91% CaO and 4.49% MgO. Fe_tO content of the slag changes from 14.91% to 1.72% from *converter* to *SMP (3 min)*. A slight decrease in Fe_tO content from 1.72% to 1.22% was reported between *SMP (3 min)* to *SMP finish*. Together with MnO, *SMP finish* % Fe_tO + %MnO value was reported as 4.80%. Slag % Fe_tO + %MnO total of the other heat was calculated as 4.00%. These values are acceptable considering the oxidation state of the slag and degree of desulfurization [24].

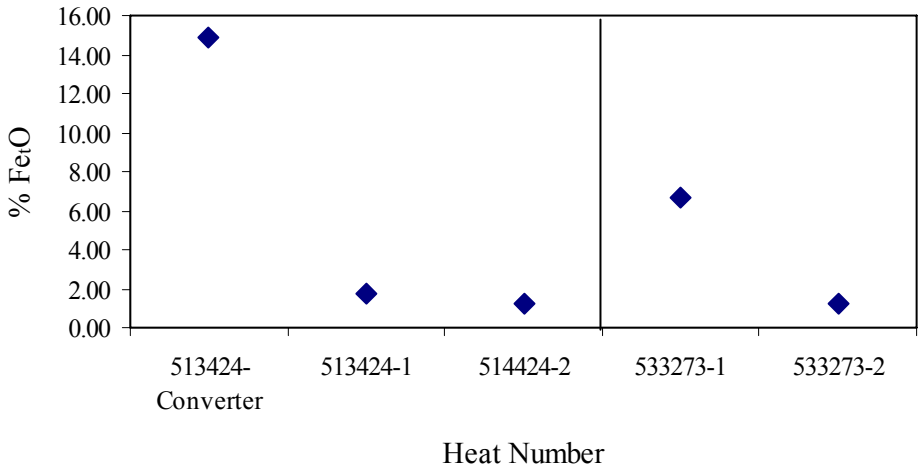

Figure 4.2 Change of %Fe_tO in converter and ladle slag for medium carbon steel qualities

4.1.3 Results of Slag Analysis of Peritectic 1 and Peritectic 2 Steel Groups

The results of Peritectic 1 and Peritectic 2 steel groups are discussed together. Slag sampling was performed in 3 heats of Peritectic 1 steels at the ladle furnace. Two heats belonging to peritectic 2 group were examined. In one of them, slag sampling at the converter stage was also performed. Slag analysis of Peritectic 1 and Peritectic 2 steel groups are presented in Table 4.5 and Table 4.6, respectively. During tapping from the converter, other than Al, coke and CaO, both high and low carbon ferromanganese as well as FeSi can be added to the steel to obtain desired chemical composition required by the steel specifications. Al-dross and CaO additions are made at the beginning of the ladle operations as in the case of low and medium carbon steel groups. Other than these, the alloys of various kinds are also added in the ladle furnace.

The heat numbered as 533267 (3942K) is in the group of Peritectic 2 steels. Converter slag sampling was performed for this heat and the chemical composition of the slag was reported as 16.18% Fe_tO, 12.14% SiO_2, 6.07% MnO, 1.20% Al_2O_3, 59.70% CaO and 1.90% MgO. During tapping from the converter, 200 kg of Al, 80 kg of coke, 600 kg of CaO and 800 kg of high carbon ferromanganese were added.

Ladle furnace sampling was made again in first 3 minutes of secondary metallurgy and the corresponding slag analysis was found as 2.94% Fe_tO, 7.91% SiO_2, 4.04% MnO, 20.17% Al_2O_3, 61.40% CaO, 2.98% MgO. Final slag sampling was conducted just before CaSi (wire) addition required by the steel quality. SMP finish analysis was given as 2.88% Fe_tO, 8.22% SiO_2, 2.52% MnO, 28.77% Al_2O_3, 53.39% CaO and 3.70% MgO.

Table 4.5 Normalized slag analysis of peritectic 1 steel group

			Normalized values (%)					
Heat Nr.	Steel Quality	Sample Nr.	Fe_tO	SiO_2	MnO	Al_2O_3	CaO	MgO
512248	4940K	1	5.06	4.00	9.66	22.90	52.44	5.36
		2**	5.45	3.65	6.93	23.61	54.11	4.85
523190	3937K	1	1.56	6.90	3.81	27.27	56.30	3.67
		2*	2.74	5.95	1.01	32.53	51.80	5.65
533277	3937K	1	5.97	6.21	4.84	16.13	63.65	2.41
		2*	5.76	6.88	3.44	28.99	50.32	3.92

* Before CaSi addition
** After CaSi addition

Table 4.6 Normalized slag analysis of peritectic 2 steel group

			Normalized values (%)					
Heat Nr.	Steel Quality	Sample Nr.	Fe_tO	SiO_2	MnO	Al_2O_3	CaO	MgO
513422	6341K	1	0.43	13.50	1.98	28.74	50.93	4.00
		2	0.76	12.96	1.01	30.87	50.09	3.86
533267	3942K	Converter	16.18	12.14	6.07	1.20	59.70	1.90
		1	2.94	7.91	4.04	20.17	61.40	2.98
		2*	2.88	8.22	2.52	28.77	53.39	3.70

* Before CaSi addition

Fe_tO content of the slag changes from 16.18% to 2.94% from *converter* to *SMP (3 min)*. During secondary applications, it remains almost the same. This is true for most of the heats belonging to either Peritectic 1 or Peritectic 2 examined here. Small variations in slag Fe_tO content was reported. Change of Fe_tO in the slag for peritectic steel qualities are illustrated in Figure 4.3 and Figure 4.4. As previously

indicated, slag % Fe_tO (and also %MnO) content is important to visualize the oxidation state of the slag and steel desulfurization ability. During secondary applications with proper slag making additions like Al-dross and CaO, % Fe_tO of the slag is expected to go down.

At the ladle furnace, type of the secondary applications and their period gain much importance considering chemical composition of the slag. Long ladle process time, heating facilities for temperature adjustment and number of ladle heating, changes of steel composition through alloy additions (FeSi, CaSi etc.), bottom stirring and its effectiveness, amount of ladle slag, and slag sampling practices may lead to some unexpected results in slag analysis. As a conclusion of this section, decrease in Fe_tO content were reported in both low C and medium C steels. Low carbon steel qualities considering their steelmaking process as a whole and the factors explained above, are the most suitable ones to see the change of unstable oxides (Fe_tO and MnO) in the ladle slag. The results for low carbon steels are important since low carbon and/or low Si qualities are difficult ones for steel desulfurization [19].

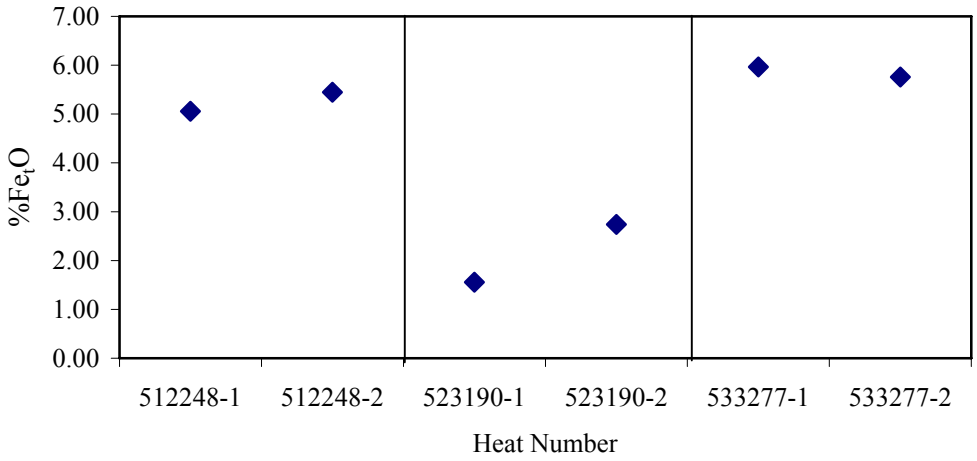

Figure 4.3 Change of %Fe_tO in converter and ladle slag for peritectic 1 steel qualities

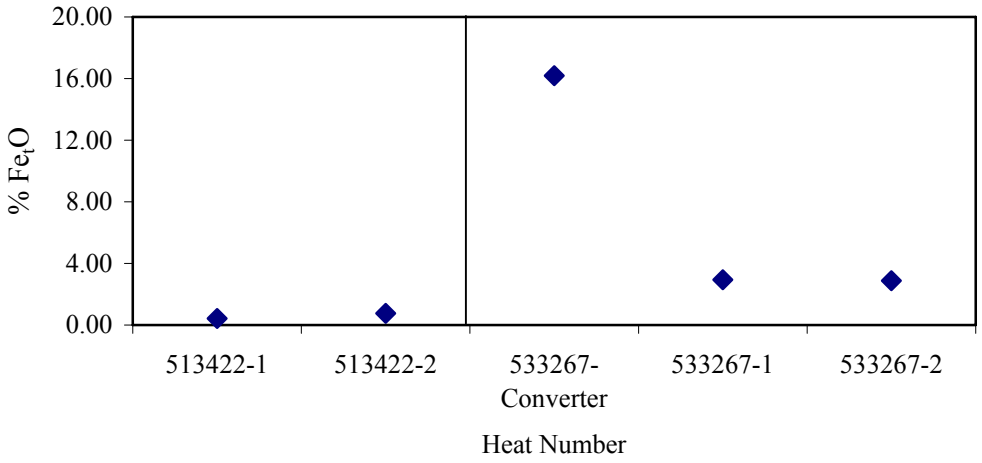

Figure 4.4 Change of % Fe_tO in converter and ladle slag for peritectic 2 steel qualities

4.2 Desulfurization Characteristics of Ladle Furnace Slags of a Low-Sulfur Steel

In steelmaking, one of the most important parameter for desulfurization is the oxygen potential of the system [47]. Oxygen potential of the system can be expressed either by oxygen activity of the steel or by Fe_tO activity of the slag. Removal of sulfur from the steel enhances when Fe_tO activity of the slag and so oxygen activity of the steel decreases. In this part, slag samples of 4937K were examined. Samples were taken both at the beginning and at the end of ladle treatment. Using chemical analysis of slag samples, the change in amount of least stable oxides (i.e. Fe_tO and MnO) in the slags could be seen. These variations were studied considering the change in iron oxide: In this section, activity coefficients of Fe_tO, γ_{Fe_tO} , were calculated for one of the low-S steel qualities, 4937K, using an empirical expression obtained by Ohta and Suito [74], given in Chapter 2. Activity calculations were performed with the program written in Mathcad. The changes in activity of Fe_tO in the slag phase, a_{Fe_tO}, were also studied in relation to the sulfur removal: The relation between *% Decrease* a_{Fe_tO} and *%DeS (measured)* was investigated for 4937K runs and some other types of steel produced in the

ERDEMİR plant. Activity coefficients of Fe_tO, γ_{Fe_tO} , were also calculated for the same heats (4937K) using steel oxygen activity data. γ_{Fe_tO} values calculated with this approach were then treated with Statistica and a linear regression equation was obtained relating γ_{Fe_tO} with the major slag components. Mathcad program written in the previous stage was revised so that steel oxygen activity could be incorporated as an input in calculations. The relationship between *% Decrease* a_{Fe_tO} and *%DeS (measured)* was studied with this approach for the same 4937K experiments and compared with one conducted previously. The same relationship was also investigated for 4937K slags using Temkin equation [27] and the polymeric anion model [28]. Variation of *%DeS (measured)* with the steel oxygen activity change at the ladle furnace was also examined.

4.2.1 Activity Calculations Using An Empirical Expression

4937K steel heats numbered as 526919, 517076, 517077, 517078, 517080, 610618, 610620, 631253, 616522 and 634021 were studied at the ladle furnace. Slag sampling was conducted at the beginning and at the end of ladle furnace treatment and XRF analyses were performed on the slag samples.

The results of the slag analysis are given in Table 4.7. There were two slag samples taken for each heat, namely at the beginning and end of slag treatment, as given in Table 4.7.

The oxygen activity in the bulk of the steel melt is calculated by using the activity of aluminum in the reaction:

$$2\underline{Al}(\%) + 3\underline{O}(\%) = Al_2O_3(s) \qquad (74)$$

In the bulk of the steel melt it is assumed that the activity of alumina is unity. The steel bulk is defined as liquid metal containing less than 1% top slag (by weight). In the slag/metal mixing zone however, the activity of oxygen is determined by the

equilibrium reactions between the liquid slag and steel [73]. In the present work, heats of the low-S steel quality, 4937K, were studied by taking slag samples to evaluate the change of oxygen activity of the steel and Fe_tO activity of the slag. For the calculation of oxygen activity of the steel and Fe_tO activity of the slag, the following exchange reaction was used:

$$Fe_tO(l) = Fe(l) + \underline{O}, \qquad \Delta G^o = 116100 - 48.4 * T(J/mole) \qquad (79)$$

Table 4.7 Normalized slag analysis of 4937K steel heats (wt%)

Heat Nr.	Sample Nr.	Fe_tO	SiO_2	MnO	Al_2O_3	CaO	MgO	Temperature (^oC)
526919	1*	6.12	6.52	5.41	25.37	48.33	7.74	1599
526919	2**	1.95	6.33	2.77	30.99	49.50	8.11	1594
517076	1	2.69	7.62	3.75	29.67	48.38	7.53	1632
517076	2	1.62	7.50	1.77	30.55	49.34	8.93	1595
517077	1	5.05	6.95	8.46	27.94	46.78	4.47	1576
517077	2	2.19	6.58	3.02	31.93	48.71	7.34	1590
517078	1	4.84	5.17	4.72	23.65	54.85	6.32	1560
517078	2	1.86	7.40	2.43	30.13	49.34	8.54	1591
517080	1	8.45	6.67	5.33	20.68	54.03	4.00	1620
517080	2	1.50	5.24	1.61	30.71	52.67	7.98	1589
610618	1	7.94	5.03	4.72	18.52	56.98	6.04	1613
610618	2	1.84	4.50	1.54	26.41	56.29	9.14	1595
610620	1	5.11	4.64	5.62	20.42	57.75	6.01	1610
610620	2	1.05	2.29	0.31	33.99	53.36	8.54	1592
631253	1	4.97	4.32	3.71	24.53	56.97	4.95	1623
631253	2	4.07	4.33	2.95	27.18	55.33	5.66	1604
616522	1	11.95	5.08	5.31	14.74	57.26	4.93	1614
616522	2	5.25	6.03	5.10	22.77	53.38	6.49	1594
634021	1	8.71	4.64	5.38	20.74	54.12	5.66	1577
634021	2	8.44	4.76	4.94	20.89	55.39	4.96	1592

* Slag sample taken at the beginning of ladle treatment.

** Slag sample taken at the end of ladle treatment

The equilibrium constant for reaction (79) can be written as

$$K_{77} = \frac{a_{\underline{O}} \cdot a_{Fe}}{a_{Fe_tO}} = \frac{a_{\underline{O}} \cdot X_{Fe}}{\gamma_{Fe_tO} \cdot X_{Fe_tO}} \qquad (80)$$

where the activity of iron, a_{Fe}, is assumed to be equal to the molar fraction of iron, X_{Fe}, in the steel melt. In the present work, X_{Fe}, values were calculated by using Mathcad program. For 4937K steel heats, X_{Fe} could be approximated as 0.99. Mole fraction of Fe_tO, X_{Fe_tO}, was also calculated using the same program. γ_{Fe_tO} values were determined using Ohta and Suito's empirical equation as given below [74]:

$$\log \gamma_{Fe_tO} = \frac{[0.676(\%MgO) + 0.267(\%Al_2O_3) - 19.07]}{(\%SiO_2)} + 0.0214(\%CaO) - 0.047 \qquad (76)$$

This empirical relation is valid for some of the slag compositions given in Table 4.7. The relation (76) is applicable when Fe_tO < 5 wt% so the experiments in which this condition was not met were not taken into account in the calculations performed with Ohta and Suito's approach. The expression given for γ_{Fe_tO} was derived at 1600 ^oC. Since the activity coefficient values do not depend very much on temperature, the relation (76) was assumed to be applicable practically at ladle furnace temperatures near 1600 ^oC.

Activity of oxygen in the slag/metal mixing zone, activity coefficient of Fe_tO, mole fraction of Fe_tO and activity of Fe_tO were calculated by a program named as *FetO* written in Mathcad (Appendix E). As indicated above, activity of Fe in the steel was assumed to be equal to molar fraction of iron, X_{Fe}, which was calculated by another program written in Mathcad. X_{Fe} could be calculated by using chemical composition of steel samples taken in ladle furnace: Program used 20 components as an input: C, Mn, P, S, Si, Al, B, Cu, N, O, Ca, Ti, Cr, Mo, V, Ni, Nb, As, Pb, Sn.

Calculated X_{Fe} values became an input in *FetO* for activity calculations. Temperature of the steel at the slag/metal mixing zone corresponding to slag sampling time was incorporated in activity calculations although activity coefficient of Fe_tO was not affected very much with temperature.

After the practices applied at the ladle furnace, a considerable decrease in molar fraction of Fe_tO (X_{Fe_tO}) was observed. Activity coefficient of Fe_tO, γ_{Fe_tO}, was found to increase during ladle furnace treatment. For almost all heats, $\%Al_2O_3$ and %MgO contents of the slags were reported to increase from 1st sample to 2nd sample. Both behaviour were in accord with the expectations: Increase in $\%Al_2O_3$ was due to slag deoxidation practice applied in secondary metallurgy while increase in %MgO was related to ladle refractory wear.

Sulfur in steel is expected to decrease while activity of Fe_tO, a_{Fe_tO}, in the slag decreases. In this respect, a relation was tried to be derived relating the decrease in a_{Fe_tO} with the decrease in S content of steel. Desulfurization in the ladle furnace was defined as $[(\%\underline{S}_{initial} - \%\underline{S}_{final}) / \%\underline{S}_{initial}] \cdot 100$ and shown by *%DeS (measured)*. Here, $\%\underline{S}_{initial}$ corresponded to the sulfur content of the steel at the beginning of ladle treatment while $\%\underline{S}_{final}$ denoted the one at the end of secondary metallurgy (LF). The change in a_{Fe_tO} was studied with *% Decrease in* a_{Fe_tO} parameter determined as $[(a_{Fe_tO\ Sample\ 1} - a_{Fe_tO\ Sample\ 2}) / a_{Fe_tO\ Sample\ 1}] \cdot 100$. With this fraction, the activity change of Fe_tO could be calculated using slag samples taken at the beginning and at the end of ladle metallurgy (1st sample and 2nd sample). Results of the program and *% Decrease in* a_{Fe_tO} and *%DeS (measured)* values for 4937K experiments are presented in Table 4.8.

Table 4.8 Results obtained by using Mathcad program and *% Decrease in* a_{Fe_tO} and *%DeS (measured)* values for 4937K experiments

Heat Nr.	Sample Nr.	γ_{Fe_tO}	X_{Fe_tO}	a_{Fe_tO}	%$\underline{S}$	*% Decrease in* a_{Fe_tO}	*% DeS (measured)*
517076	1	1.561	0.024	0.038	0.0061	13	23
	2	2.284	0.015	0.033	0.0047		
517077	1	0.523	0.047	0.024	0.0056	-17	18
	2	1.403	0.020	0.028	0.0046		
517078	1	0.306	0.043	0.013	0.0050	-154	-12
	2	1.991	0.017	0.033	0.0056		
610620	1	0.135	0.045	$6.01*10^{-3}$	0.0105	72	60
	2	0.178	$9.55*10^{-3}$	$1.70*10^{-3}$	0.0042		
631253	1	0.112	0.044	$4.97*10^{-3}$	0.0055	-45	9
	2	0.196	0.037	$7.19*10^{-3}$	0.0050		

% Decrease in a_{Fe_tO} and *% Desulfurization* data present in Table 4.8 were used in a Mathcad program to obtain the relationship between the former and the latter. *% Decrease in* a_{Fe_tO} values were decided to be the x-axis of the graph while *% Desulfurization* data being y-axis written as *%DeS (measured)*, for the sake of simplification. As seen in Figure 4.5, a linear relation was obtained between the *% Decrease* a_{Fe_tO} and *%DeS (measured)*. As *% Decrease in* a_{Fe_tO} increased, meaning a larger decrease in a_{Fe_tO}, *%DeS (measured)* increased. This relation between the calculated a_{Fe_tO} and *%DeS (measured)* values was in accord with the expectations. It is known that a good steel desulfurization at the secondary metallurgy necessitates a steel having oxygen activity as low as possible [23]. Another way of statement is that desulfurization at the ladle furnace requires low a_{Fe_tO} and so sufficiently fluid slag satisfying desired level of slag-metal reaction. The experimental data was treated in the Mathcad program so the best line of equation was found as:

$$\%DeS(measured) = 27.35 + 0.298 * (\%Decrease\ in\ a_{Fe_tO}) \qquad (81)$$

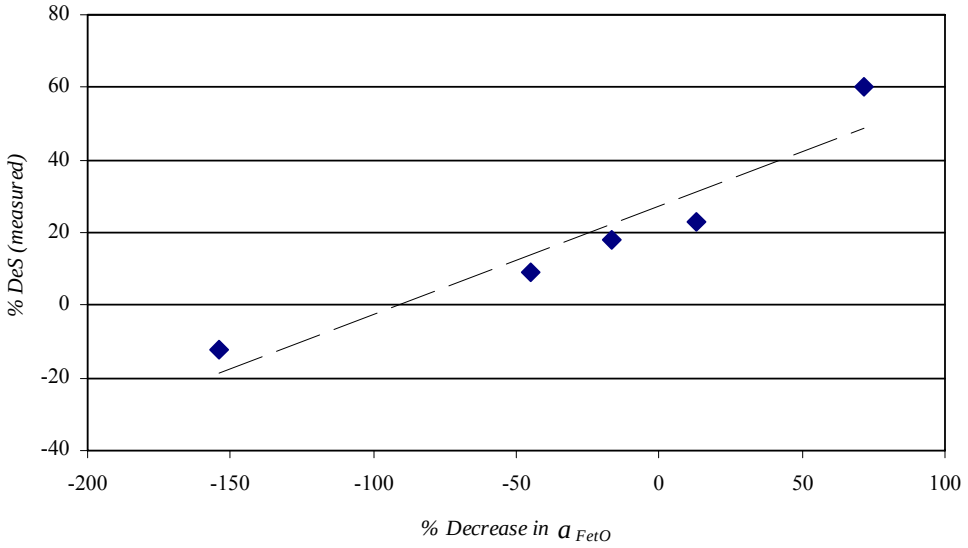

Figure 4.5 The variation of *% Decrease in* a_{Fe_tO} with *%DeS (measured)* for 4937K runs

In the heat numbered as 517078 given in Table 4.8, *% Decrease in* a_{Fe_tO} was found as a negative value meaning an increase in a_{Fe_tO}. Considering the increase in a_{Fe_tO} only, it was a condition affecting the degree of desulfurization adversely. Evidently, a considerable increase in a_{Fe_tO} was the possible reason of poor desulfurization at the ladle. In this heat, the measured sulfur composition of the steel samples showed a negative *%DeS (measured)* value meaning an increase in sulfur content during ladle treatment.

According to the data obtained and the corresponding relation given in (81) about 28% of desulfurization was achieved even though no decrease in a_{Fe_tO} was observed. From this point on, *%DeS (measured)* was reported to continue increasing with decreasing a_{Fe_tO}. However, a significant increase in *%DeS (measured)* seemed to require much larger decrease in a_{Fe_tO} values. This was an

expected result since considerable degree of desulfurization was possible as long as a considerable decrease in unstable oxides (The most important one being Fe_tO) in the slag was attained.

The variation of *%DeS (measured)* with *% Decrease in* a_{Fe_tO} was also examined for the other slags produced in the ERDEMİR plant. Similar calculations were conducted for them using Mathcad software. Common property of them was that sulfur limit of all of them (except for 4933K) was above 100 ppm. Total of 20 heats were grouped into 3 categories as follows:

- Low C - Low Si: C content of the steel qualities presented in this group was 0.02-0.06 %, while Si concentration being 0.035% maximum.
  (Qualities of experiments conducted: 7112K, 6424K, 6223K and 7612K)

- 4933K: C content: 0.03-0.07%; Si content: 0.030% maxiumum. Due to its similarity to 4937K, 4933K was studied as a separate group since C, Mn and Nb content of 4933K is slightly lower than 4937K and S composition of 4933K is limited to 0.008% maximum.

- High C: C content of the steel qualities present in this group was 0.12-0.19%, while Si concentration was generally 0.100% maximum. This group was called as high C only to indicate C concentration of steel was considerably higher than the one in low C - low Si (i.e. High C group here should not be understood as its general meaning in steelmaking terminology [97]: 0.12-0.19% C range is not in the range of high C steels)
  (Qualities of experiments conducted: 6044K, 3942K, 4242K and 6341K)

The change of *%DeS (measured)* with *% Decrease in* a_{Fe_tO} is shown in Figure 4.6. The same relation obtained for 4937K steel quality given in Figure 4.5 is also presented in Figure 4.6. Considering the trend curves of data obtained for all groups, the highest *%DeS (measured)* values were observed in 4937K steel quality

experiments. This was in agreement with the expectations since the strongest sulfur removal practices were applied for 4937K and therefore the highest *%DeS (measured)* values were anticipated. The lowest desulfurization data were obtained in low C- low Si group (red coloured dash line). The qualities in this group had not strong limitation on sulfur content [95]. Desulfurization behavior of 4933K and high C group lied in between. Only three heats of 4933K were examined. For 4933K steel quality, desulfurization practices applied in ladle furnace is not as effective as that of 4937K. Therefore, the data obtained for 4933K is below 4937K, as expected. Experimental data of high C group is also below 4937K trend line. Like low C - low Si group, this is due to their steel specification which does not require to lower S content. On the other hand, *%DeS (measured)* values of high C group stayed above low C - low Si group. This was also an expected result since sulfur removal becomes difficult as C and/or Si content of steel decreases [19]. That is to say, as long as the same practices applied, steels having higher C and/or Si concentration show greater desulfurization ability.

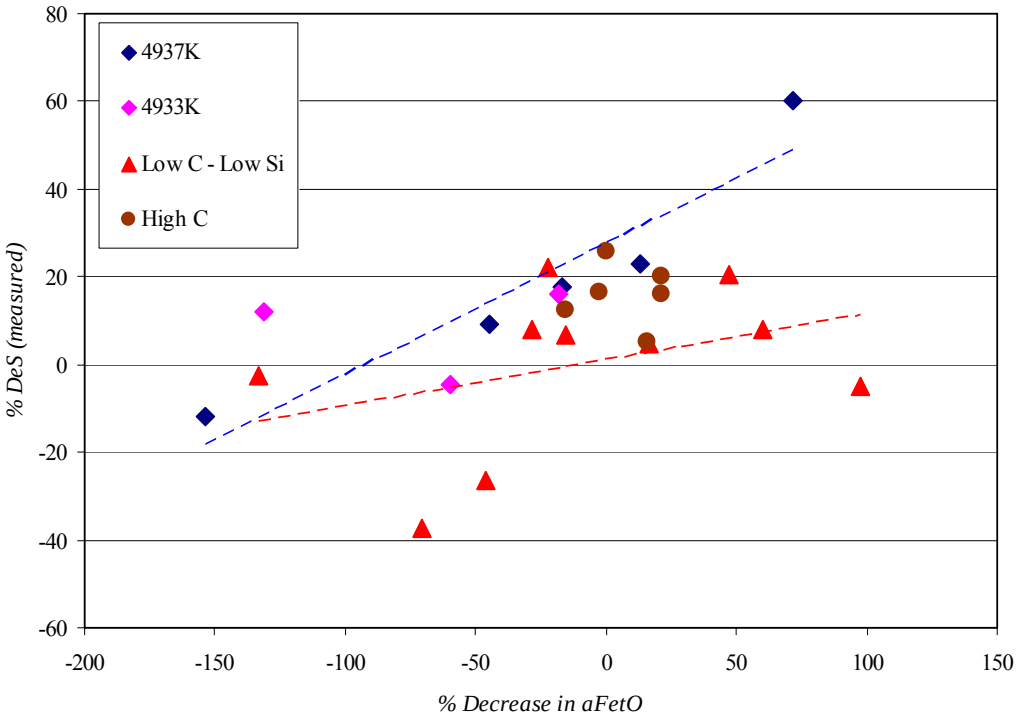

Figure 4.6 The variation of *% Decrease in* a_{Fe_tO} with *%DeS (measured)* for 4937K and other slag samples produced in ERDEMİR plant

4.2.2 Activity Calculations Using Steel Oxygen Activities

As indicated previously, oxygen activity of a steel bath can be calculated using the following equation for Al-killed steels [73]:

$$Al_2O_3(s) = 2\underline{Al}(\%) + 3\underline{O}(\%) \qquad \text{(74-reversed)}$$

In the past, many laboratory experiments were conducted to measure oxygen activity of liquid steel using the EMF technique. Oxygen sensors were introduced together with these studies. The working principles of oxygen sensors were given in literature, in detail [101]. To be consistent with the commercial oxygen sensor readings, the following apparent equilibrium constant may be used for reaction (74-reversed) for pure Al_2O_3 as the reaction product [49].

$$k_a = \frac{[\%Al]^2 \cdot [ppmO \cdot f_O]^3}{a_{Al_2O_3}} \qquad (82)$$

where

$$\log k_a = -\frac{62680}{T} + 32.54 \qquad (83)$$

The alumina activity is with respect to pure solid Al_2O_3. The effect of Al on the activity coefficient of oxygen dissolved in liquid steel is given by $-\log f_O = 3.9 * [\%Al]$. At low concentrations of aluminum, $f_{Al} \approx 1.0$

Another point to be clarified is that in the commercial oxygen sensor system, the EMF reading of the oxygen activity is displayed on the instrument panel in terms of ppm O, as though the activity coefficient $f_O = 1.0$ in the Al-killed steel. If the deoxidized steel contains 0.05% Al, the apparent oxygen activity using equation

(82) will be $[ppmO \cdot f_O]$ = 3.62; noting that at 0.05% Al, $f_O = 0.64$, the apparent concentration of dissolved oxygen will be 3.62/0.64 = 5.65 ppm O [49].

In the previous section, the activity coefficient of Fe_tO for low sulfur quality, 4937K, was determined by using an empirical relation obtained from the literature [74]. This relation is valid for a certain slag composition range which is given previously. As a different approach, it is also possible to calculate activity coefficient of Fe_tO using steel oxygen activity data. One type of oxygen sensors commonly used in practice is named as Celox (produced by Electronite) and it is currently used in ERDEMİR steelmaking plant at the secondary metallurgy [102]. It is used almost in every heat in ladle furnace where desulfurization experiments have been performed in the scope of this thesis study. After fine adjustment of steel composition at the ladle furnace, (i.e. before sending the ladle to the continuous caster) steel oxygen activity is measured and monitored. Although the results of whole steel samples especially soluble Al content of the steel should be evaluated to ensure sufficient deoxidation, it is a helpful tool at the first glance to understand whether the complete deoxidation of steel is accomplished or not. While slag sampling is assumed to be conducted at the time of steel sampling, oxygen activity mesaurement time more or less coincides with the steel sampling time. Oxygen activity measurement time is recorded like steel sampling time therefore it is possible to analyse the average time difference between the former and the latter. Generally speaking, oxygen activity measurement is performed before the last steel sampling. In some cases oxygen activity is measured at the beginning of ladle treatment. This measurement is also conducted before the first steel sample at the ladle furnace.

The difference between the oxygen activity measurement time and the chemical analysis time was studied for 4937K steel quality. The distribution of data was illustrated as a histogram using Statistica and is shown in Figure 4.7. Fifty one heats of 4937K were examined and the average time difference between the oxygen activity measurement time and the steel sampling time was found as 2.04 minutes

with a standard deviation of 1.81 minutes. Only in 22% of the heats the two samplings were seen to be performed in the same minute. In reality, since the mesurement time is stored in database in 'hour:minute' format and the seconds are not included, this percentage must be greater. It was shown that average ladle treatment time for 4937K was around 50 minutes. Therefore, average of 2 minutes difference between the two samples can be neglected considering the ladle treatment time so steel oxygen activity data is assumed to be recorded at the same time of steel sampling (and also at the same time of slag sampling; according to the assumption made in Chapter 3).

Similar work was performed for 7112K steel quality (C: 0.02-0.04%; Si: 0.030% max.) and the difference between the oxygen activity measurement time and the steel sampling time is presented in Figure 4.8. The average time difference was reported as 2.30 minutes with a standard deviation of 2.30 minutes. In the [0,3] minutes region 7112K quality showed similar distribution with 4937K and therefore the assumption given above can be taken also true for 7112K quality.

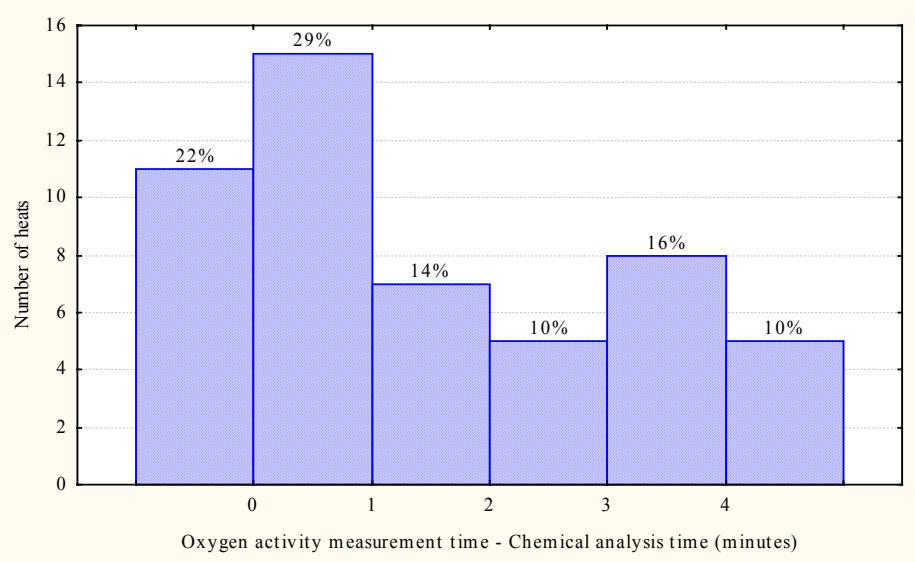

Figure 4.7 Distribution of difference between oxygen activity measurement time and chemical analysis time for 4937K steel quality heats (51 heats)
(Average: 2.04, minimum: 0, maximum: 7, std. deviation: 1.81)

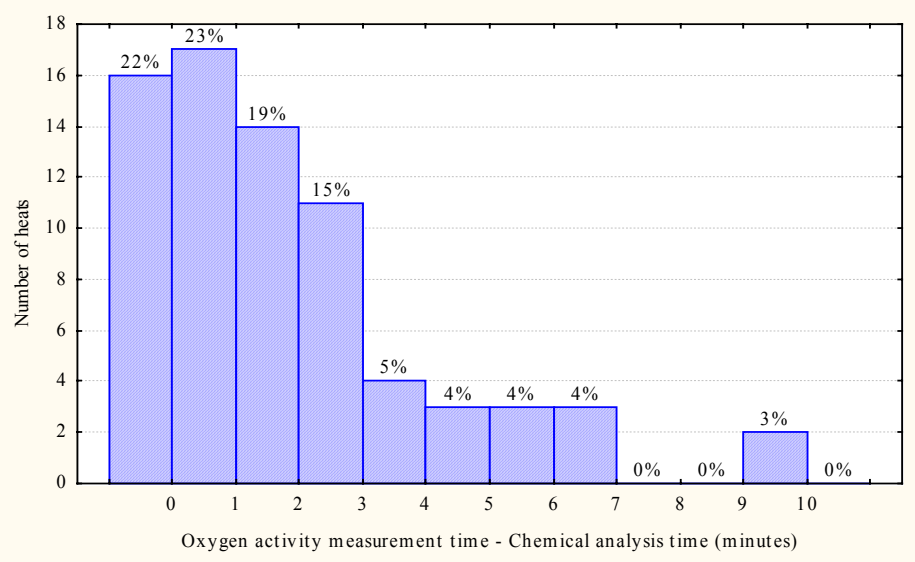

Figure 4.8 Distribution of difference between oxygen activity measurement time and chemical analysis time for 7112K steel quality heats (73 heats)
(Average: 2.30, minimum: 0, maximum: 10, std. deviation: 2.30)

The measured steel oxygen activity data were used in the calculation of γ_{Fe_tO} according to the reaction (79) and the relation (80). Therefore, the Mathcad program written for the calculation of γ_{Fe_tO} was changed such that oxgen activity value was given as an input while activity coefficient of Fe_tO were calculated and presented as an output of the program. The modified program and sample output are presented in Appendix F.

γ_{Fe_tO} values calculated by using steel oxygen activities were then treated with Statictica software to obtain a relation between γ_{Fe_tO} and major slag components. For this purpose, a multiple regression analysis was conducted. In that analysis, γ_{Fe_tO} was determined as dependent variable while SiO_2, Al_2O_3, CaO and MgO were selected as independent variables. Together with the multiple regression method, the following relation was obtained:

$$\gamma_{Fe_tO} = -0.162 - 0.0006(\%SiO_2) + 0.0046(\%Al_2O_3) + 0.0011(\%CaO) + 0.0067(\%MgO)$$

$$(R = 0.93;\ R^2 = 0.86;\ \text{Adjusted}\ R^2 = 0.82) \qquad (84)$$

The regression analysis conducted in the present study was based on 4937K heats. The slag compositions of each steel quality may differ from one another due to the differences of practices applied after BOF and during secondary metallurgy. For example, ultra low carbon steel qualities are tapped from the converter in rimming condition in order to use oxygen dissolved in liquid steel for effective decarburization in vacuum degasser. Therefore, deoxidation is not applied during tapping from the converter. For this reason, in those heats the slag present on top of liquid steel contains at least 15.0-20.0% Fe_tO which is the sign of highly oxidizing slag. Generally, first slag sample of Al-killed low C steel qualities at the ladle furnace contains around 10.0% Fe_tO although these are not given here. The desulfurization behaviour of these slags corresponding to those qualities shows significant difference, and therefore expressions obtained regarding to activity coefficients and activities should show considerable differences from one another.
The relation between γ_{Fe_tO} (measured a_O) and γ_{Fe_tO} (regression formula) is presented in Figure 4.9.

The relation (84) given above can also be used to predict steel oxygen activity. In some cases, at the beginning of ladle treatment no celox measurements are made. Therefore the activity coefficient of Fe_tO, γ_{Fe_tO}, calculated by expression (84) can be used to calculate steel oxygen activity for 4937K heats corresponding to the first slag samples. Minimum-maximum values of slag composition for 4937K slags are illustrated in Table 4.9.

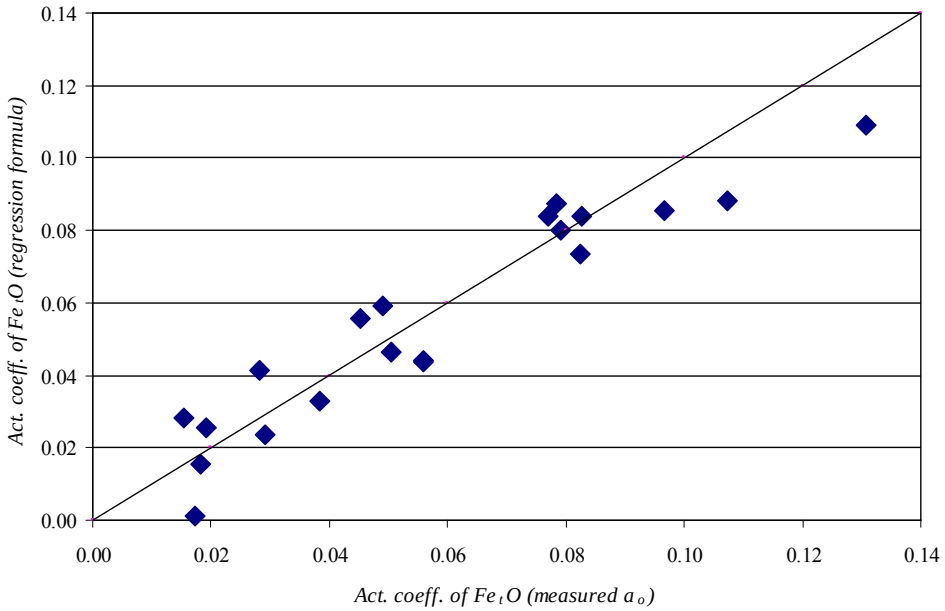

Figure 4.9 The relation between γ_{Fe_tO} (measured a_O) and γ_{Fe_tO} (regression formula)

Table 4.9 Minimum-maximum values of slag composition for 4937K slags (wt%)

	Fe_tO	SiO_2	MnO	Al_2O_3	CaO	MgO
Minimum	1.05	2.29	0.31	14.74	46.78	4.00
Maximum	11.95	7.62	8.46	33.99	57.75	9.14

The activity coefficient of Fe_tO, γ_{Fe_tO}, calculated using steel oxygen activity data can be used to obtain activity of Fe_tO in slag, a_{Fe_tO}. The activity of Fe_tO of the first slag samples are expected to be greater than the ones corresponding to the second slag samples. Together with the ladle practices applied to decrease the sulfur content of the steel, activity of Fe_tO, a_{Fe_tO}, in slag should be decreasing towards the end of ladle metallurgy. To visualise the degree of change of activity of Fe_tO, *% Decrease in* a_{Fe_tO} term was again used. It was defined previously as $[(a_{Fe_tO_{Sample\ 1}} - a_{Fe_tO_{Sample\ 2}}) / a_{Fe_tO_{Sample\ 1}}] * 100$. In the same manner, the changes of

a_{Fe_tO} were also studied in relation to sulfur removal data obtained in the ladle as conducted in the calculations using Ohta and Suito's regression analysis. *% Decrease in* a_{Fe_tO} with *%DeS (measured)* calculated with this method are shown in Table 4.10. *% Decrease in* a_{Fe_tO} with *%DeS (measured)* relationship was also treated graphically. The results are illustrated with pink coloured square dots in Figure 4.10 together with those obtained with Ohta and Suito's regression equation.

The scattered data were also tried to be represented with a best line so a pink coloured dashed line was obtained to illustrate the tendency of *%DeS (measured)* with the change in *% Decrease in* a_{Fe_tO}. As an example, using the best line one can read from the Figure 4.10 that *%DeS (measured)* value of 30.0 corresponds to a *% Decrease in* a_{Fe_tO} value of approximately 35.0.

Table 4.10 *% Decrease in* a_{Fe_tO} and *%DeS (measured)* values for 4937K experiments
(γ_{Fe_tO} values calculated by using steel oxygen activities)

4937K heats	$a_{FetO}(1)$	$a_{FetO}(2)$	*% Decrease in* a_{Fe_tO}	$\%\underline{S}_{initial}$	$\%\underline{S}_{final}$	*%DeS (measured)*
526919	0.0052	0.0017	67.70	0.0071	0.0050	29.58
517076	0.0018	0.0015	15.47	0.0061	0.0047	22.95
517077	0.0026	0.0016	37.31	0.0056	0.0046	17.86
610618	0.002	0.0013	37.50	0.0079	0.0038	51.90
610620	0.0011	0.0012	-12.96	0.0105	0.0042	60.00
631253	0.0009	0.0018	-105.81	0.0055	0.0050	9.09
616522	0.0018	0.0013	27.37	0.0056	0.0044	21.43
634021	0.0012	0.0014	-20.51	0.0040	0.0039	2.50

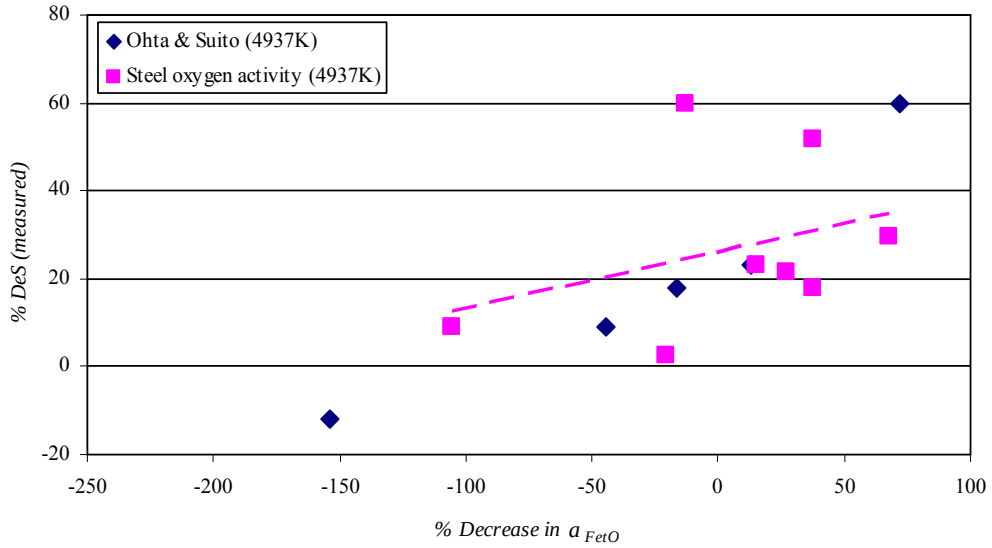

Figure 4.10 The variation of *% Decrease in* a_{Fe_tO} with *%DeS (measured)* for 4937K experiments

To confirm this behaviour, an experiment (625067) was conducted with a *% Decrease in* a_{Fe_tO} value of around 35.0 to see whether a similar *%DeS (measured)* value (i.e. near 30.0) could be found or not. As explained before, oxygen potential of the system can be expressed either by oxygen activity of the steel or by Fe_tO activity of the slag. As it can be seen from relation (80), oxygen activity of the steel and Fe_tO activity of the slag are directly proportional quantities and both represent the similar meaning considering desulfurization. Therefore, *% Decrease in* a_{Fe_tO} can possibly be replaced with *% Decrease in* a_O. As a result of this replacebility, through celox measurements at the beginning and at the end of ladle treatment, *% Decrease in* a_O could be calculated immediately during experiments. Since there is no online slag analysis measurement device in the ladle furnace, a_{Fe_tO} could not be calculated at the time of ladle process.

In the heat of 4937K steel quality numbered as 625067, at the beginning of ladle treatment steel oxygen activity value of 5.48 ppm was monitored using celox

measurement. The analysis of first steel sample indicated a sulfur value of 0.0059%. Slag samples were taken both at the beginning and at the end of ladle treatment. The celox measurement at the end of ladle treatment indicated an oxygen activity of 3.50 ppm. Therefore, *% Decrease in* a_O was calculated as [(5.48-3.50)/5.48]*100 = 36.13. The last steel sample of the heat gave a sulfur value of 0.0038%; so *%DeS (measured)* value was turned out to be as [(0.0059-0.0038)/0.0038]*100 = 35.59. Using the best line equation, *% Decrease in* a_O value of 36.13 corresponds to *%DeS (measured)* value of 30.77(Figure 4.10). Therefore, *%DeS (measured)* value obtained in the ladle were close to the one calculated from the best line equation. In conclusion, the result of this experiment confirmed that the behaviour of *%DeS (measured)* with the change in *% Decrease in* a_{Fe_tO} could be represented with the relation cited in Figure 4.10. The slag samples taken during ladle treatment were analysed and activity calculations were performed. *% Decrease in* a_{Fe_tO} value of the experiment was found as 30.60 being a similar value with *% Decrease in* a_O, as expected. Normalized slag analysis of the 4937K run, *% Decrease in* a_O, *%DeS (measured)* and *% Decrease in* a_{Fe_tO} values are illustrated in Table 4.11.

Table 4.11 Normalized slag analysis of the 4937K experiment (625067) and the activity values

		Normalized values (%)						Temp. (°C)
Heat Nr.	Sample Nr.	Fe_tO	SiO_2	MnO	Al_2O_3	CaO	MgO	
625067	1	6.30	3.36	4.80	21.92	59.38	3.80	1616
	2	3.86	5.57	4.33	24.30	55.96	5.05	1595
Heat Nr.	Sample Nr.	Steel Oxygen Activity * (ppm)	a_{Fe_tO}	*%Decrease in* a_O	%S initial	%S final	*%DeS (measured)*	*%Decrease in* a_{Fe_tO}
625067	1	5.48	0.0026	36.13	0.0059	0.0038	35.59	30.60
	2	3.50	0.0018					

* Treated as oxygen activity when $f_O = 1$.

In ERDEMİR steelmaking plant, steel qualities of various kinds are currently produced. More than 50 % of the slab production belongs to low carbon (LC) steel qualities (C: 0.005-0.08%). 4937K is one of the low carbon steel grades. The behaviour of 4937K slags was studied in the scope of the present work, in detail. The desulfurization data and slag analysis of LC steel qualities of various types were also examined [103]. In that respect, low carbon steels having carbon content of 0.02-0.06% were analysed. These qualities were Al-killed steel grades like 4937K and their silicon content was restricted to 0.035% max. The slag compositions were normalized and activity coefficient calculations were conducted in the same manner: Steel oxygen activity values were utilized. The relation obtained by Ohta and Suito was not applicable to those slags since Fe_tO content of them were mostly larger than 5 wt%. Normalized slag analysis of LC heats are presented in Table 4.12. Slag compositions corresponding to heat a, b and c providing the highest *% DeS (measured)* values were taken into account. *% Decrease in* a_{Fe_tO} values were calculated. *% Decrease in* a_{Fe_tO} and *%DeS (measured)* values for LC heats are illustrated in Table 4.13. The corresponding data for LC heats are superimposed to Figure 4.10 and therefore all are shown in Figure 4.11.

Table 4.12 Normalized slag analysis of LC heats

			Normalized values (%)						Steel
Heat	LC heats	Sample Nr.	Fe_tO	SiO_2	MnO	Al_2O_3	CaO	MgO	Temp. (^oC)
a	526878	1	9.12	5.07	1.80	25.60	50.96	7.10	1609
		2	4.29	4.44	1.35	30.67	50.24	8.97	1601
b	536511	1	4.35	10.51	2.17	28.59	47.21	7.04	1597
		2	1.95	9.65	0.84	31.87	47.94	7.73	1601
c	518622	1	9.21	3.99	2.62	24.42	53.30	6.07	1600
		2	3.48	4.39	1.64	31.05	46.86	12.51	1595

Table 4.13 *% Decrease in* a_{Fe_tO} and *%DeS (measured)* values for LC heats (γ_{Fe_tO} values calculated by using steel oxygen activities)

Heat	LC heats	$a_{FetO}(1)$	$a_{FetO}(2)$	*% Decrease in* a_{Fe_tO}	$\%\underline{S}_{initial}$	$\%\underline{S}_{final}$	*%DeS (measured)*
a	526878	0.0017	0.0022	-31.05	0.0072	0.0053	26.39
b	536511	0.0023	0.0017	25.51	0.0067	0.0046	31.34
c	518622	0.0016	0.00157	4.00	0.0112	0.0073	34.82

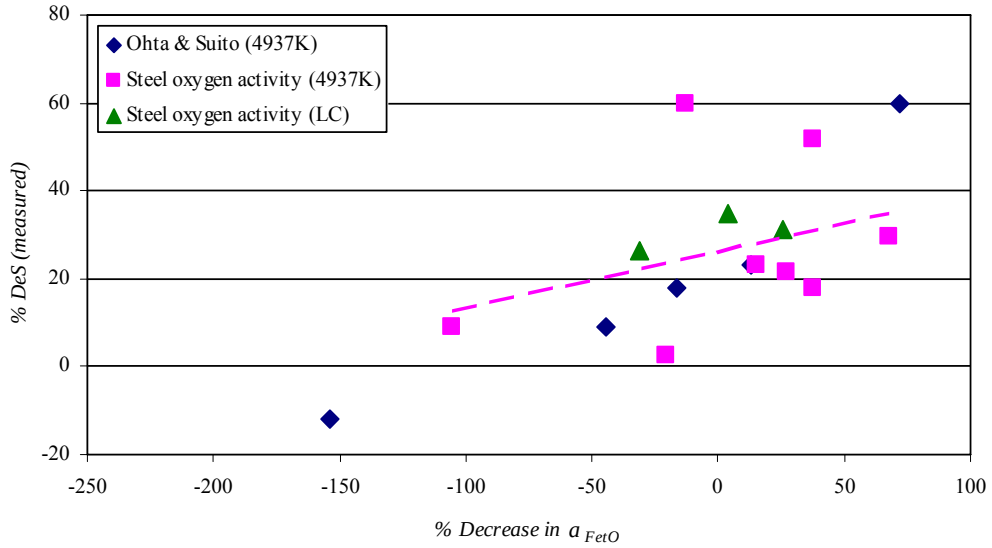

Figure 4.11 The variation of *% Decrease in* a_{Fe_tO} with *%DeS (measured)* for 4937K and LC heats

In both methods of approach (Ohta and Suito & Steel oxygen activity), *%DeS (measured)* was found to increase as *% Decrease in* a_{Fe_tO} increased. This tendency was in accord with the expectations. The relation obtained by using measured steel oxygen activities for 4937K steel quality was of course valid for a limited slag composition range compared to the one cited by Ohta and Suito [74]. On the other hand, since calculations conducted using steel oxygen activities directly outlined the results related to 4937K, this approach was considered to be more suitable for 4937K slags. In conclusion, the formulation relating γ_{Fe_tO} with the major slag

components derived in this study was found to be representative for 4937K slags, showing similar behaviour with the one obtained by Ohta and Suito. Slag compositions of some LC heats gave similar results like that of 4937K quality considering *%DeS (measured)* and *% Decrease in* a_{Fe_tO} values. Since LC steel qualities take considerable portion of slab production, this point is important to show the general desulfurization behaviour of ERDEMİR slags. Thermodynamically, sulfur slag-metal distribution ratio depends mainly on metal composition, slag composition and oxygen potential of the system [17]. Kinetically, good steel desulfurization requires sufficient time for slag-metal reactions to reach equilibrium. The data obtained in the scope of this work reflected directly the operating conditions of the steelmaking shop, where it may be something difficult to allocate time for reactions to reach equilibrium state. On the other hand, the necessary time should be allowed for a heat to ensure desired level of desulfurization. This behaviour could also be seen from Figure 4.11.

4.2.3. Activity Calculations Using Temkin Equation

In this section, the relationship between *% Decrease in* a_{Fe_tO} and *%DeS (measured)* was investigated using Temkin equation [7,27]. The results obtained from Temkin equation for 4937K runs were then compared with the ones obtained using steel oxygen activities and Ohta and Suito's formula [74].

Being the first quantitative interpretation of slag-metal equilibria based on the ionic constitution of basic slags, Temkin's model states that silicon, phosphorus and aluminum exist only in complex SiO_4^{4-} , PO_4^{3-} and AlO_3^{3-} anions. In basic slags, other than these complex anions, O^{2-} ions and R^{2+} metal ions from the basic RO oxides (e.g. CaO, MgO, MnO and FeO) are present. For CaO, Al_2O_3, SiO_2, MgO, MnO, FeO slag system examined in the scope of this PhD thesis study, the dissociation scheme can be written as follows [7]:

$$wSiO_2 + yAl_2O_3 + zRO = w\ SiO_4^{4-} + 2y\ AlO_3^{3-} + (z-2w-3y)\ O^{2-} + z\ R^{2+} \quad (85)$$

where w, y and z represents number of moles of each constituent. The slag is said to be basic when (z-2w-3y) is a positive value, i.e. free oxygen ions exist [7].

As indicated in Chapter 2, according to theory of Temkin, thermodynamic activity of the molten oxide is the activity product of ionic fractions over cationic and anionic matrices [27]. The activity of ferrous oxide in a slag can therefore be expressed as [7]:

$$a_{FeO} = N_{Fe^{2+}} \cdot N_{O^{2-}} \tag{86}$$

where the ionic fractions of iron and oxygen are the fractions of these ions referred to the total number of ions of the same sign [7]:

$$N_{Fe^{2+}} = \frac{n_{Fe^{2+}}}{\sum n_{cations}} \tag{87}$$

$$N_{O^{2-}} = \frac{n_{O^{2-}}}{\sum n_{anions}} \tag{88}$$

Number of moles of anions and cations present in CaO-Al_2O_3-SiO_2-MgO-Fe_tO-MnO slag system and anionic, cationic fractions and activity of iron oxide were calculated using a program written in Mathcad. This program and a sample output are illustrated in Appendix G. Iron oxide present in the slags was again assumed to contain only Fe^{2+} ions and denoted as Fe_tO. The results of calculations were tabulated and presented in Table 4.14.

Activity of iron oxide, a_{Fe_tO}, values calculated using Temkin equation were then treated to obtain the relationship between *% Decrease in* a_{Fe_tO} and *%DeS (measured)* for 4937K slags. The relation obtained using Temkin model is shown in Figure 4.12 together with the ones obtained from Ohta and Suito's formula and steel oxygen activities. The trend lines are also presented in Figure 4.12.

Table 4.14 Anionic and cationic fractions and activity of iron oxide in $CaO\text{-}Al_2O_3\text{-}SiO_2\text{-}MgO\text{-}Fe_tO\text{-}MnO$ slag system using Temkin equation

4937 Runs	S. Nr.	Fe_tO	SiO_2	MnO	Al_2O_3	CaO	MgO	$n_{Fe^{2+}}$	Σ ations	$N_{Fe^{2+}}$	$n_{O^{2-}}$	Σ nions	$N_{O^{2-}}$	a_{Fe_tO}		
526919	1	6.12	6.52	5.41	25.37	48.33	7.74	0.085	1.218	0.070	0.254	0.860	0.295	0.021		
517076	1	2.69	7.62	3.75	29.67	48.38	7.53	0.037	1.142	0.033	0.016	0.724	0.0217	0.001		
517080	1	8.45	6.67	5.33	20.68	54.03	4.00	0.117	1.257	0.093	0.427	0.943	0.452	0.042		
610618	1	7.94	5.03	4.72	18.52	56.98	6.04	0.110	1.345	0.082	0.633	1.080	0.586	0.048		
610620	1	5.11	4.64	5.62	20.42	57.75	6.01	0.071	1.332	0.053	0.576	1.054	0.547	0.029		
631253	1	4.97	4.32	3.71	24.53	56.97	4.95	0.069	1.262	0.055	0.397	0.950	0.418	0.023	*%Decr. in* a_{Fe_tO}	*%DeS (meas.)*
616522	1	11.95	5.08	5.31	14.74	57.26	4.93	0.166	1.387	0.120	0.784	1.157	0.677	0.081		
634021	1	8.71	4.64	5.38	20.74	54.12	5.66	0.121	1.305	0.093	0.540	1.024	0.527	0.049		
526919	2	1.95	6.33	2.77	30.99	49.50	8.11	0.027	1.153	0.023	0.030	0.743	0.041	0.001	95.36	29.58
517076	2	1.62	7.50	1.77	30.55	49.34	8.93	0.023	1.152	0.020	0.003	0.727	0.004	0.0001	87.80	22.95
517080	2	1.50	5.24	1.61	30.71	52.67	7.98	0.021	1.184	0.018	0.106	0.795	0.133	0.002	94.46	25.32
610618	2	1.84	4.50	1.54	26.41	56.29	9.14	0.026	1.281	0.020	0.354	0.947	0.374	0.007	84.47	51.9
610620	2	1.05	2.29	0.31	33.99	53.36	8.54	0.015	1.185	0.012	0.109	0.814	0.134	0.002	94.33	60
631253	2	4.07	4.33	2.95	27.18	55.33	5.66	0.057	1.228	0.046	0.284	0.889	0.319	0.015	35.64	9.09
616522	2	5.25	6.03	5.10	22.77	53.38	6.49	0.073	1.260	0.058	0.390	0.936	0.416	0.024	70.31	21.43
634021	2	8.44	4.76	4.94	20.89	55.39	4.96	0.117	1.300	0.090	0.527	1.016	0.519	0.047	4.35	2.5

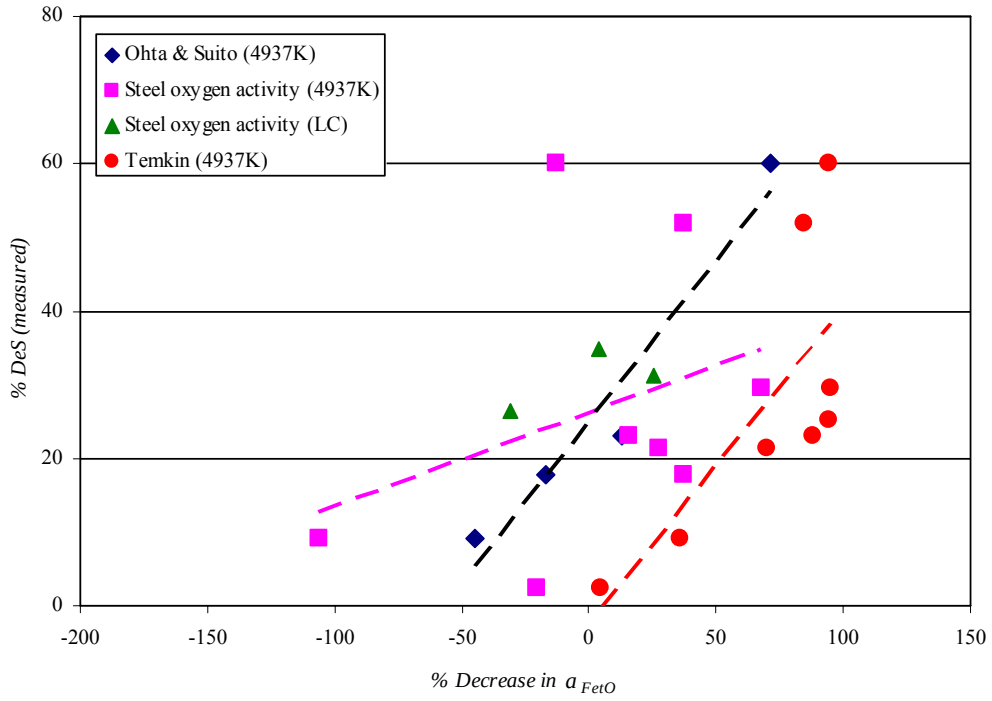

Figure 4.12 The relationship between *% Decrease in* a_{Fe_tO} and *%DeS (measured)* using a) Ohta and Suito's regression equation, b) Steel oxygen activity values, c) Theory of Temkin

As it can be seen from Figure 4.12, similar results were obtained with Temkin equation. Calculated activity changes were reported to correspond lower *%DeS (measured)* values in Temkin's approach. In other words, for the same *%DeS (measured)* data, higher *% Decrease in* a_{Fe_tO} values were obtained with Temkin equation. Therefore, the trendline of the values calculated from Temkin model were found to settle right side of the ones obtained from Ohta and Suito's regression equation. The possible cause of this shift may be attributed to differences of components incorporated in calculations. In the calculations using theory of Temkin, all 6 major components were taken into account for activity of Fe_tO determination, whereas 4 components of slag system, namely CaO, Al_2O_3, SiO_2 and MgO, were used to calculate activity coefficient of Fe_tO in Ohta and Suito's approach. Other than this shift, the slopes of the trendlines obtained from Ohta & Suito and Temkin were found to be nearly the same. *% Decrease in*

a_{Fe_tO} values showed similar variations with *%DeS (measured)* in both approaches. Therefore, it was concluded that the two approaches applied to 4937K slags were found to give similar results as far as the relation between *% Decrease in* a_{Fe_tO} and *%DeS (measured)* was considered.

The results obtained from Temkin equation were found to show similar tendency with the ones obtained from steel oxygen activities in that *%DeS (measured)* values were reported to increase with *% Decrease in* a_{Fe_tO}. As discussed in Section 4.2.2, the results obtained by using steel oxygen activities was concluded to be representative for 4937K slags showing also similar behaviour with the one obtained by using Temkin model.

4.2.4 Activity Calculations Using Polymeric Anion Model

In this section, the relationship between *% Decrease in* a_{Fe_tO} and *%DeS (measured)* was investigated using the polymeric anion model and the results obtained for 4937K slags were compared with the ones given in previous sections.

According to the polymeric anion model, the silicate ions consist either of linear or branched chains of general formula $Si_nO_{3n+1}^{2(n+1)-}$ [28]. Considering the polymers having branched chain configurations, Masson et.al. [28,104-106] suggested some k_{11} values for different binary systems: k_{11} value for FeO containing binary system at 1600 ^oC was suggested as 1.0. For the calculations regarding to steelmaking slags examined in the current PhD thesis, k_{11} value of 1.0 was therefore determined to be used. Using the relation (17) given in Chapter 2, the following reactions were obtained for n values starting from 1 to 4:

$$n=1 \qquad SiO_4^{4-} + SiO_4^{4-} \Leftrightarrow Si_2O_7^{6-} + O^{2-} \tag{89}$$

$$n=2 \qquad SiO_4^{4-} + Si_2O_7^{6-} \Leftrightarrow Si_3O_{10}^{8-} + O^{2-} \tag{90}$$

$$n=3 \qquad SiO_4^{4-} + Si_3O_{10}^{8-} \Leftrightarrow Si_4O_{13}^{10-} + O^{2-} \tag{91}$$

$$n = 4 \qquad SiO_4^{4-} + Si_4O_{13}^{10-} \Leftrightarrow Si_5O_{16}^{12-} + O^{2-} \tag{92}$$

From the equilibrium constants of these reactions, the following equations were obtained. Here, Si denotes the equilibrium number of moles of SiO_4^{4-}, Si_2 shows the equilibrium number of moles of $Si_2O_7^{6-}$, and so on. Abbreviation of (oxy) represents the equilibrium number of moles of (O^{2-}). k_{12}, k_{13} and k_{14} can be calculated using relation (18) given in Chapter 2.

$$Si_2 = \frac{k_{11}Si^2}{(oxy)} \tag{93}$$

$$Si_3 = \frac{k_{11}k_{12}Si^3}{(oxy)^2} \tag{94}$$

$$Si_4 = \frac{k_{11}k_{12}k_{13}Si^4}{(oxy)^3} \tag{95}$$

$$Si_5 = \frac{k_{11}k_{12}k_{13}k_{14}Si^5}{(oxy)^4} \tag{96}$$

Since the number of moles of SiO_2 present in the slag samples can be found from the slag analysis, the following mass balance equation can be written:

$$Si + 2Si_2 + 3Si_3 + 4Si_4 + 5Si_5 = \frac{(SiO_2)}{60} \tag{97}$$

The equilibrium number of moles of (O^{2-}) present in the slags can be formulated considering the basic and the acidic oxides as follows:

$$(oxy) = \frac{(FeO)}{72} + \frac{(MnO)}{71} + \frac{(CaO)}{56} + \frac{(MgO)}{40} - 3 \cdot \frac{(Al_2O_3)}{102} + 2 \cdot \frac{(SiO_2)}{60} - 4Si - 7Si_2 - 10Si_3 - 13Si_4 - 16Si_5 \quad (98)$$

The oxides given in parantheses are the normalized slag analysis in wt% and can be found in Table 4.7.

The set of nonlinear equations from (93) to (98) were solved for each slag sample. Si, Si_2, Si_3, Si_4, Si_5 and (oxy) values were obtained using Mathcad program. A sample run of this program is illustrated in Appendix H. Anionic fraction of (O^{2-}) can be calculated from the following relation:

$$N_{O^{2-}} = \frac{(oxy)}{(oxy) + Si + Si_2 + Si_3 + Si_4 + Si_5 + 2 \cdot \frac{(Al_2O_3)}{102}} \quad (99)$$

Here, aluminum in the slag is supposed to exist in AlO_3^{3-} form as stated in Temkin model [7]. Cationic fraction of (Fe^{2+}) is the same as calculated in Section 4.2.3. Therefore, a_{Fe_tO} is the multiplication of cationic fraction of (Fe^{2+}) with anionic fraction (O^{2-}). Results obtained from Mathcad program and activity of iron oxide values calculated for 4937K slags were tabulated and and given in Appendix H.

Using a_{Fe_tO} values calculated, the relation between *% Decrease in* a_{Fe_tO} and *%DeS (measured)* was then investigated. The relation obtained using the polymeric anion model is shown in Figure 4.13 together with the results obtained from Ohta & Suito's formula, steel oxygen activities and Temkin equation. The points obtained from the polymeric anion model were indicated with brown-colour plus signs and a brown-colour trendline was also depicted in Figure 4.13.

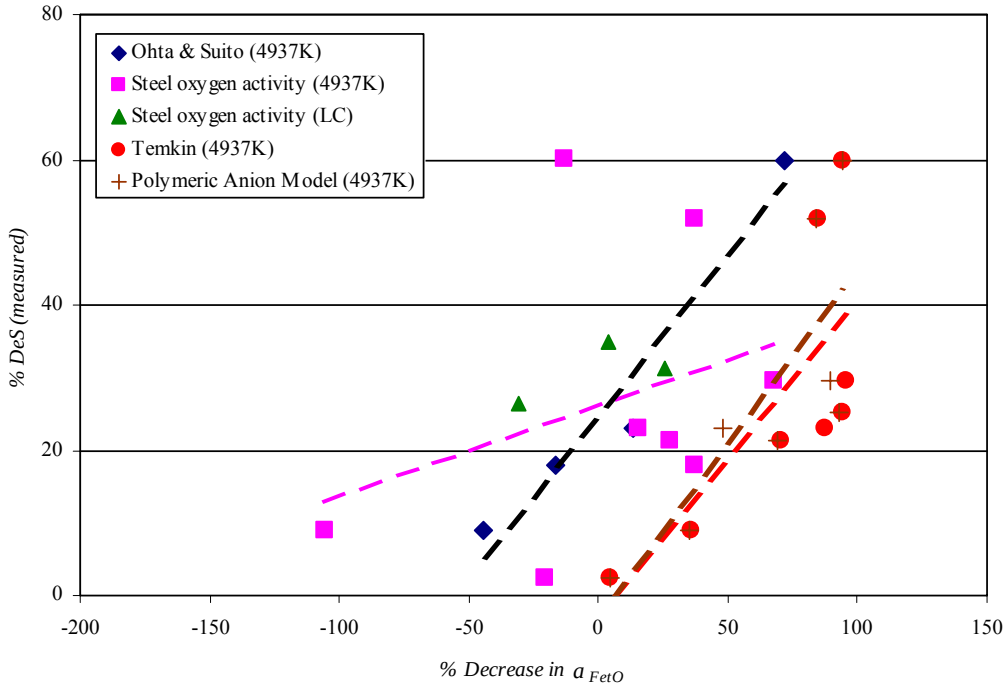

Figure 4.13 The relationship between *% Decrease in* a_{Fe_tO} and *%DeS (measured)* using a) Ohta and Suito's regression equation, b) Steel oxygen activity values, c) Theory of Temkin, d) Polymeric anion model

As seen from Figure 4.13, similar results were found from the polymeric anion model. According to Temkin model, 4 oxygen atoms are needed to form a complex SiO_4^{4-} anion. On the other hand, according to the polymeric anion model less than 4 oxygen atoms are used in the formation of silicate anions indicating more free oxygen ions present in the slags. This can be seen from comparing $n_{O^{2-}}$ values of Table 4.14 and Table H.1. Application of the polymeric anion model gave therefore higher anionic fractions of (O^{2-}) and eventually higher a_{Fe_tO} values. Considering *% Decrease in* a_{Fe_tO} values, similar results were found for both models. The trendline obtained for the polymeric anion model is slightly above the one obtained for Temkin eqution.

The results obtained from the polymeric anion model showed a similar tendency with the ones calculated from Ohta and Suito's formula. Similar to the discussion made in Section 4.2.3, for the same *%DeS (measured)* data, higher *% Decrease in* a_{Fe_tO} values were obtained with the polymeric anion model. The slopes of trendlines obtained from both approaches were found to be nearly the same.

4.2.5 Relation Between Percentage of Sulfur Removal and Change in Steel Oxygen Activity

In the scope of the current study, the relation between the steel oxygen activity change and % desulfurization at the ladle furnace was studied for 4937K experiments. Change in steel oxygen activity at the ladle furnace was investigated with *% Decrease in* a_O parameter defined as $[(a_{O\,initial} - a_{O\,final})/a_{O\,initial}]\cdot 100$ where $a_{O\,initial}$ and $a_{O\,final}$ correspond to the steel oxygen activities at the beginning and at the end of secondary refining, respectively. Percentage of sulfur removal was designated as *%DeS (measured)*, as defined in Section 4.2.1.

The relation between *% Decrease in* a_O and *%DeS (measured)* was illustrated in Figure 4.14. As seen from the scattered data presented, *%DeS (measured)* was found to increase as *% Decrease in* a_O increased. Together with the top slag application for 4937K, the extent of desulfurization enhanced with the decrease in steel oxygen activity. This result was in accord with the expectations since the degree of desulfurization increases as the oxygen potential of the system decreases. Using least square method, a best line representing the relation was also depicted in Figure 4.14. The desulfurization behaviour obtained with the measured steel oxygen activity change was found to be similar with the one concerning % Decrease in a_{Fe_tO}, given in Figure 4.10.

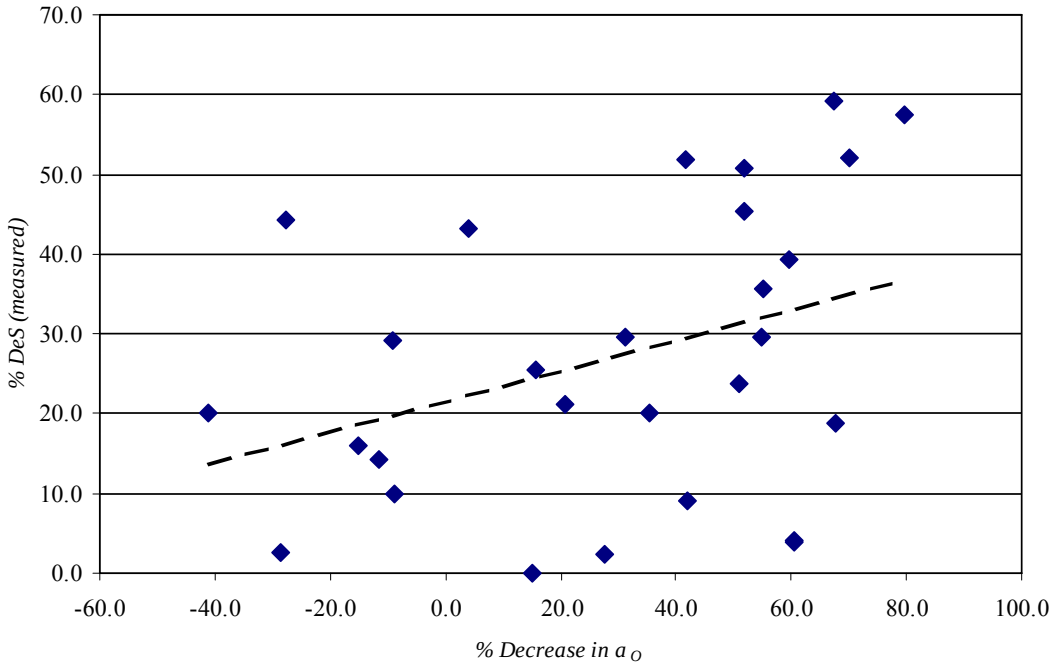

Figure 4.14 The variation of *% Decrease in* a_O with *%DeS (measured)* for 4937K (28 runs)

4.3 Statistical Interpretation of % Desulfurization

In some preliminary work in Erdemir [107], desulfurization practice for the steel qualities 4937K, 9060K and 9065K at the secondary metallurgy plant was outlined. In that work, chemical composition and production route including typical alloy additions and top and bottom stirring data were discussed, in detail. Heats of these qualities performed in the year 2004 were examined as a whole and effect of ladle furnace process time on desulfurization was presented for each quality. Here, the same qualities were examined in such a way that amount of desulfurization was illustrated as a histogram obtained with Statistica. To determine amount of desulfurization, %desulfurization, defined as $[(\%\underline{S}_{initial} - \%\underline{S}_{final})/\%\underline{S}_{initial}]*100$, was studied for the same qualities mentioned above. $\%\underline{S}_{initial}$ and $\%\underline{S}_{final}$ were as defined in this work .

% Desulfurization value of 51 heats conducted in the year 2005 were examined and presented in histogram given in Figure 4.15 for 4937K steel. Average $[(\%S_{initial} - \%S_{final}) / \%S_{initial}] * 100$ value for 4937K quality steel was found as 29.29% showing a standard deviation of 20.77%. Sixtyfive heats of 9060K linepipe quality steel were cast in 2005 and %Desulfurization data calculated for this quality steel are shown as a histogram in Figure 4.16. Average %Desulfurization value was found as 21.78% with a standard deviation of 17.15%. Change of sulfur content of the steel produced as 9065K pipeline quality was also examined. Results of 233 heats were illustrated in Figure 4.17. Average %Desulfurization value was calculated as 23.16% with a standard deviation of 15.37%.

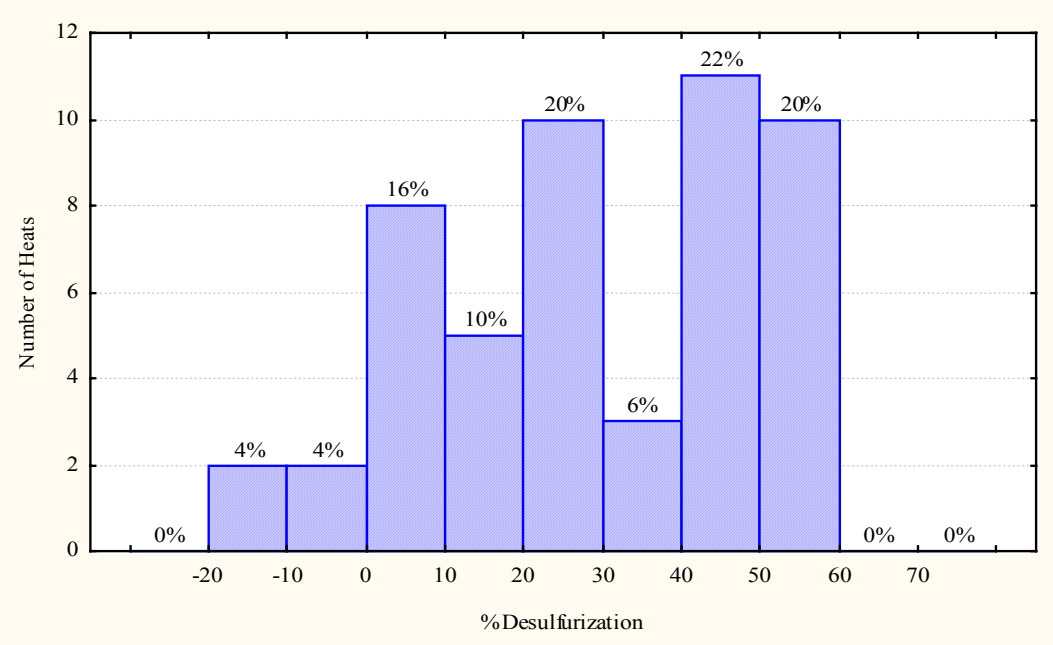

Figure 4.15 Distribution of % Desulfurization for 4937K steel heats (51 heats)
(Average: 29.29%, minimum: -12.50%, maximum: 60%, std. deviation: 20.77%)

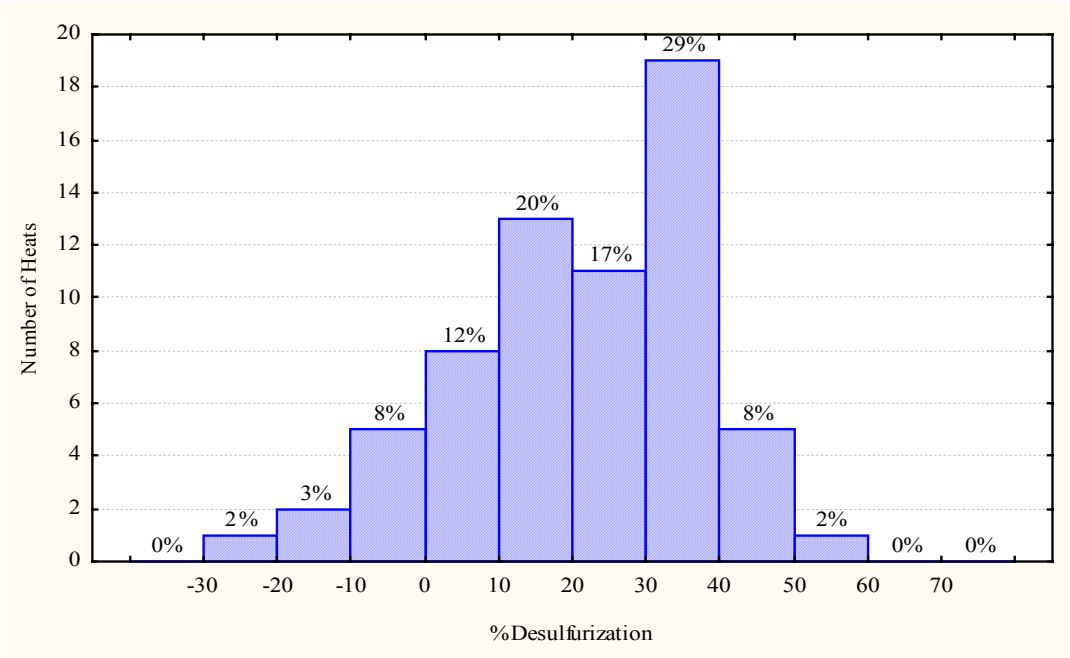

Figure 4.16 Distribution of % Desulfurization for 9060K steel heats (65 heats)
(Average: 21.78%, minimum: -25.00%, maximum: 51.85%, std.deviation: 17.15%)

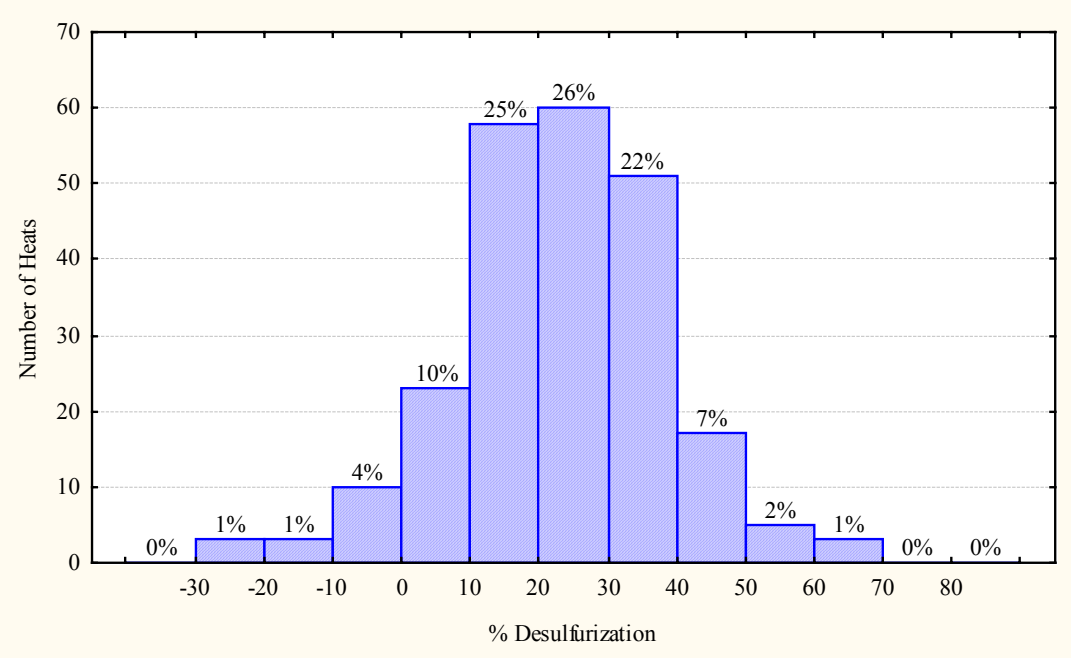

Figure 4.17 Distribution of % Desulfurization for 9065K steel heats (233 heats)
(Average: 23.16%, minimum: -28.57%, maximum: 64.04%, std.deviation: 15.37%)

Careful examination of %Desulfurization data of these steel qualities revealed that average sulfur removal during secondary metallurgy was the largest (around 29%) in 4937K steel. %Desulfurization data obtained in pipeline steel qualities, 9060K and 9065K, gave lower average sulfur removal, being 21.78% and 23.16%, respectively. These results are in accord with the expectations and they are closely related to the nature of ladle practices applied in the secondary metallurgy. Heats belonging to 4937K quality are normally treated with top slag application in ladle furnace and S content of the steel is intended to be lowered below 50 ppm which is a specification requirement of this type of steel. To achieve this, as well as the ladle operations, the converter end blow sulfur is tried to be set in more tight limits during production. In other words, conditions are set to lower sulfur content of hot metal as much as possible in desulfurization process before the converter stage. On the other hand, in 9060K and 9065K quality steel heats, specification limit of sulfur is 100 ppm so strong treatment of sulfur removal need not to be applied in ladle furnace in many cases compared to 4937K quality steel. Moreover, as indicated in the preliminary work in Erdemir plant [107], one of the most important parameters considering desulfurization in ladle furnace is the time and it mostly becomes important to satisfy the time requirement of slab production in continuous casting machines. Therefore, it may not be possible to decrease sulfur to much lower levels due to time limitation of the process, which will hopefully be overcome with the establishment of the second ladle furnace in 2007 in ERDEMİR plant.

4.4 Inclusion Morphologies of Ca-treated Steel Qualities

Shape control of sulfide inclusions includes formation of stable sulfide compounds, which precipitated with a small size and globular shape so that no deformation of inclusions can happen during rolling. The extent of sulfide shape control that can be achieved during solidification of calcium-treated steel depends on the total oxygen, sulfur and calcium contents of the steel. The following criteria were derived for the tundish compositions of aluminum-killed steels to give adequate sulfide shape control in the final product (Table 4.15) [2].

Table 4.15 Tundish composition ranges for Al-killed steels to achieve acceptable sulfide shape control [2]

O (ppm) as aluminate inclusions	Ca (ppm)	Mn (%)	S (ppm)
25	20-30	0.4-0.6	<20
25	20-30	1.3-1.5	<30
12	15-20	0.4-0.6	<10
12	15-20	1.3-1.5	<15

In steels with a total oxygen content of 10 ppm or less and relatively high sulfur contents, e.g.>100 ppm, sulfide shape control by means of calcium treatment is obviously not feasible [2].

Ca-treatment is currently applied to many steel qualities produced in ERDEMİR. It is important especially for hot-rolled steel products which are to be used in applications containing shaping (e.g. bending). CaSi wire injection is conducted during secondary metallurgy either in chemical heating station or in ladle furnace. As well as its power in inclusion shape control, Ca-treatment is found to be useful to improve castability of liquid steel (may be helpful to increase the content of $C_{12}A_7$ type liquid inclusions). Inclusion modification using CaSi injection is limited to the steel qualities having S of 0.010% maximum to prevent formation of CaS(s) which may lead to decrease castability, as indicated above. In the same way, excessive use of CaSi wire leads to the same result and therefore should be avoided.

Inclusions are characterized by size, shape, concentration and distribution rather than chemical composition. According to the terminology relating to metallography, inclusions may be divided into 4 different types: A-type: Sulfide, B-type: Alumina, C-type: Silicate, D-type: Globular oxide. Inclusion population within a given lot of steel varies with position. Therefore, the lot must be

statistically sampled in order to access its inclusion content. One of the most popular inclusion rating methods is JK inclusion rating which is a method of measuring non-metallic inclusions based on the Swedish Jernkontoret procedures. Another method, worst-field rating is a rating in which the specimen is rated for each type of inclusions by assigning the value for the highest severity rating observed of that inclusion type anywhere on the specimen surface. In the microscopic studies the specimen geometry is important: The recommended polished surface area of a specimen for the microscopical determination of inclusion content is 160 mm^2. For flat-rolled products, the section shall also be perpendicular to the rolling plane [100].

In the worst field inclusion rating method, severity level numbers which are determined by the total length of inclusions in one field at 100 magnification (for A, B and C types) or number of inclusions in one field (for D type) are used. Severity levels scale starts from 0 and ends at 5 (0, 1/2, 1, 1 ½, …, 5). Severity number increases as the number or total length of inclusions increases. For each specimen, (e.g. total of 6 specimens) 8 severity numbers should be determined from the worst field (Type-A thin, Type-A heavy, Type-B thin, Type-B heavy, and so on). Whether an inclusion is to be selected either thin or heavy depends upon the width of inclusion. Size ranges are given for inclusions for this purpose in the standard. At the end of 6^{th} specimen 48 severity numbers should be written in the chart. For each type, an average value is obtained and reported. These average values more or less indicate the inclusion characteristics of the product examined. Number of specimen is important for increasing the accuracy of the results [100].

In relation to Ca-treatment five different heats of chassis steel, wheel steels and pipe line steels were examined in an optical microscope. Samples taken from hot rolled products were prepared according to ASTM E45-97 (Reapproved 2002) standard in ERDEMİR laboratories [100]. The details of specimen preparation are not included in the scope of the current work. D type (globular) oxide inclusions

are expected for calcium-treated Al-killed steels. Chemical analysis of these heats is presented in Table 4.16.

Table 4.16 Heats subjected to inclusion morphology studies (wt%)

Heat Number	Steel Quality	Type	C	Si	Mn	S (ppm)	Ca (ppm)	Al (sol.)	Al (tot.)	Al (ins.)
621726	4936K	Chassis Steel	0.08	0.077	0.74	43	31	0.042	0.0451	0.0031
516741	3942K	Wheel Steel	0.015	0.049	0.67	100	40	0.0343	0.0396	0.0053
535723	9061K	Pipe Line Steel	0.094	0.182	1.50	41	28	0.0277	0.0299	0.0023
515753	9042K	Pipe Line Steel	0.15	0.219	0.99	70	33	0.0457	0.0486	0.0029
526215	9052K	Pipe Line Steel	0.096	0.199	0.99	50	45	0.043	0.047	0.0045

The first two heats, namely 4936K and 3942K steel qualities are Ca treated Al-killed steels. The criteria given previously in Table 4.15 indicate the necessary amount of Ca must be present in steel to ensure acceptable inclusion globularization [2]. To determine the amount of Ca to be used in steelmaking, the most important parameters are sulfur content and O (ppm) in steel. Total O content of solidified steel is closely related with deoxidation of steel. From the insoluble Al content of steel, Al(ins.), the amount of Al_2O_3 inclusions present can be calculated by multiplying Al (ins.) with [Mole wt. of Al_2O_3 / 2*At. wt. of Al]. Therefore from this simple stoichiometry, O present in Al_2O_3 inclusions can easily be obtained [108]. This is a common approach for Al-killed steels. For the heats numbered as 621726 and 516741 total O content of steel is calculated as 28 ppm and 47 ppm, respectively. Considering the chemical analysis of the first and the second heats again, the total oxygen content and sulfur concentration in steel are relatively higher than the ones given in Table 4.15. Therefore, for complete inclusion shape control, the calcium present in steel should be higher than the values given in Table

4.15. For this reason, 20-60 ppm of Ca is aimed in final steel analysis for most of the calcium treated steels produced in ERDEMİR plant. A general concluding remark is that the target Ca content of steel can be lowered provided that the sulfur and Al(ins) concentrations are brought to much lower levels.

Inclusion morphology of the heats given above were photographed by the image analyzer and presented in the following figures (Figures 4.18 to 4.22). Image analyzer of CLEMEX CIR 3.5 model was used. D-type globular oxide inclusions were observed in all heats. Careful examination of photographs reveals that average severity levels may differ from one another and generally an average value between 1 and 2 is observed. This degree of severity is mostly acceptable in many cases. At a glance, one of the main evidences indicating that Ca-treatment is not sufficiently performed is the presence of A-type inclusions (sulfide), the most important one being MnS. On the other hand, no A-type inclusion is observed in the photographs. As a final note, one of the key issues about specimen preparation is that a polished, microscopically flat section is to be achieved in order that the sizes and shapes of inclusions are accurately shown. To obtain satisfactory and consistent inclusion ratings, the specimen must have a polished surface free of artifacts such as pitting, foreign material (for example polishing media), and scratches [100].

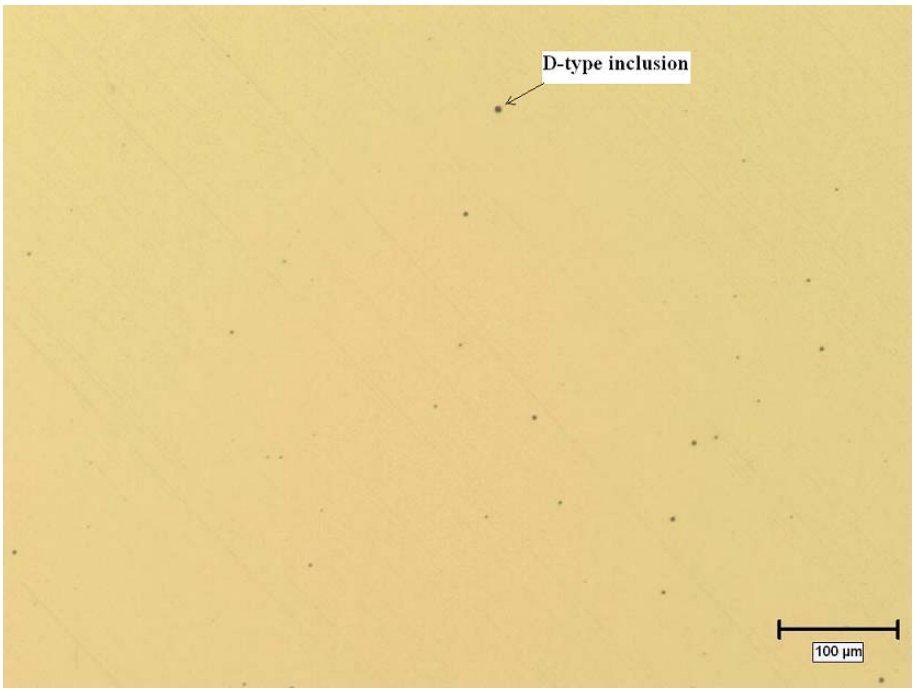

Figure 4.18 Inclusion morphology of 4936K steel quality (Photograph taken by image analyzer; 100 magnification)

Figure 4.19 Inclusion morphology of 3942K steel quality (Photograph taken by image analyzer; 100 magnification)

Figure 4.20 Inclusion morphology of 9061K steel quality (Photograph taken by image analyzer; 100 magnification)

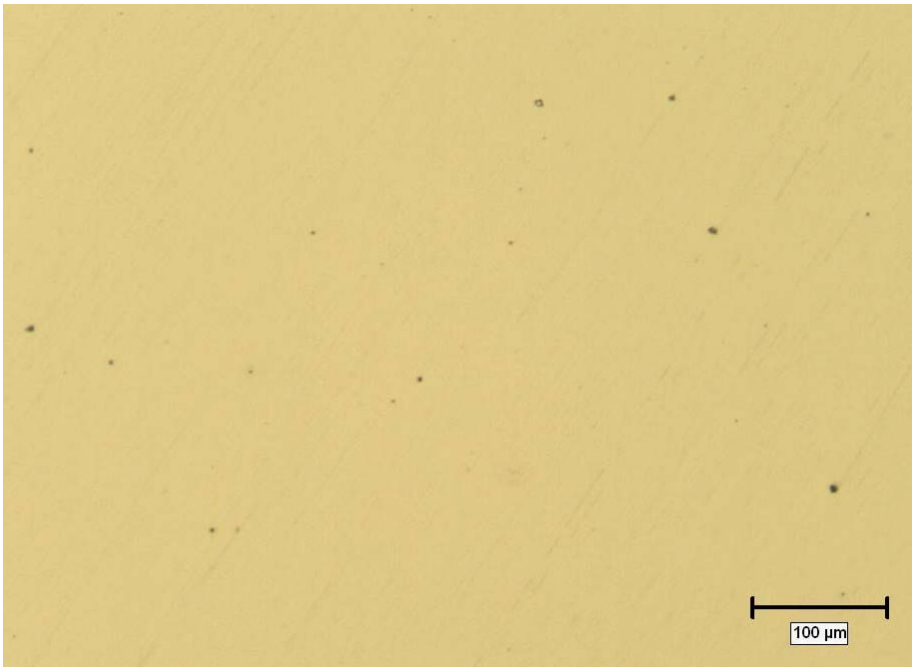

Figure 4.21 Inclusion morphology of 9042K steel quality (Photograph taken by image analyzer; 100 magnification)

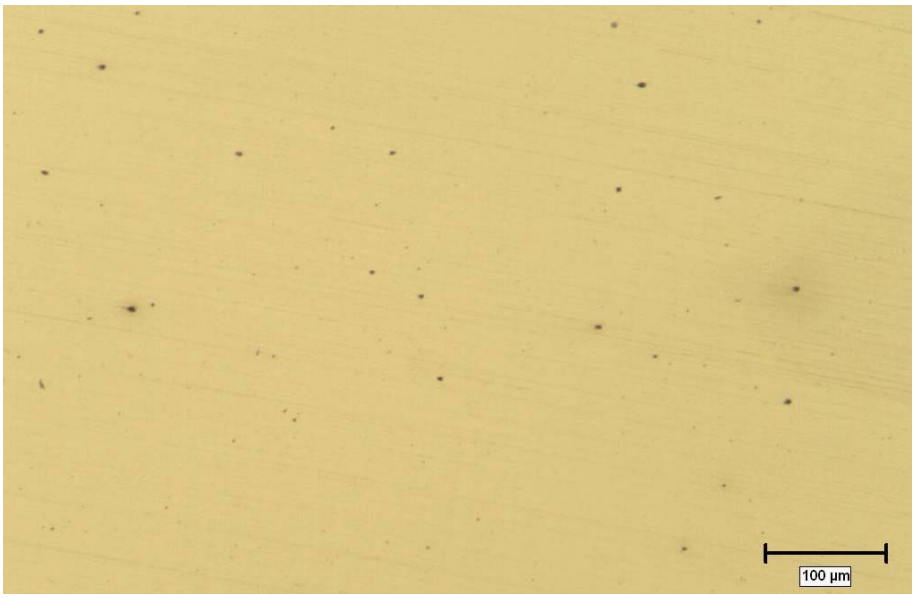

Figure 4.22 Inclusion morphology of 9052K steel quality (Photograph taken by image analyzer; 100 magnification)

Two steel samples taken from hot rolled product of 4936K quality were prepared for SEM analysis. SEM-EDS analysis was performed by using JEOL JSM-5600 scanning electron microscope. Heat subjected to SEM-EDS analysis are illustrated in Table 4.17. Three inclusions were examined for each sample. SEM-EDS analysis confirmed the findings of image analyzer studies. According to EDS patterns obtained, Fe, Mn, Ca, Al and S peaks were observed. The photographs and the peaks obtained indicates the presence of globular type $CaO.Al_2O_3$ inclusions (Figures 4.23 to 4.34). Peaks of Ca, Mn and S is a clear evidence of CaS-MnS ring type morphology, which is aimed in Ca-treatment, as shown in Figure 2.12.

Table 4.17 Heats subjected to SEM-EDS studies (wt%)

Heat Number	Steel Quality	Appl.	C	Si	Mn	S (ppm)	Ca (ppm)	Al (sol.)	Al (tot.)	Al (ins.)
626786	4936K	Chassis Steel	0.063	0.049	0.77	66	34	0.035	0.039	0.0032
635946	4936K	Chassis Steel	0.053	0.045	0.74	63	28	0.039	0.046	0.0068

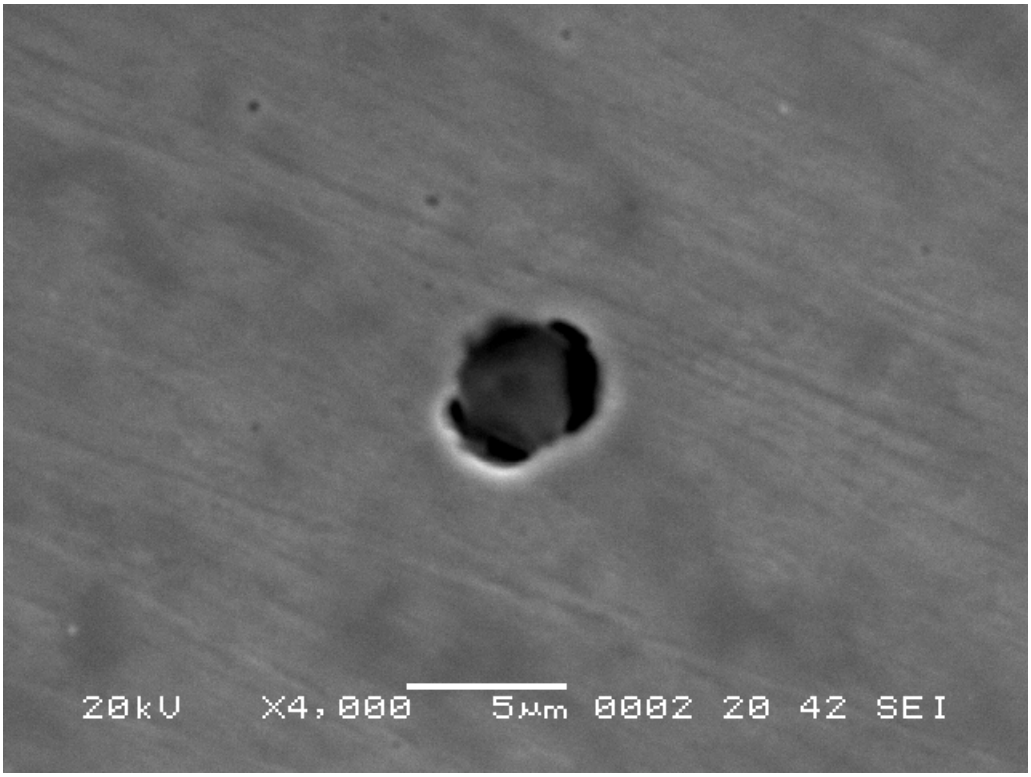

Figure 4.23 SEM photograph of an inclusion; Point-1 (Heat number: 626786)

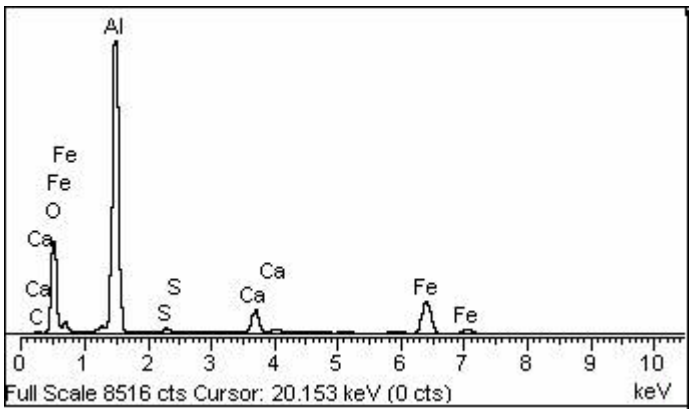

Figure 4.24 EDS pattern of Figure 4.23

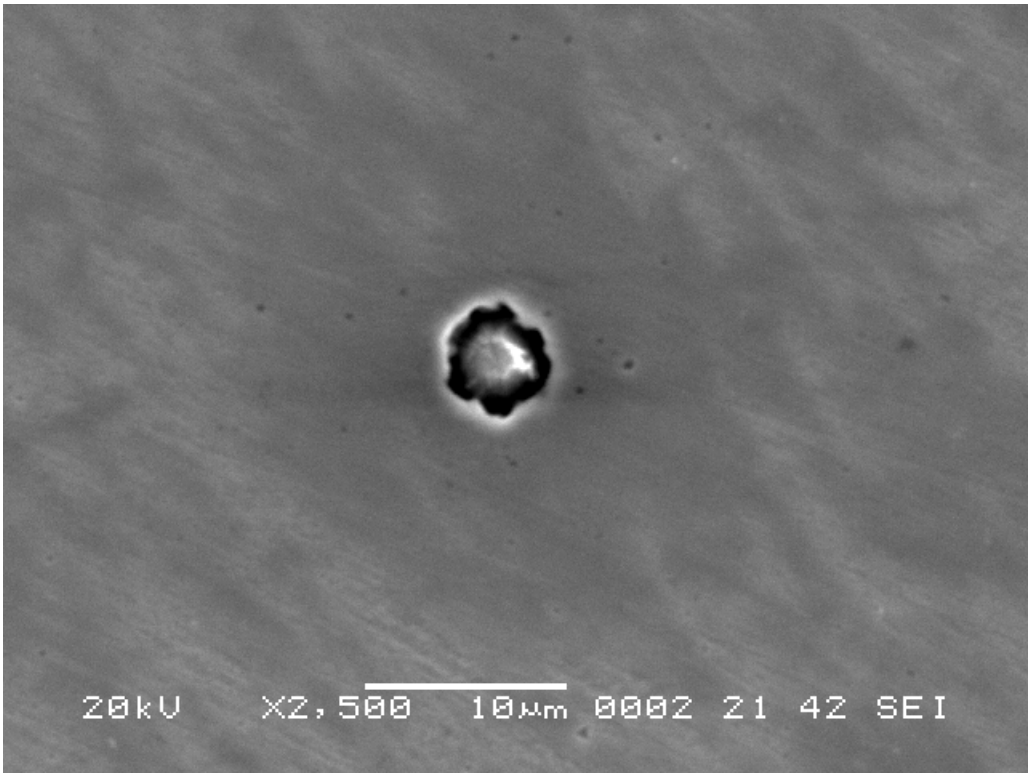

Figure 4.25 SEM photograph of an inclusion; Point-2 (Heat number: 626786)

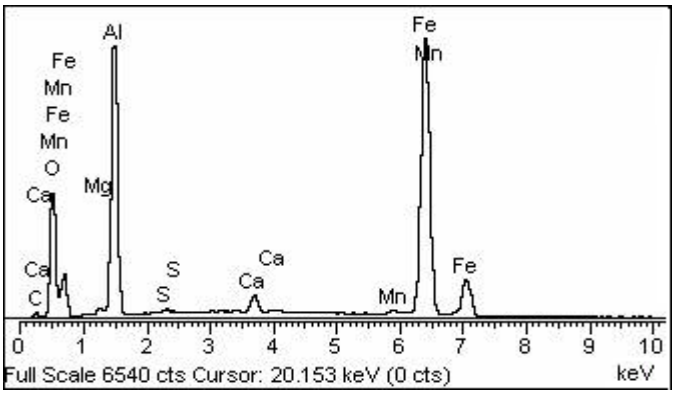

Figure 4.26 EDS pattern of Figure 4.25

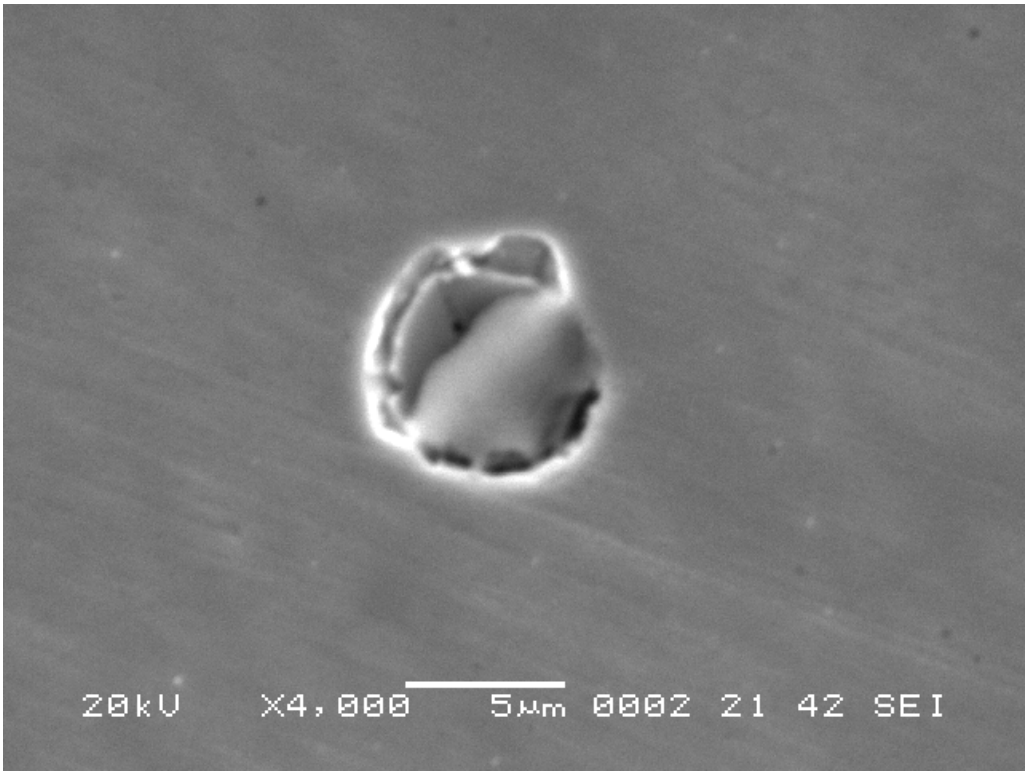

Figure 4.27 SEM photograph of an inclusion; Point-3 (Heat number: 626786)

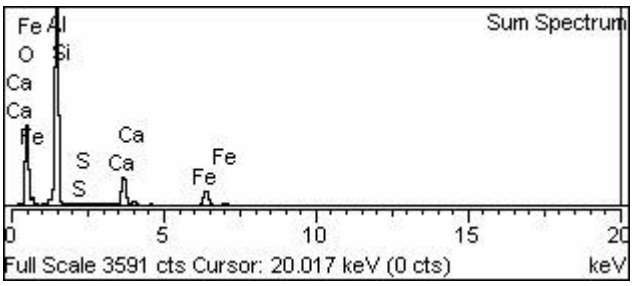

Figure 4.28 EDS pattern of Figure 4.27

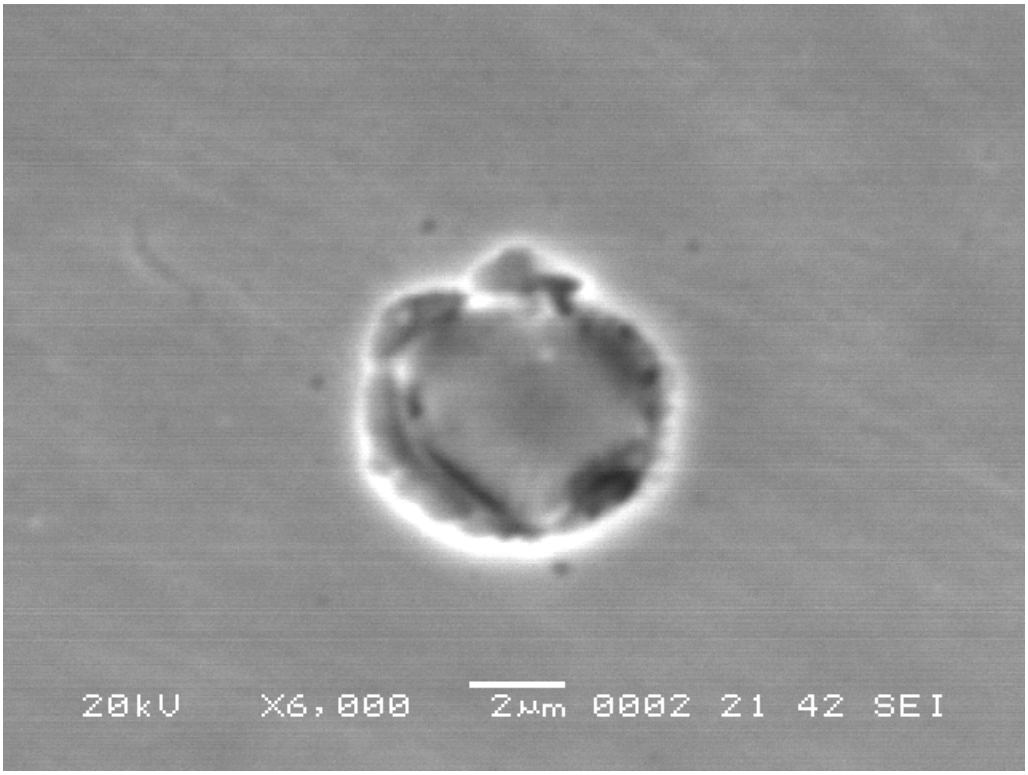

Figure 4.29 SEM photograph of an inclusion; Point-1 (Heat number: 635946)

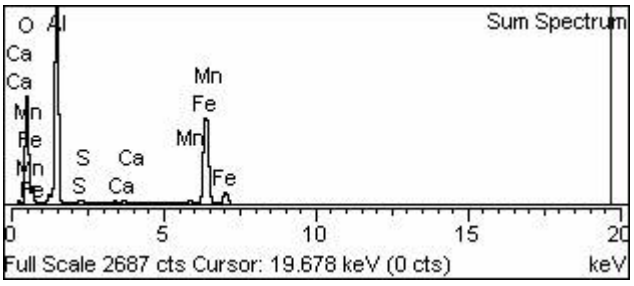

Figure 4.30 EDS pattern of Figure 4.29

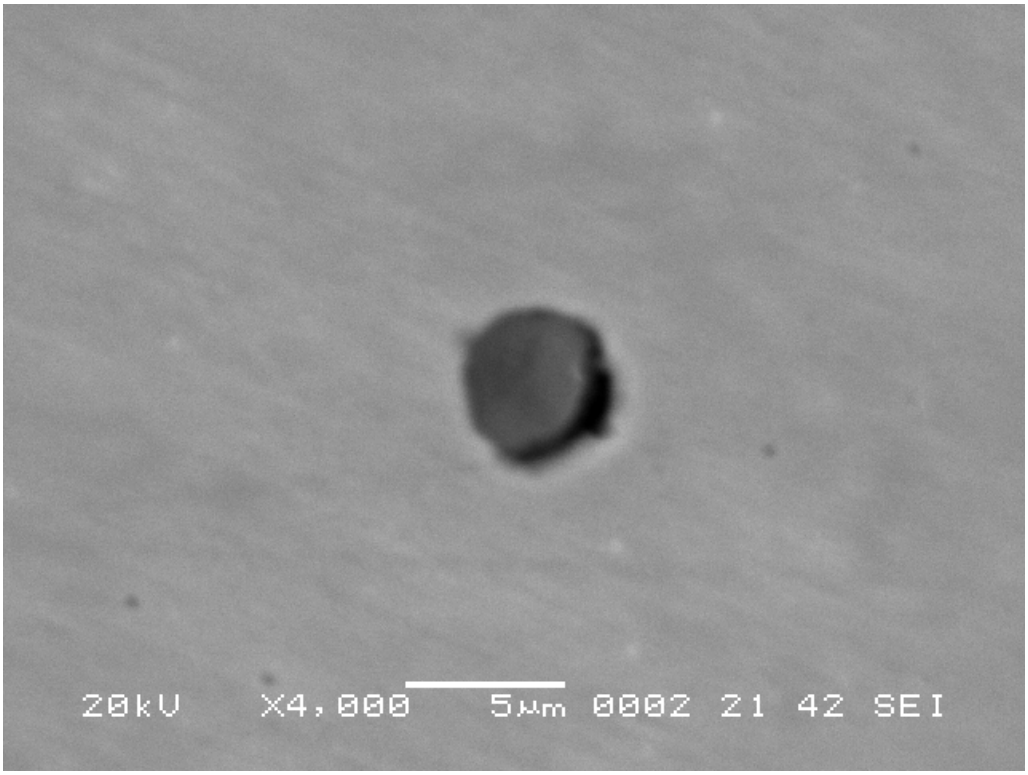

Figure 4.31 SEM photograph of an inclusion; Point-2 (Heat number: 635946)

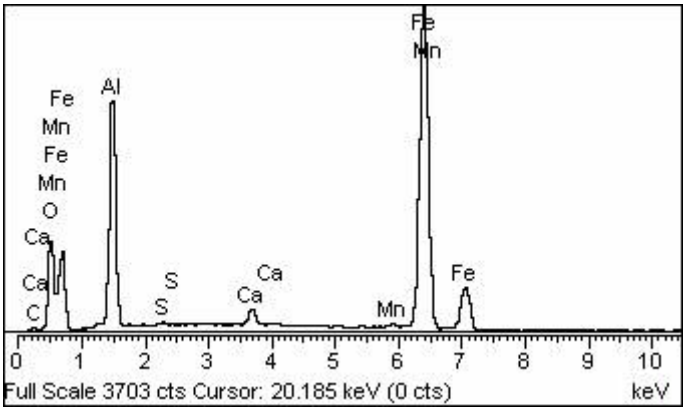

Figure 4.32 EDS pattern of Figure 4.31

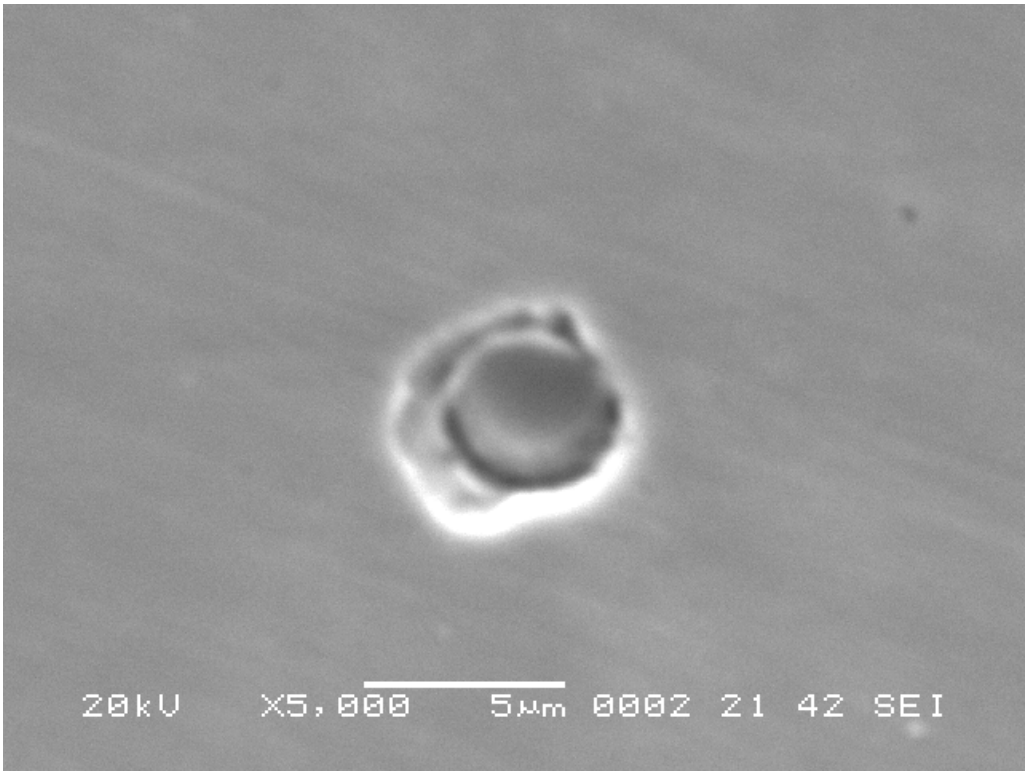

Figure 4.33 SEM photograph of an inclusion; Point-3 (Heat number: 635946)

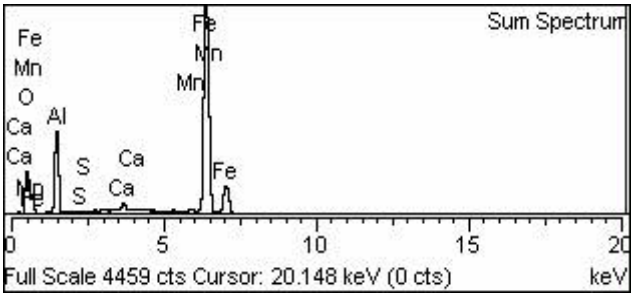

Figure 4.34 EDS pattern of Figure 4.33

CHAPTER 5

CONCLUSIONS

From the results of this study, the following conclusions can be drawn:

1. Investigation of the slags of some steel quality groups produced in ERDEMİR showed that unstable oxides (Fe_tO and MnO) can be studied best with the low-C steel quality group.

2. Examination of a member of this low-C quality group (heats of low-S steel quality, 4937K) showed that for all heats $\%Al_2O_3$ and %MgO contents of the slags were reported to increase with time. Both behaviour were in accord with the expectations: Increase in $\%Al_2O_3$ was due to slag deoxidation practice applied in secondary metallurgy while increase in %MgO was related to ladle refractory wear.

3. The relationship between *% Decrease in* a_{Fe_tO} and *% DeS (measured)* using Ohta and Suito's regression formula [74] showed that for 4937K heats *% DeS (measured)* values were found to increase with *% Decrease in* a_{Fe_tO} .

4. With the same regression formula [74], experiments conducted for some other steels produced in ERDEMİR plant showed that the highest *% DeS (measured)* values were obtained for 4937K steel quality, the lowest ones belonged to low C-low Si group while 4933K and high C stayed in between. This is closely related to the fact that an increase in C and/or Si content of liquid iron (or steel) lead to an increase in activity coefficient of sulfur indicating removal of sulfur from metal to slag is more favorable [19].

5. Results obtained from statistical works showed that the time of oxygen activity measurement and that of steel sampling could be assumed as the same considering the total process period of ladle furnace operation. This assumption enabled to study the relation between the change of oxygen potential of the steel-slag system and *% DeS (measured)*.

6. As a different approach, for the same 4937K steel quality heats, activity coefficients of Fe_tO, γ_{Fe_tO}, were calculated using steel oxygen activity values obtained during ladle treatment. A regression equation relating γ_{Fe_tO} with the major slag components was obtained ($R = 0.93$). Investigation of γ_{Fe_tO} using steel oxygen activities showed that the regression equation proposed was representative for 4937K slags.

7. In both methods of approach (Ohta and Suito [74] & Steel oxygen activity), *% DeS (measured)* was found to increase as *% Decrease in* a_{Fe_tO} increased. This tendency was in accord with the expectations. The relation obtained by using measured steel oxygen activities for 4937K steel quality was of course valid for a limited slag composition range compared to the one cited by Ohta and Suito [74]. On the other hand, since the calculations conducted using steel oxygen activities directly outlined the results related to 4937K, this approach was considered to be more suitable for 4937K slags. In conclusion, the formulation relating γ_{Fe_tO} with the major slag components derived in this study was found to be representative for 4937K slags, showing similar behaviour with the one obtained using Ohta and Suito's formula [74]. Slag compositions of some LC heats gave similar results like that of 4937K quality considering *% DeS (measured)* and *% Decrease in* a_{Fe_tO} values. Change of *% DeS (measured)* with steel oxygen activity was also investigated for 4937K: A linear relationship between the former and the latter was obtained.

8. Investigation of the relationship between *% Decrease in* a_{Fe_tO} and *%DeS (measured)* with Temkin equation [7,27] showed that similar results were found using Temkin equation and Ohta and Suito's formula [74]. For the same *% DeS (measured)* values, higher *% Decrease in* a_{Fe_tO} values were obtained with Temkin equation. The possible cause of this shift may be attributed to the differences of components incorporated in calculations. The results obtained from Temkin equation were reported to show similar tendency with the ones obtained from steel oxygen activities. Application of the polymeric anion model [28] to 4937K slags gave analogous results with Temkin model. Since less than 4 oxygen atoms are used in the formation of silicate anions, higher anionic fractions of (O^{2-}) and eventually higher a_{Fe_tO} values were obtained using the polymeric anion model. Considering the relationship between *% Decrease in* a_{Fe_tO} and *%DeS (measured)*, the trendline for the polymeric anion model was found to settle slightly above the one for Temkin model, showing similar tendency with the one obtained from Ohta and Suito's formula.

9. Examination of some steel qualities in relation to sulfur removal at the ladle furnace showed that average %desulfurization at the secondary metallurgy was the largest (29.29%) in 4937K. %Desulfurization data obtained in pipeline steels, 9060K and 9065K, were found to be less, being 21.78% and 23.16%, respectively. These results were in accord with the expectations and closely related to the nature of ladle practices applied at the ladle furnace.

10. In relation to the necessity of formation of less harmful inclusions to suppress adverse effects of sulfur, inclusion morphologies of Ca-treated steel qualities were investigated. Morphological investigations showed that D-type globular inclusions were observed with an average severity level ranging from 1 to 2. As indicated in Chapter 2, through shape control of sulfur containing inclusions, inclusion precipitation takes place at the earlier stages of steel solidification and therefore small-sized and globular shape inclusions which do not deform during rolling

processes are obtained. SEM-EDS studies confirmed the findings of image analyzer and showed typical Ca-treated inclusion morphologies, as desired.

CHAPTER 6

SUGGESTIONS FOR FUTURE WORK

Following items, especially with the settlement of the new ladle furnace, should be conducted in the scope of a future work:

i) Experiments should also be performed for steel qualities having different slag compositions to obtain γ_{Fe_tO} relations for them as found for 4937K in the present work.

ii) Related to low-sulfur steels, effect of some process parameters on ladle desulfurization should be studied. These are;

-Ladle process time,
-Bottom stirring rate,
-Amount of Al-dross and CaO addition, etc.

iii) In relation to production of ultra-low S steel qualities (S<10 to 20 ppm), powder injection desulfurization method should be experimented at the new ladle furnace.

iv) Inclusion morphologies of 4937K steel quality should be investigated together with the corresponding slag compositions and activities calculated from them.

REFERENCES

1. Kiessling, R., Non-metallic Inclusions in Steel, Part III: The Origin and Behaviour of Inclusions and Their Influence on the Properties of Steels, The Metals Society, London, Second Edition, pp. 74-110, 1978.

2. Kor, G.J.W., and Glaws, P.C., The Making, Shaping and Treating of Steel, Steelmaking and Refining Volume, The AISE Steel Foundation, Pittsburgh, PA, 11th Edition, Chapter 11: Ladle Refining and Vacuum Degassing, pp. 687, 693, 1998.

3. Luyckx, L., "Steel Ladle Desulfurization Compositions and Methods of Steel Desulfurization", United States Patent, March 6, 1979.

4. Jaffre, D., Effect of the Elements on Steel Properties: A Summary, Chaparral Steel, Midlothian, Texas, pp. 1-18, 2003.

5. FactSage™ 5.5, www.factsage.com, Fe-S Phase Diagram, last accessed date: September 2007.

6. Sharma, R.C., and Chang, Y.A., "Thermodynamics and Phase Relationships of Transition Metal-Sulfur Systems: Part III. Thermodynamic Properties of the Fe-S Liquid Phase and the Calculation of the Fe-S Phase Diagram", Metallurgical Transactions B, 10B, pp. 103-108, 1979.

7. Ward, M.A., An Introduction to the Physical Chemistry of Iron and Steelmaking: Figure 16 taken from "Richardson, F.D., and Jeffes, J., The Thermodynamics of Substances of Interest in Iron and Steelmaking, Part III-Sulphides, J. Iron St. Inst., vol. 171, pp. 165-175, 1952", Edvard Arnold Ltd., London, pp. 59, 1962.

8. Yarwood, J.C., Flemings, M.C., Elliott, J.F., "Inclusion Formation in the Fe-O-S System", Metallurgical Transactions B, Vol. 2, No. 9, pp. 2573-2582, Sept. 1971.

9. Kor, G.J.W., and Turkdogan, E.T., "Sulfides and Oxides in Fe-Mn Alloys: Part III. Formation of Oxysulfides During Freezing of Steel", Metallurgical Transactions B, Vol. 3, No. 5, pp. 1269-1278, May. 1972.

10. Turkdogan, E.T., Physicochemical Properties of Molten Slags and Glasses, The Metals Society, London, pp. 226, 1983.

11. Turkdogan, E.T., Kor, G.J.W., Darken, L.S., Gurry, R.W., "Sulfides and Oxide in Iron-Manganese Alloys. I. Phase Relations in Iron-Manganese-Sulfur-Oxygen System", Metallurgical Transactions B, Vol. 2, No. 6, pp. 1561-1570, 1971.

12. Kiessling, R., Non-metallic Inclusions in Steels, Part 5, The Institute of Metals, London, pp. 54-58, 64, 1989.

13. Sims, C.E., and Dahle, F.B., Trans. Am. Foundrymen's Soc., Vol. 46, pp. 65, 1938.

14. Kiessling, R., and Lange, N., Non-metallic inclusions in steel, Part II: "Inclusions Belonging to the Systems $MgO\text{-}SiO_2\text{-}Al_2O_3$, $CaO\text{-}SiO_2\text{-}Al_2O_3$ and Related Oxide Systems. Sulphide Inclusions", The Iron and Steel Institute, pp. 114-127, 1966.

15. Baker, T.J., and Charles, J.A., "Deformation of MnS Inclusions in Steel", J. Iron Steel Inst., Vol. 210, pp. 680-690, 1972.

16. Barbadillo, J.J., and Snape, E., editors, Sulfide Inclusions in Steel, Proceedings of an International Symposium, 7-8 November 1974-New York, American Society for Metals, 1975.

17. Sevinç, N., Demir-Çelik Üretiminde Kükürt, Seminer Notları, Karabük, 2-6 1985.

18. Sherman, C.W., Elvander, H. I., and Chipman, J., **"**Thermodynamic Properties of Sulfur in Molten Iron-Sulfur Alloys", Journal of Metals, Vol. 188, pp. 334-340, 1950.

19. Banya, S., and Chipman, J., Trans AIME, Vol. 245, pp. 133 and pp. 391, 1969.

20. Lupis, C.H.P., Chemical Thermodynamics of Materials, North Holland, 1983.

21. Turkdogan, E.T., Physical Chemistry of High Temperature Technology, Academic Press, 1980.

22. Fincham, C.J.B, and Richardson, F.D., Proc. R. Soc. A, Vol. 223, pp. 40-62, 1954.

23. Andersson, AT., Jönsson, P.G., and Nzotta, M.M., "Application of the Sulfide Capacity Concept on High Basicity Ladle Slags Used in Bearing-Steel Production", ISIJ International, Vol. 39, No. 11, pp. 1140-1149, 1999.

24. Pretorius, E., Slag Short Course, LWB Refractories, Process Tech. Group, pp. 105-121.

25. Karakaya, İ., MetE 527 Advanced Chemical Metallurgy, METU Lecture Notes.

26. Mills, K.C., "The Influence of Structure on the Physico-chemical Properties of Slags", ISIJ International, Vol. 33, No. 1, pp. 148-155, 1993.

27. Moretti, R., and Ottonello, G., "Polymerization and Disproportionation of Iron and Sulfur in Silicate Melts: Insights from an Optical Basicity-Based Approach", Journal of Non-Crystalline Solids, 323, pp. 111-119, 2003.

28. Masson, C.R., Smith, I.B., and Whiteway, S.G., "Activities and Ionic Distributions in Liquid Silicates: Application of Polymer Theory", Canadian Journal of Chemistry, Vol. 48, pp. 1456-1464, 1970.

29. Duffy, J.A., and Ingram, M.D., "Establishment of an Optical Scale for Lewis Basicity in Inorganic Oxyacids, Molten Salts, and Glasses", J. Amer. Chem. Soc., Vol. 93 (24), pp. 6448-6454, 1971.

30. Gaye, H., and Welfringer, J., "Modelling of the Thermodynamic Properties of Complex Metallurgical Slags", edited by Fine, H.A., and Gaskell, D.R., Second International Symposium on Metallurgical Slags and Fluxes, The Metallurgical Society of AIME, pp.357-375, 1984.

31. Nzotta, M.M., Sichen, Du, and Seetharaman, S., “Sulfide Capacities in Some Multi Component Slag Systems”, ISIJ International, Vol. 38, No. 11, pp. 1170-1179, 1998.

32. Duffy, J.A., and Ingram, M.D., “Comments on the Application of Optical Basicity to Glass”, Journal of Non-Crystalline Solids, 144, pp. 76-80, 1992.

33. Reddy, R.R., Ahammed, Y.N., Gopal, K.R., Abdul Azeem, P., and RaO, T.V.R., “Correlation Between Optical Basicity, Electronegativity and Electronic Polarizability for Some Oxides and Oxysalts”, Optical Materials, 12, pp. 425-428, 1999.

34. Sosinsky, D.J., and Sommerville, I.D., Metallurgical and Materials Transactions B, 17B, pp. 331-337, 1986.

35. Young, R.W., Duffy, J.A., Hassall, G.J., and Xu, Z., “Use of Optical Basicity Concept for Determining Phosphorus and Sulfur Slag-Metal Partitions”, Ironmaking and Steelmaking, Vol. 19, No. 3, pp. 201-219, 1992.

36. Lehmann, J., Gaye, H., and Rocabois, P., “The IRSID Slag Model For Steelmaking Process Control”, http://www.yosh.ac.il/research/mmt/MMT-2000/papers/89-96.doc, last accessed date: September 2007.

37. Kapoor, M.L., and Frohberg, M.G., Chemical Metallurgy of Iron and Steel, The Iron and Steel Institute, London, pp. 17-22, 1973.

38. Gaye, H., Riboud, P.V., and Welfringer, J., “Use of a Slag Model to Describe Slag-Metal Reactions and Precipitation of Inclusions”, Ironmaking and Steelmaking, Vol. 15, No. 6, 319-322, 1988.

39. Kjellqvist, L., “Studies of Steel/Slag Equilibria Using Computational Thermodynamics”, Licentiate Thesis, KTH, Stockholm, Sweden, pp. 5-6, April 2006.

40. Gaye, H., Riboud, P.V., and Welfringer, J., “Slag Modelling: A Tool for Evaluating Metallurgical Treatments”, Fifth International Iron and Steel Congress, Process Technology Proceedings, Volume 6, Washington, DC, A Publication of the Iron and Steel Society, Book 3, pp. 631-639, 1986.

41. Rocabois, P., Lehmann, J., Gaye, H., Wintz., M., "Kinetics of Precipitation of Non-Metallic Inclusions During Solidification of Steel", Journal of Crystal Growth, 198/199, pp. 838-843, 1999.

42. Lehmann, J., Rocabois, P., Gaye, H., "Kinetic Model of Non-Metallic Inclusions' Precipitation During Steel Solidification", Journal of Non-Crystalline Solids, 282, pp. 61-71, 2001.

43. Nzotta, M.M., Sichen, Du, and Seetharaman, S., "A Study of the Sulfide Capacities of Iron-Oxide Containing Slags", Metallurgical and Materials Transactions B, 30B, pp. 909-920, 1999.

44. Hao, N., Li, H., Wang, H., Wang, X., and Wang, W., "Application of the Sulphide Capacity Theory on Refining Slags during LF Treatment", Journal of University of Science and Technology Beijing, Vol. 13, Number 2, pp. 112-116, April 2006.

45. Wang, C., Lu, Q., Zhang, S., and Li, F., "Study of the Sulfide Capacity of CaO-SiO_2-Al_2O_3-MgO-Fe_tO Slags", Journal of University of Science and Technology Beijing, Vol. 13, Number 3, pp. 213-217, June 2006.

46. Banya, S., Hobo, M., Kaji, T., Itoh, T., and Hino, M., "Sulphide Capacity and Sulphur Solubility in CaO-Al_2O_3 and CaO-Al_2O_3-CaF_2 Slags", ISIJ International, Vol. 44, No. 11, pp. 1810-1816, 2004.

47. Turkdogan, E.T., "Physicochemical Aspects of Reactions in Ironmaking and Steelmaking Processes", Transactions ISIJ, Vol. 24, pp. 591-611, 1984.

48. Fruehan, R.J., Ladle Metallurgy, Principles and Practices, A Publication of the Iron and Steel Society, Chapter 1, pp. 1-2, 1985.

49. Turkdogan, E.T., and Fruehan, R.J., The Making, Shaping and Treating of Steel, Steelmaking and Refining Volume, The AISE Steel Foundation, Pittsburgh, PA; 11th Edition, Chapter 2: Fundamentals of Iron and Steelmaking, pp. 144-145, 149, 1998.

50. Strassburger, J.H., editor, Blast Furnace - Theory and Practice, AIME, Gordon and Breach Science Publishers, Vol. 2, pp. 987-1040, 1969.

51. Turkdogan, E.T., and Martonik, L.J., "Sulfur Solubility in Iron-Carbon Melts Coexistent with Solid CaO and CaS", Trans. Iron Steel Inst. Jpn., Vol. 23, No. 12, pp. 1038-1044, 1983.

52. Turkdogan, E.T., "Slags and Fluxes for Ferrous Ladle Metallurgy", Ironmaking and Steelmaking, Vol. 12, No. 2, pp. 64-78, 1985.

53. Emi, T., and Iida, Y., Iron and Steelmaker, pp. 20, Feb. 1984.

54. Seshadri, V., Da Silva, C.A., Da Silva, I.A., and Von Krüger, P., "A Kinetic Model Applied to the Molten Pig Iron Desulfurization by Injection of Lime-based Powders", ISIJ International, Vol. 37, No. 1, pp. 21-30, 1997.

55. Chushao, X., and Xin, T., "The Kinetics of Desulfurization of Hot Metal by CaO-CaF_2 Based Fluxes", ISIJ International, Vol. 32, No. 10, pp. 1081-1083, 1992.

56. Haastert, H.P., Meischner, W., Rellemeyer, H., Peters, K.H., Iron and Steel Engineer, pp. 71, Oct. 1975.

57. Zou, Z., Zou, Y., Zhang, L., and Wang, N., "Mathematical Model of Hot Metal Desulphurization by Powder Injection", ISIJ International, Vol. 41, Supplement, pp. S66-S69, 2001.

58. Coudure, J.M., and Irons, G.A., "The Effect of Calcium Carbide Particle Size Distribution on the Kinetics of Hot Metal Desulphurization" ISIJ International, Vol. 34, No. 2, pp. 155-163, 1994.

59. Lovold, K., "Desulfurization of Hot Metal by Injection of Magnesium Granules", Ironmaking Steelmaking, Vol. 7, No. 1, pp. 41, 1980.

60. Kurzinski, E.F., "Desulfurization of Fe-Status and Evaluation", Iron Steel Eng., Vol. 53, No. 4, pp. 59-71, Apr. 1976.

61. DuMond, T.C., “Mag-Coke Creates Big Stir in Desulfurization”, Iron Age, Vol. 211, No. 24, pp. 75-77, June 1973.

62. Recknagel, W., and Hater, M., “Desulphurization of Hot Metal to Produce Low Sulphur Contents in Steel”, Ironmaking Steelmaking, Vol. 8, No. 2, pp. 81-84, 1981.

63. Jin, Y., Bi, X.G., and Yu, S.R., “Kinetic Model for Powder Injection Desulfurization”, Acta Metallurgica Sinica (English Letters), Vol. 19, No. 4, pp. 258-264, 2006.

64. Bahout, B., Bienvenu, Y., Denier, G., “External Desulphurization of Iron by Pneumatic Injection of Soda Ash in 200 tonne Ladles”, Ironmaking Steelmaking, Vol.5, No.4, p.162-167, 1978.

65. Suito, H., Ishizaka, A., Inoue, R., and Takahashi, Y., “Simultaneous Dephosphorization and Desulfurization of Carbon-saturated Iron by Sodium Carbonate-Sodium Sulfate Flux”, Transactions ISIJ, Vol. 21, pp. 156-164, 1981.

66. Moriya, T., and Fujii, M., “Dephosphorization and Desulfurization of Molten Pig Iron by Na_2CO_3”, Transactions ISIJ, Vol. 21, pp. 732-741, 1981.

67. Iwai, H., and Kunisada, K., “Desulfurization and Simultaneous Desulfurization and Dephosphorization of Molten Iron by Na_2O-SiO_2 and Na_2O-CaO-SiO_2 Fluxes”, ISIJ International, Vol. 29, No. 2, pp. 135-139, 1989.

68. Hernandez, A., Romero, A., Chavez, F., Angeles, M., and Morales, R.D., “Dephosphorization and Desulfurization Pretreatment of Molten Iron with CaO-SiO_2-CaF_2-FeO-Na_2O Slags”, ISIJ International, Vol. 38, No. 2, pp. 126-131, 1998.

69. Choi, J., Kim, D., and Lee, H., “Reaction Kinetics of Desulfurization of Molten Pig Iron Using CaO-SiO_2-Al_2O_3-Na_2O Slag Systems”, ISIJ International, Vol. 41, No. 3, pp. 216-224, 2001.

70. Van Niekerk, W.H., and Dippenaar, R.J., “Thermodynamic Aspects of Na_2O and CaF_2 Containing Lime-based Slags Used for the Desulphurization of Hot Metal”, ISIJ International, Vol. 33, No. 1, pp. 59-65, 1993.

71. Turkdogan, E.T., “Theoretical Aspects of Sulfide Formation in Steel”, taken from ref. 16, pp. 1-22.

72. Desulfurization in Secondary Steelmaking, CRC Press LLC, 2001.

73. Andersson, A.T., Jonsson, T.I., and Jönsson, P.G., “A Thermodynamic and Kinetic Model of Reoxidation and Desulphurization in the Ladle Furnace”, ISIJ International, Vol. 40, No. 11, pp. 1080-1088, 2000.

74. Ohta, H., and Suito, H., “Activities of SiO_2 and Al_2O_3 and Activity Coefficients of Fe_tO and MnO in CaO-SiO_2-Al_2O_3-MgO Slags”, Metallurgical and Materials Transactions B, Volume 29B, pp. 119-129, 1998.

75. Andersson, A.T., Hallberg, M., Jonsson, L., Jönsson, P., “Slag-metal Reactions during Ladle Treatment with Focus on Desulphurisation”, Ironmaking and Steelmaking, Vol. 29, No. 3, pp. 224-232, 2002.

76. Andersson, A.T., Jönsson, P., and Hallberg, M., “Optimisation of Ladle Slag Composition by Application of Sulphide Capacity Model”, Ironmaking and Steelmaking, Vol. 27, No. 4, pp. 286-293, 2000.

77. Patsiogiannis, F., Pal, U.B., and Bogan, R.S., “Laboratory Scale Refining Studies on Low Carbon Aluminum Killed Steels Using Synthetic Fluxes”, ISIJ International, Vol. 34, No. 2, pp. 140-149, 1994.

78. Elliott, J.F., Lynch, D.C., and Braun, T.B., “Criticism of the Flood-Grjotheim Ionic Treatment of Slag-Equilibria”, Metallurgical Transactions B, 6B, pp. 495-501, 1975.

79. Patsiogiannis, F., and Pal, U.B., “Incorporation of Sulfur in an Optimized Ladle Steelmaking Slags”, ISIJ International, Vol. 36, No. 4, pp. 402-409, 1996.

80. Turkdogan, E.T., “Slag Composition Variations Causing Variations in Steel Dephosphorization and Desulphurization in Oxygen Steelmaking”, ISIJ International, Vol. 40, No. 9, pp. 827-832, 2000.

81. Tsujino, R., Nakashima, J., Hırai, M., and Yamada, Y., “Behavior of Desulfurization in Ladle Steel Refining with Powder Injection at Reduced Pressures”, ISIJ International, Vol. 29, No. 1, pp. 92-95, 1989.

82. Wang, L., Lin, Q., Ji, J., Lan, D., “New Study Concerning Development of Application of Rare Earth Metals in Steels”, Journal of Alloys and Compounds, 408-412, pp. 384-386, 2006.

83. Pielet, H.M., and Bhattacharya, D., “Thermodynamics of Nozzle Blockage in Continuous Casting of Calcium-Containing Steels” Metallurgical Transactions B, Vol. 15, pp. 547-562, 1984.

84. Faulring et.al., “Process for Continuous Castings of Aluminum-Deoxidized Steel”, United States Patent, March 2, 1982.

85. Turkdogan, E.T., “Retrospect on Technology Innovations in Ferrous Pyrometallurgy”, Canadian Metallurgical Quarterly, Vol. 40, No. 3, pp. 255-308, 2001.

86. Blais, C., L’Espérance, G., LeHuy, H., Forget, C., “Development of an Integrated Method for Fully Characterizing Multiphase Inclusions and Its Application to Calcium-Treated Steels”, Materials Characterization, 38, pp. 25-37, 1997.

87. Ito, Y., Suda, M., Kato, Y., Nakato, H., and Sorimachi, K., “Kinetics of Shape Control of Alumina Inclusions with Calcium Treatment in Line Pipe Steel for Sour Service”, ISIJ International, Vol. 36, Supplement, pp. S148-S150, 1996.

88. Han, Z.J., Liu, L., Lind, M., and Holappa, L., “Mechanism and Kinetics of Transformation of Alumina Inclusions by Calcium Treatment”, Acta Metallurgica Sinica (English Letters), Vol. 19, No. 1, pp. 1-8, February 2006.

89. Lind, M., “Mechanism and Kinetics of Transformation of Alumina Inclusions in Steel by Calcium Treatment”, Doctoral Thesis, “CaO-Al_2O_3 phase diagram from FactSage”, Helsinki University of Technology Publications in Materials Science and Engineering, September 2006.

90. Ye, G., Jönsson, P., and Lund, T., "Thermodynamics and Kinetics of the Modification of Al_2O_3 Inclusions", ISIJ International, Vol. 36, Supplement, pp. S105-S108, 1996.

91. Steelmaking Department web page, Ladle Furnace, Ereğli Iron and Steel Works Co.(ERDEMİR), (Unpublished), 2006.

92. VAI document for Slag Free Tapping System, ERDEMİR BOF Capacity Improvement and Modernization.

93. Turkdogan, E.T., Fundamentals of Steelmaking, Chapter 5: Physochemical Properties of Molten Slags, 2nd Ed., The Institute of Materials, Cambridge University Press, p. 142, 1996.

94. Xu, X., Hwang, J., Greenlund, R., Huary, X., Luo, J., and Anschuetz, S., "Quantitative Determination of Metallic Iron Content in Steelmaking Slag", Journal of Minerals & Materials Characterization & Engineering, Vol. 2, No. 1, pp. 65-70, 2003.

95. Chemical Analysis Application Table for Continuous Casting Qualities, Ereğli Iron and Steel Works Co.(ERDEMİR), (Unpublished), 2007.

96. Al-dross specification, Ereğli Iron and Steel Works Co. (ERDEMİR), (Unpublished), 2006.

97. Steel quality groups according to C content, Know-how information, Ereğli Iron and Steel Works Co.(ERDEMİR), (Unpublished), 2006.

98. OS 4460 User Manual, Chapter 2, Simplified Technical Description Part.

99. CS344 C-S User Manual, Characteristics Part.

100. Standard Test Methods for Determining the Inclusion Content of Steel, ASTM E45-97 (Reapproved 2002).

101. Turkdogan, E.T., Fruehan, R.J., “Review of Oxygen Sensors for Use in Steelmaking and of Deoxidation Equilibria”, Ladle Metallurgy Principles and Practices, Publication of the Iron and Steel Society, Appendix, pp. 57-66, 1985.

102. Celox Oxygen Activity Measurement Devices, User Manual.

103. Aydemir, O., “Usage of Aluminum Dross for Slag Treatment in Secondary Steelmaking to Decrease Amount of Reducible Oxides in Ladle Furnace”, MSc. Thesis (Unpublished), Middle East Technical University, Ankara, 2006.

104. Whiteway, S.G., Smith, I.B., and Masson, C.R., “Theory of Molecular Size Distribution in Multichain Polymers”, Canadian Journal of Chemistry, Vol. 48, pp. 33-45, 1970.

105. Smith, I.B., and Masson, C.R., “Activities and Ionic Distributions in Cobalt Silicate Melts”, Canadian Journal of Chemistry, Vol. 49, pp. 683-690, 1971.

106. Masson, C.R., “Thermodynamics and Constitution of Silicate Slags”, J. Iron Steel Inst., Vol. 210, pp. 89-96, 1972.

107. Keskinkılıç, E., “PhD. Thesis Progress Report (Unpublished)”, Middle East Technical University, December, 2004.

108. Dressel, G.L., “Short Communication: Calcium Wire Injection”, Iron and Steelmaker, Skull Session, pp. 28, April 2000.

109. Ulrich Grethe, Andeas Berghöfer, Harry Amsler, and Manfred Winkelmann, Slag Free Tapping with the INTERSTOP Tap Hole Gate TAP120 for Clean Steel Production, Technical Report.

110. http://mpe-us.com/slag_detection.htm, last accessed date: September 2007.

APPENDIX A

ELLINGHAM DIAGRAM FOR SULFIDES

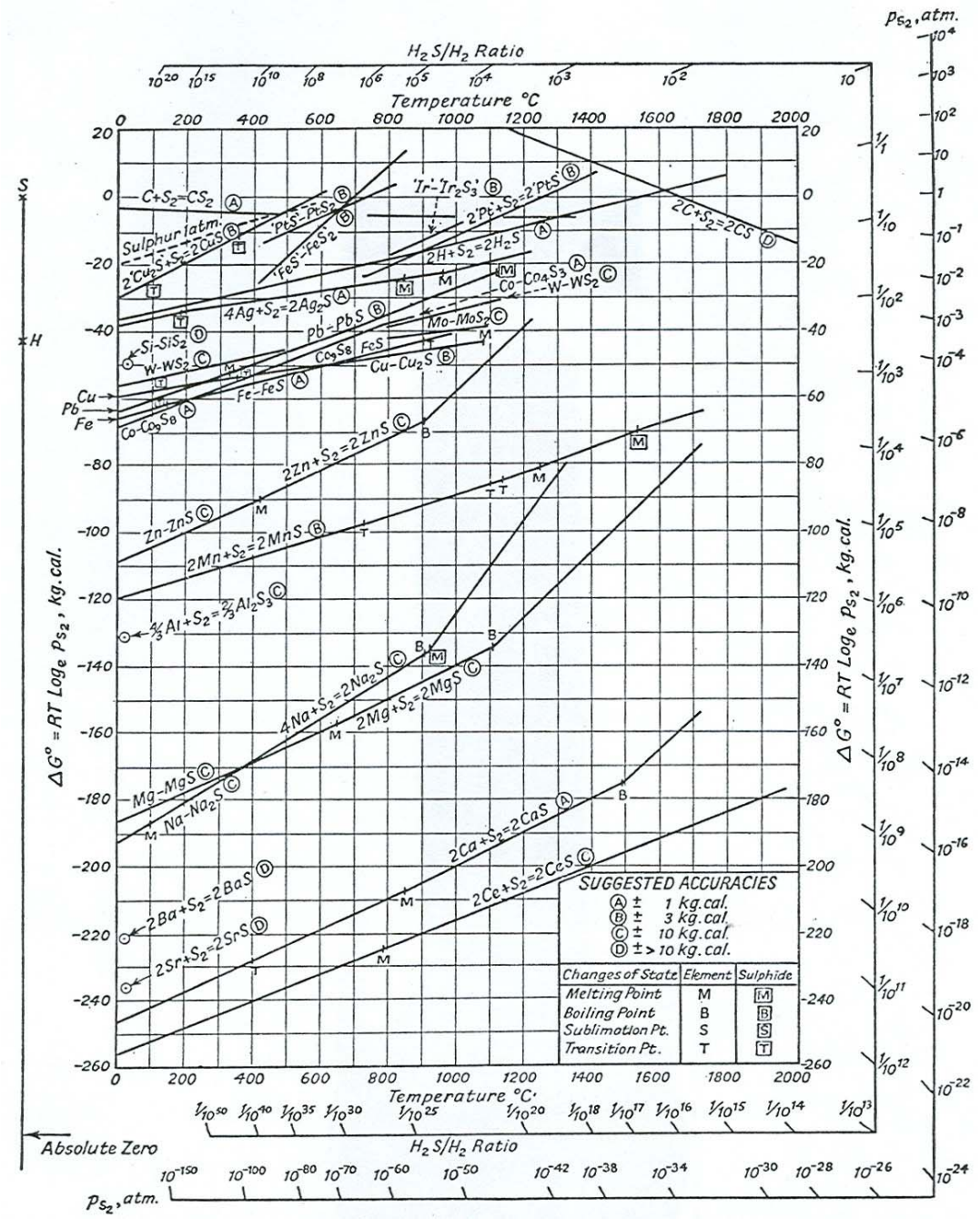

Figure A.1 The standard free energy of formation of metallurgically important sulfides as a function of temperature [7]

APPENDIX B

Fe-S-O TERNARY SYSTEM

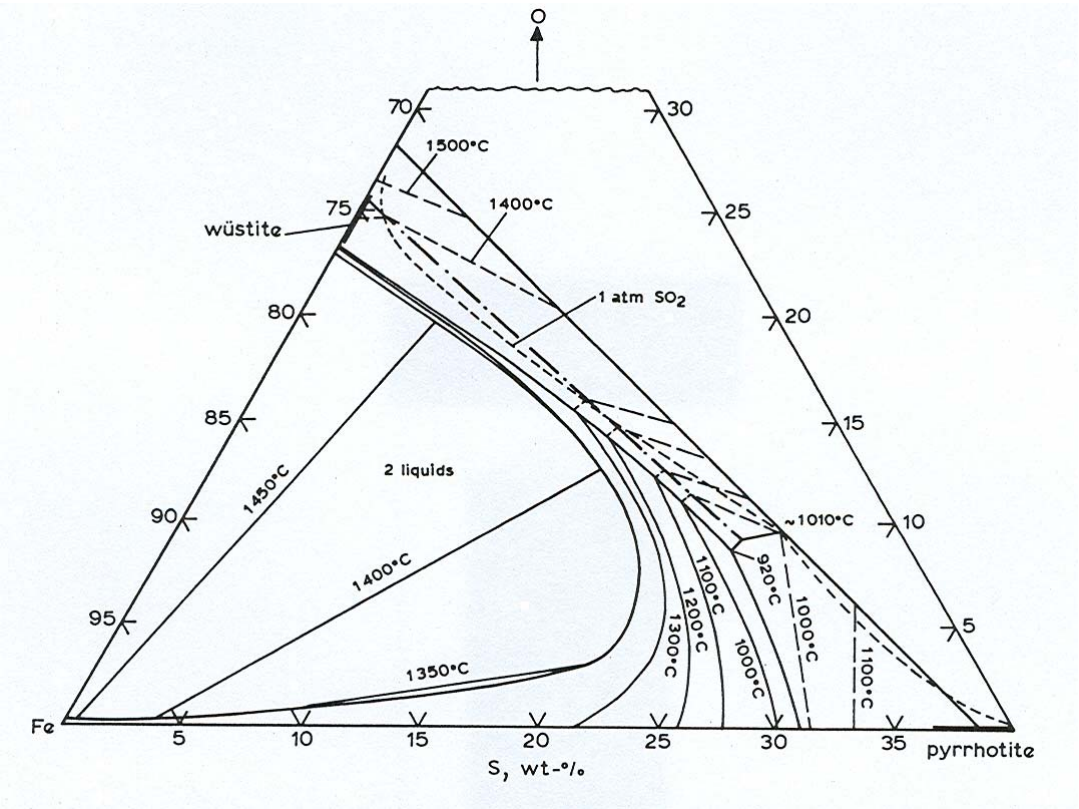

Figure B.1 Projection of the miscibility gap boundary and the liquidus isotherms on the composition diagram for the system Fe-S-O [10].

APPENDIX C

SLAG FREE TAPPING SYSTEM

Slag-free tapping is the key to “ultra clean steel” production. Steel grades, where the high demands are on a low phosphorus and sulfur content, can only be assured through slag free tapping. Furthermore, the handling procedure in subsequent processes is clearly improved using this method and the production costs can be significantly reduced.

Basic oxygen furnace (BOF) converters require special slag detection and slag retaining systems. The various systems currently in use are illustrated in Figure C.1 [109].

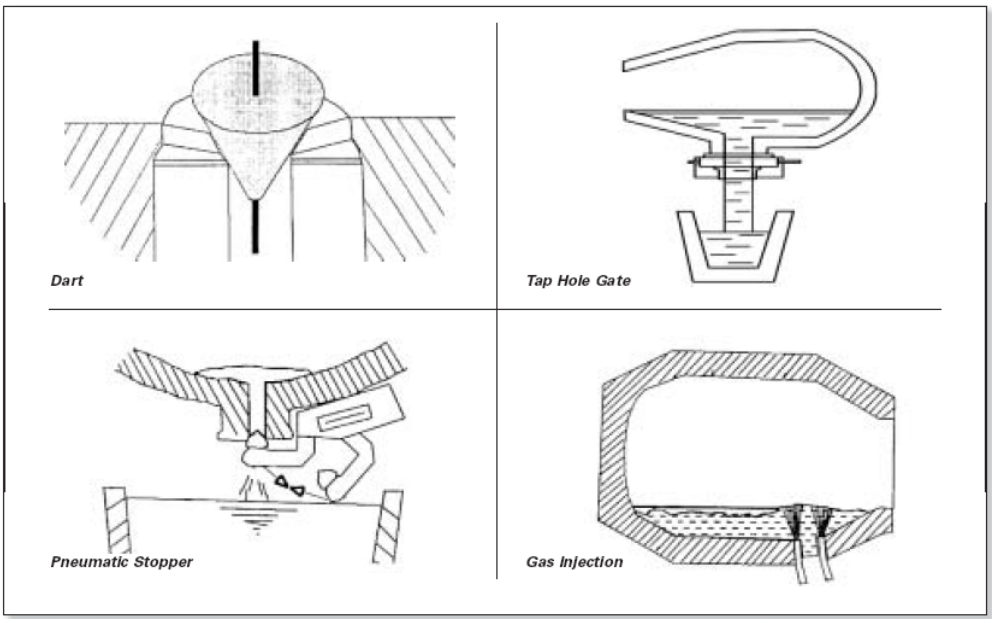

Figure C.1 Converter slag retaining systems [109]

The pneumatic slag stopper present in ERDEMİR converters serves for closing tap hole towards the end of tapping in order to minimize slag carry-over by separating steel and slag. The principle of the system is to retain slag by injecting air through a nozzle into the tap hole. The sealing function is performed pneumatically and does not depend on the surface condition of the closing members (General arrangement of slag free tapping system is given in Figure C.2) [92].

The nozzle is fixed at the end of the swivel arm. The actuation of the swivel arm with nozzle is performed by a pneumatic cylinder. Slewing is controlled automatically by the EMLI-S.I.O. Slag Indication System. The system, however, can also be controlled manually upon pushbutton by the operator. The time for slewing the slag stopper from open to closed position is approximately 1 second and is adjustable.

Simultaneously with the slewing motion a pusher integrated into the slewing shaft is opened automatically, the nozzle is supplied with N_2 to retain slag in the vessel. Immediately after slewing-in the nozzle, the vessel is tilted up into vertical position, meanwhile the nozzle is slewed out and the shaft integrated pusher for the retaining medium becomes closed automatically.

The impulse for opening the slag stopper can be initiated manually or automatically depending on converter position or time. The mechanical equipment (slewing cylinder, swivel arm, supporting etc.) is fixed in a detachable way. The design of the slag stopper assumes that the three converters are identical in design and dimensions. Differences in dimension due to deformation of the converter are compensated by the fixation bracket [92].

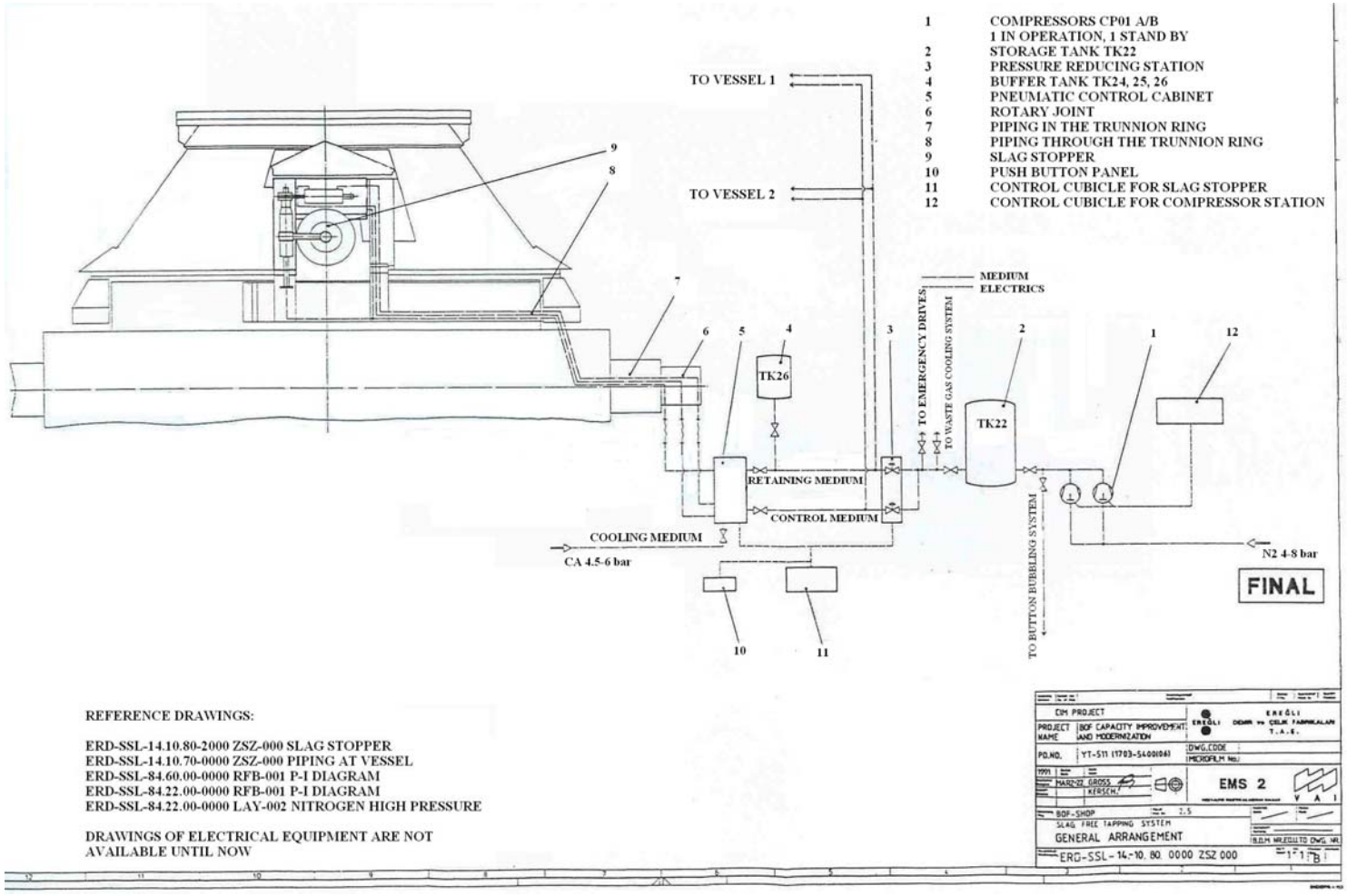

Figure C.2 General arrangement of slag free tapping system [92]

In order to obtain optimum results with the slag stopper regular cleaning and repair of the tap hole is a precondition as well as careful maintenance of the equipment. At extremely high demands on slag-free tapping, the nozzle can already be slewed-in into the steel stream before slag emerges, however, an essentially shorter life of the equipment (especially of the nozzle) must be considered.

To protect the cylinder and the nozzle against too high temperature they are cooled with air taken from the line of the retaining medium. To avoid a too high consumption of high pressure N_2, the cooling medium is taken from the works supply during the time between tapping. Changing over from cooling medium to a high pressure control and retaining medium is performed at the pneumatic control panel [92].

The EMLI-S.I.O.-Slag Indication System is the complementary system to the "Pneumatic Slag Stopper" (Figure C.3) [110].

The application of this combination provides for fully automatical operation of the "Slag Stopper System" and excludes the subjective influence of the operator in deciding time for closing the slag stopper. The EMLI-S.I.O. System provides objective criteria for slag detection, especially in the case where the operator cannot distinguish between steel and slag (e.g. heavy fume formation, high tapping temperatures) and at operating conditions with worn tap hole where a large amount of slag leaves the converter within a short time. The pneumatic Slag Stopper closes automatically in response to the "Slag Alarm"-signal produced by the EMLI-S.I.O.-Slag Indication System [110].

Figure C.3 EMLI™ Slag Indication Oxygen Vessel (EMLI-SIO) - for real-time slag detection on B.O.F. furnaces [110]

The **EMLI™** Slag detection systems work on the principle that the penetration depth of steel is much less than the penetration depth of slag. This means that slag is virtually invisible to the electromagnetic signal generated by the **EMLI™** electronics. For example, in the **EMLI™** SIO system, the signal received when the tap hole of the BOF is filled with slag is very close to the signal received when the tap hole is filled with air. When the tap hole is filled with steel a significant portion of the magnetic field is blocked and therefore the received signal is greatly reduced. The **EMLI™** microprocessor can recognize this signal change and generate alarms as required. Principle of the system is presented in Figure C.4 [110].

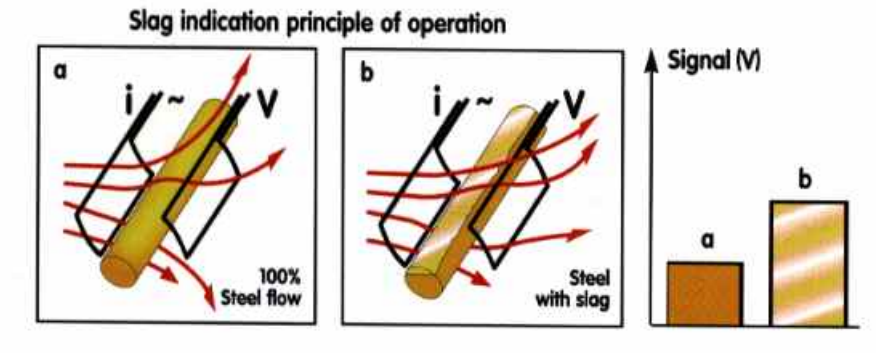

Figure C.4 Principle of EMLI^{TM} Slag Detection System [110]

APPENDIX D

THEORETICAL CALCULATION FOR CARRY-OVER SLAG

A typical converter charge contains around 104 ton of hot metal, 24 ton of scrap, and 6.5 ton of CaO.

A typical converter slag consists of
18% Fe_tO, 12% SiO_2, 8% MnO, 45% CaO, 3% MgO and 1% P_2O_5.

During tapping, an average of 210 kg of Al, 40 kg of coke and 600 kg of CaO are added to the ladle.

A typical first slag sample taken in the ladle furnace has an analysis of

5% Fe_tO, 5% SiO_2, 2% MnO, 25% Al_2O_3, 53% CaO, 3.50% MgO and 0.2% P_2O_5.

The source of 25% Al_2O_3 in the slag is the deoxidation reaction given below:

$$2\underline{Al}(\%) + 3\underline{O}(\%) = Al_2O_3(s) \qquad (74)$$

The first steel sample taken at the ladle furnace contains around 0.03% Al. Therefore (0.03/100)*120000 kg = 36 kg of Al present in steel.

210-36 = 174 kg is used for deoxidation reaction.

(174/27) kg moles of Al forms (1/2)*(174/27) kg moles = 3.22 kg moles Al_2O_3

3.22 kg moles of Al_2O_3 is 3.22*102 kg = 329 kg Al_2O_3.

The slag present in the ladle from the previous heat is around 200 kg. This contains around (30/100)*200 = 60 kg Al_2O_3.

Therefore, total Al_2O_3 in the slag is approximately 400 kg. So the total slag amount is roughly given as 400/0.25 = 1.6 ton. The previous studies conducted and careful examination of the system showed that this amount can be around 1.8 ton. Mass balance calculations are rather rough and small differences in percentages give very different values. However, the calculations give fairly good estimates for the amount of slag present in the ladle.

Typical slag amount at the ladle and its components are listed as follows:

540 kg CaO (Lime contains around 90% CaO min.)
330 kg Al_2O_3 (From deoxidation reaction)
200 kg slag (From previous heat)
100 kg MgO (From refractories)
Total: Around 1.6 ton from the calculation given above.

Therefore carry-over slag amount: 1600-(540+330+200+100) = 430 kg.

In reality carry-over slag amount is around 600-650 kg. Generally, theoretical values are found to be less than real values. This is attributed to the assumptions made during calculations.

APPENDIX E

MATHCAD PROGRAM, *FetO*, FOR ACTIVITY CALCULATIONS

This program calculates activity of oxygen in the slag/metal mixing zone by the exchange reaction between Fe_tO in the slag and oxygen in the steel melt:

$Fe_tO(l)=Fe(l)+O$

The activity coefficient of Fe_tO, γ_{FetO}, is calculated using the expression from Ohta and Suito .The program outlines

1. Activity of oxygen in the slag/metal mixing zone
2. Activity coefficient of Fe_tO
3. Mole fraction of Fe_tO
4. Activity of Fe_tO.

$$\text{FetO}(\text{CaO}, \text{Al2O3}, \text{SiO2}, \text{MgO}, \text{FeO}, \text{MnO}, \text{XFeSteel}, T) :=$$

$$\text{logActivityCoeff} \leftarrow \frac{0.676\,\text{MgO} + 0.267\,\text{Al2O3} - 19.07}{\text{SiO2}} + 0.0214\,\text{CaO} - 0.047$$

$$\text{ActivityCoeff} \leftarrow 10^{\text{logActivityCoeff}}$$

ActivityCoeff

$$\text{XFeO} \leftarrow \frac{\frac{\text{FeO}}{72}}{\frac{\text{CaO}}{56} + \frac{\text{Al2O3}}{112} + \frac{\text{SiO2}}{60} + \frac{\text{MgO}}{40} + \frac{\text{MnO}}{71} + \frac{\text{FeO}}{72}}$$

$$\text{activityO} \leftarrow \frac{\text{ActivityCoeff} \cdot \text{XFeO} \cdot e^{\left(\frac{-116100}{8.314\,T} + \frac{48.4}{8.314}\right)}}{\text{XFeSteel}}$$

$$\text{actFeO} \leftarrow \text{ActivityCoeff} \cdot \text{XFeO}$$

$$\begin{pmatrix} \text{activityO} \\ \text{ActivityCoeff} \\ \text{XFeO} \\ \text{actFeO} \end{pmatrix}$$

$$\text{FetO}(\text{CaO}, \text{Al2O3}, \text{SiO2}, \text{MgO}, \text{FeO}, \text{MnO}, \text{XFeSteel}, T)$$

Heat No: 526919

$$\text{FetO}(48.33, 25.37, 6.52, 7.74, 6.12, 5.41, 0.988, 1872) = \begin{pmatrix} 8.628 \times 10^{-3} \\ 0.801 \\ 0.055 \\ 0.044 \end{pmatrix}$$

$$\text{FetO}(49.50, 30.99, 6.33, 8.11, 1.95, 2.77, 0.987, 1867) = \begin{pmatrix} 5.071 \times 10^{-3} \\ 1.489 \\ 0.018 \\ 0.026 \end{pmatrix}$$

Heat no: 517076

$$\mathrm{FetO}(\mathrm{CaO}, \mathrm{Al2O3}, \mathrm{SiO2}, \mathrm{MgO}, \mathrm{FeO}, \mathrm{MnO}, \mathrm{XFeSteel}, \mathrm{T})$$

$$\mathrm{FetO}(48.38, 29.67, 7.62, 7.53, 2.69, 3.75, 0.99, 1905) = \begin{pmatrix} 8.49 \times 10^{-3} \\ 1.561 \\ 0.024 \\ 0.038 \end{pmatrix}$$

$$\mathrm{FetO}(49.34, 30.55, 7.50, 8.93, 1.62, 1.77, 0.99, 1868) = \begin{pmatrix} 6.407 \times 10^{-3} \\ 2.284 \\ 0.015 \\ 0.033 \end{pmatrix}$$

Heat no: 517077

$$\mathrm{FetO}(\mathrm{CaO}, \mathrm{Al2O3}, \mathrm{SiO2}, \mathrm{MgO}, \mathrm{FeO}, \mathrm{MnO}, \mathrm{XFeSteel}, \mathrm{T})$$

$$\mathrm{FetO}(46.78, 27.94, 6.95, 4.47, 5.05, 8.46, 0.99, 1849) = \begin{pmatrix} 4.369 \times 10^{-3} \\ 0.523 \\ 0.047 \\ 0.024 \end{pmatrix}$$

$$\mathrm{FetO}(48.71, 31.93, 6.58, 7.34, 2.19, 3.02, 0.99, 1863) = \begin{pmatrix} 5.311 \times 10^{-3} \\ 1.403 \\ 0.02 \\ 0.028 \end{pmatrix}$$

Heat no: 517078

$$\mathrm{FetO}(\mathrm{CaO}, \mathrm{Al2O3}, \mathrm{SiO2}, \mathrm{MgO}, \mathrm{FeO}, \mathrm{MnO}, \mathrm{XFeSteel}, \mathrm{T})$$

$$\mathrm{FetO}(54.85, 23.65, 5.17, 6.32, 4.84, 4.72, 0.99, 1833) = \begin{pmatrix} 2.198 \times 10^{-3} \\ 0.306 \\ 0.043 \\ 0.013 \end{pmatrix}$$

$$\mathrm{FetO}(49.34, 30.13, 7.40, 8.54, 1.86, 2.43, 0.99, 1864) = \begin{pmatrix} 6.322 \times 10^{-3} \\ 1.991 \\ 0.017 \\ 0.033 \end{pmatrix}$$

Heat no: 517080

$$\mathrm{FetO}(\mathrm{CaO}, \mathrm{Al2O3}, \mathrm{SiO2}, \mathrm{MgO}, \mathrm{FeO}, \mathrm{MnO}, \mathrm{XFeSteel}, \mathrm{T})$$

$$\mathrm{FetO}(54.03, 20.68, 6.67, 4, 8.45, 5.33, 0.99, 1893) = \begin{pmatrix} 4.905 \times 10^{-3} \\ 0.304 \\ 0.076 \\ 0.023 \end{pmatrix}$$

$$\mathrm{FetO}(52.67, 30.71, 5.24, 7.98, 1.5, 1.61, 0.99, 1862) = \begin{pmatrix} 2.757 \times 10^{-3} \\ 1.084 \\ 0.013 \\ 0.015 \end{pmatrix}$$

APPENDIX F

MODIFIED MATHCAD PROGRAM, *ModifiedFetO*, FOR ACTIVITY CALCULATIONS

FetO(l)=Fe(l)+O

The activity coefficient of FetO, γFetO, is calculated using steel oxygen activity data.

The program outlines

1. Steel oxygen activity
2. Activity coefficient of FetO
3. Mole fraction of FetO
4. Activity of FetO.

$$\text{ModifiedFetO}(CaO, Al2O3, SiO2, MgO, FeO, MnO, activityO, XFeSteel, T) := \left| \begin{array}{l} XFeO \leftarrow \dfrac{\frac{FeO}{72}}{\frac{CaO}{56}+\frac{Al2O3}{112}+\frac{SiO2}{60}+\frac{MgO}{40}+\frac{MnO}{71}+\frac{FeO}{72}} \\ ActivityCoeff \leftarrow \dfrac{XFeSteel \cdot activityO}{XFeO \cdot e^{\left(\frac{-116100}{8.314 \cdot T}+\frac{48.4}{8.314}\right)}} \\ actFeO \leftarrow ActivityCoeff \cdot XFeO \\ \begin{pmatrix} activityO \\ ActivityCoeff \\ XFeO \\ actFeO \end{pmatrix} \end{array} \right.$$

$$\text{ModifiedFetO}(CaO, Al2O3, SiO2, MgO, FeO, MnO, activityO, XFeSteel, T)$$

Heat No: 526919

$$\text{ModifiedFetO}(48.33, 25.37, 6.52, 7.74, 6.12, 5.41, 0.000713, 0.988, 1872) = \begin{pmatrix} 7.13 \times 10^{-4} \\ 0.066 \\ 0.055 \\ 3.625 \times 10^{-3} \end{pmatrix}$$

$$\text{ModifiedFetO}(49.50, 30.99, 6.33, 8.11, 1.95, 2.77, 0.000322, 0.987, 1867) = \begin{pmatrix} 3.22 \times 10^{-4} \\ 0.095 \\ 0.018 \\ 1.668 \times 10^{-3} \end{pmatrix}$$

APPENDIX G

MATHCAD PROGRAM, *TemkinFetO*, FOR ACTIVITY CALCULATIONS

This program calculates activity of FetO using Temkin equation:

aFetO=a(Fe2+)*a(O2-)

$$\text{TemkinFetO}(\text{CaO},\text{Al2O3},\text{SiO2},\text{MgO},\text{FeO},\text{MnO}) := \left|\begin{array}{l} \text{nFe} \leftarrow \frac{\text{FeO}}{72} \\ \text{nMn} \leftarrow \frac{\text{MnO}}{71} \\ \text{nCa} \leftarrow \frac{\text{CaO}}{56} \\ \text{nMg} \leftarrow \frac{\text{MgO}}{40} \\ \text{TotalCations} \leftarrow \text{nFe} + \text{nMn} + \text{nCa} + \text{nMg} \\ \text{NFe} \leftarrow \frac{\text{nFe}}{\text{TotalCations}} \\ \text{nSiO4} \leftarrow \frac{\text{SiO2}}{60} \\ \text{nAlO3} \leftarrow 2\cdot\frac{\text{Al2O3}}{102} \\ \text{nO} \leftarrow \frac{\text{FeO}}{72} + \frac{\text{MnO}}{71} + \frac{\text{CaO}}{56} + \frac{\text{MgO}}{40} - 2\cdot\frac{\text{SiO2}}{60} - 3\cdot\frac{\text{Al2O3}}{102} \\ \text{TotalAnions} \leftarrow \text{nSiO4} + \text{nAlO3} + \text{nO} \\ \text{NO} \leftarrow \frac{\text{nO}}{\text{TotalAnions}} \\ \text{aFetO} \leftarrow \text{NFe}\cdot\text{NO} \\ \text{aFetO} \end{array}\right.$$

TemkinFetO(CaO,Al2O3,SiO2,MgO,FeO,MnO)

Heat No: 526919

TemkinFetO(48.33,25.37,6.52,7.74,6.12,5.41) = 0.021

TemkinFetO(49.50,30.99,6.33,8.11,1.95,2.77) = 0.001

APPENDIX H

MATHCAD PROGRAM FOR CALCULATION OF THE VARIABLES OF POLYMERIC ANION MODEL AND THE RESULTS OBTAINED FOR 4937K SLAGS

This program calculates the equilibrium number of moles of SiO_4^{4-}, $Si_2O_7^{6-}$, $Si_3O_{10}^{8-}$, $Si_4O_{13}^{10-}$, $Si_5O_{16}^{12-}$, (O^{2-}) anions present in 4937K slags according to the polymeric anion model.

Variables:

A: $n_{SiO_4^{4-}}$, B: $n_{Si_2O_7^{6-}}$, C: $n_{Si_3O_{10}^{8-}}$, D: $n_{Si_4O_{13}^{10-}}$, E: $n_{Si_5O_{16}^{12-}}$, F: $n_{O^{2-}}$

Initial guesses: $A := 0.07 \quad B := 0.01 \quad C := 0.0025 \quad D := 0.0007 \quad E := 0.0002 \quad F := 0.50$

$k11 := 1$

$$k12 := k11\cdot(3\cdot 2 + 1)\cdot\frac{(3\cdot 2 + 2)}{2\cdot(2\cdot 2 + 3)\cdot(2 + 1)}$$

$$k13 := k11\cdot(3\cdot 3 + 1)\cdot\frac{(3\cdot 3 + 2)}{2\cdot(2\cdot 3 + 3)\cdot(3 + 1)}$$

$$k14 := k11\cdot(3\cdot 4 + 1)\cdot\frac{(3\cdot 4 + 2)}{2\cdot(2\cdot 4 + 3)\cdot(4 + 1)}$$

Inputs:

$SiO2 := 4.76 \quad FeO := 8.44 \quad MnO := 4.94 \quad CaO := 55.39 \quad MgO := 4.96 \quad Al2O3 := 20.89$

Given

$$B = k11\cdot\frac{A^2}{F} \quad C = k11\cdot k12\cdot\frac{A^3}{F^2} \quad D = k11\cdot k12\cdot k13\cdot\frac{A^4}{F^3} \quad E = k11\cdot k12\cdot k13\cdot k14\cdot\frac{A^5}{F^4}$$

$$A + 2\cdot B + 3\cdot C + 4\cdot D + 5\cdot E = \frac{SiO2}{60}$$

$$F = \frac{FeO}{72} + \frac{MnO}{71} + \frac{CaO}{56} + \frac{MgO}{40} - 3\cdot\frac{Al2O3}{102} + 2\cdot\frac{SiO2}{60} - 4\cdot A - 7\cdot B - 10\cdot C - 13\cdot D - 16\cdot E$$

$$\text{Find}(A, B, C, D, E, F) = \begin{pmatrix} 0.061 \\ 6.99\times 10^{-3} \\ 1.064\times 10^{-3} \\ 1.855\times 10^{-4} \\ 3.502\times 10^{-5} \\ 0.537 \end{pmatrix}$$

Table H.1 Results obtained for 4937K slags ($k_{11} = 1.0$)

4937K Runs	S. Nr.	$N_{Fe^{2+}}$	$n_{SiO_4^{4-}}$	$n_{Si_2O_7^{6-}}$	$n_{Si_3O_{10}^{8-}}$	$n_{Si_4O_{13}^{10-}}$	$n_{Si_5O_{16}^{12-}}$	$n_{O^{2-}}$	$N_{O^{2-}}$	a_{Fe_tO}		
526919	1	0.07	0.062	0.014	0.003974	0.001333	0.0004842	0.282	0.3274	0.023		
517076	1	0.033	0.033	0.014	0.008184	0.005364	0.003808	0.078	0.1077	0.004		
517080	1	0.093	0.074	0.012	0.002745	0.0006977	0.000192	0.447	0.4745	0.044		
610618	1	0.082	0.066	0.006883	0.00095	0.0001503	0.00002574	0.642	0.5949	0.049		
610620	1	0.053	0.061	0.006396	0.000892	0.0001424	0.00002464	0.585	0.5551	0.029		
631253	1	0.055	0.053	0.006956	0.001212	0.0002421	0.00005235	0.407	0.4287	0.024		
616522	1	0.12	0.07	0.006146	0.000722	0.0000972	0.00001417	0.792	0.6839	0.082		
634021	1	0.093	0.06	0.006632	0.000972	0.0001632	0.00002967	0.549	0.5364	0.050	% Decr. in a_{Fe_tO}	%DeS
526919	2	0.023	0.031	0.012	0.00662	0.004026	0.002652	0.079	0.1063	0.002	89.33	29.58
517076	2	0.02	0.03	0.014	0.008148	0.005613	0.004188	0.067	0.0920	0.002	48.22	22.95
517080	2	0.018	0.039	0.011	0.004376	0.001936	0.0009271	0.135	0.1699	0.003	93.07	25.32
610618	2	0.02	0.053	0.007747	0.001502	0.0003338	0.00008032	0.366	0.3867	0.008	84.15	51.9
610620	2	0.012	0.023	0.004598	0.001211	0.0003654	0.0001194	0.118	0.1450	0.002	94.09	60
631253	2	0.046	0.049	0.007972	0.001741	0.0004357	0.0001181	0.297	0.3340	0.015	34.83	9.09
616522	2	0.058	0.067	0.011	0.002459	0.0006212	0.0001699	0.408	0.4360	0.025	69.19	21.43
634021	2	0.09	0.061	0.00699	0.001064	0.0001855	0.00003502	0.537	0.5286	0.048	4.63	2.5

CURRICULUM VITAE

PERSONAL INFORMATION

Surname, Name: Keskinkılıç, Ender
Nationality: Turkish (TC)
Date and Place of Birth: 17 April 1977 , Üsküdar
Marital Status: Single
Phone: +90 312 337 05 57
email: keskinkilic@yahoo.com

EDUCATION

Degree	Institution	Year of Graduation
MS	METU Metallurgical and Materials Engineering	2001
BS	METU Metallurgical and Materials Engineering	1999
High School	Yenimahalle Mustafa Kemal High School, Ankara	1994

WORK EXPERIENCE

Year	Place	Enrollment
2003- Present	Ereğli Iron and Steel Works Co. (ERDEMİR)	Metallurgical Engineer
1999-2003	METU Department of Metallurgical and Materials Engineering	Research Assistant
1998 August	CER Döküm	Intern Engineering Student
1997 August	MAN A.Ş.	Intern Engineering Student

FOREIGN LANGUAGES

Advanced English

CERTIFICATION

Six-Sigma Green Belt Certificate (from Kent State University; 5-9 October 2004)

PUBLICATIONS

1. Keskinkılıç, E., Geveci, A., "Denizli-Tavas Manganez Cevherlerinden Silikomanganez Üretimi", 11th International Metallurgy and Materials Congress, İstanbul, 5-8 June 2002.

2. Keskinkılıç, E., Geveci, A., "Effect of Certain Variables on Silicomanganese Production from Denizli-Tavas Mn Ore", 3rd Balkan Conference on Metallurgy, Ohrid, Macedonia, 24-27 September 2003.

3. Geveci, A., Keskinkılıç, E., “Study of Smelting Parameters in the Production of Silicomanganese from Denizli-Tavas Manganese Ores of Turkey”, 2004 TMS Annual Meeting, Charlotte, North Carolina, 14-18 March 2004.

4. Geveci, A., Keskinkılıç, E., Topkaya, Y.A., "Desulfurization in the Ladle Furnace Using Industrial Slags", Sohn International Symposium on Advanced Processing of Metals and Materials: Principles, Technologies and Industrial Practice *(invited)*, San Diego, California, 27-31 August 2006.

5. Geveci, A., Keskinkılıç, E., Topkaya, Y.A., "Pota Fırını Curuflarının Kükürt Giderme Davranışlarının İncelenmesi", 13th International Metallurgy and Materials Congress, İstanbul, 9-11 November 2006.

6. Keskinkılıç, E., Geveci, A., Topkaya, Y.A., “Desulfurization Characteristics of Ladle Furnace Slags of a Low-Sulfur Steel”, Canadian Metallurgical Quarterly, *accepted on June 17, 2007*.

HOBBIES

Sports especially football, watching TV, playing chess.